Thesis in Partial Fulfillment of the Requirements for the Degree of Master in Aeronautics

Numerical Study of The Reactive Flow Behaviour in Gas Turbine Combustor

Realized by:

Redjem Aymen

Yahiaoui Imad Eddine

Promoter:

Renane Rachid

Co-Promoter:

Chegrani Ahmed

Promo: 2019/2020

Acknowledgement

First and for most I want I am grateful to God and we could never be thankful enough for his guidance he gave us, the wisdom to make the right decisions and the courage and willingness to finish this work, hoping that his light will guide us toward more success in the future.

We give our deepest gratitude to Mr R.Renane and Mr A.Chegrani for the help and continuous orientation they provided us during work.

We would like to thank the members of the jury for accepting to evaluate our humble work.

Finally yet importantly, we would like to thank everyone who contributed to this work with their ideas and collaborations that helped improve and refine this work.

Dedication

This study is wholeheartedly dedicated to our beloved parents, who have been the source of inspiration, who continually provided their moral and financial support.

To our brothers and sisters, relatives, Mentors and friends who shared their advices and encouragement to finish this work.

Abstract

This work is a contribution to the numerical study of gas turbine cycles, more specifically; it studies the final state of combustion. The numerical analysis is based on a ten-dissociation sub-reactions kinetic model of Ethylene, which allows the calculation of the reaction products molar fractions using a Newton-Raphson method based Matlab code, which at first requires the calculation of the Jacobian matrix for the 11 variables system. The mole numbers will be then injected into a Bisection method based Matlab code, which uses the both, the reactants and products enthalpy to guess the adiabatic flame temperature up to a maximum precision. The study also includes an Ansys simulation of a combustor model made in SolidWorks with the measures of the P9005 micro-gas turbine combustor, which allows for a comparison between the Matlab Program Results, the simulation results and some results and benchmarks runs from different articles. The study also includes the effect of pre-heat inlet air on the final temperature and the parameters contributing to the production of pollutant in the products.

Résumé

Ce travail est une contribution à l'étude numérique des cycles des turbines à gaz, plus spécifiquement; il étudie l'état final de la combustion. L'analyse numérique est basée sur un modèle cinétique à dix sous-réactions de dissociation de l'éthylène, qui permet le calcul des fractions molaires des produits de réaction en utilisant un code Matlab basé sur la méthode Newton-Raphson, qui dans un premier temps nécessite le calcul de la matrice Jacobéenne du système d'équations à 11 variables. Les nombres de moles calculés seront ensuite injectés dans un code Matlab basé sur la méthode de dichotomie, qui calcule la différence entre l'enthalpie des réactifs et des produits pour un état d'équilibre pour estimer la température de la flamme adiabatique avec une haute précision. L'étude comprend également une simulation Ansys d'un modèle de chambre de combustion réalisé dans SolidWorks avec les mesures de la chambre de combustion de la micro-turbine à gaz P9005, ce qui permet une comparaison entre les résultats du programme Matlab, les résultats de la simulation et certains résultats et benchmarks tirés de différents articles. L'étude comprend également l'effet de préchauffage de l'air d'admission sur la température finale et l'étude des paramètres qui contribuent à la production de polluant dans les produits.

Nomenclature

P, p	Pressure
N, n	Moles Number
M	Molar Mass
m	Mass
V	Volume
v	Specific Volume/Velocity
R	Gas Constant
Xi	Mole Fraction
CxHy	Hydrocarbon
A/F	Air/fuel Ratio
Φ	Equivalence Ratio
Q, q	Heat
W	Work
U, u	Internal energy/Mass specific internal energy
Δ	Change
g	Gravitational acceleration
S	Entropy
KB	Boltzmann's constant
Ω	Microstate Number
H	Enthalpy
d	Perfect differential
δ	Partial differential
G	Gibbs free energy
$\bar{g}_{i,T}^{0}$	Gibbs is function of the pure species
$\bar{h}_{\iota}(T)$	Standardized enthalpy
$\bar{h}_{f,i}^{0}(T_{ref})$	Enthalpy of formation at standard reference state

C_v	Volume specific heat capacity
C_p	Pressure specific heat capacity
η_{th}	Theoretical efficiency
r_p	Pressure ratio
r_w	Work ratio
K	Reaction rate constant
Kp	Equilibrium constant
α	Tangential angle at compressor inlet
V_1	Relative velocity of the air
C_2	Absolute velocity
C_{w2}	Absolute Tangential velocity component
C_{r2}	Absolute Tangential radial component
U	Blade speed
σ	Slip factor
T_{0x}	Stagnation temperature at x station
ψ	Loss factor
C_a	Axial velocity
η_c	Overall isentropic efficiency
η_s	Isentropic efficiency in a stage
W_s	Stage work
λ_N	The loss coefficient for the nozzle blades
r_c	Fuel mole number
H_r	Reactants Enthalpy
H_p	Products Enthalpy
N_t	Total number of moles
T_{ad}	Adiabatic temperature
T_i	Initial temperature

1-1 <u>Background study</u>

A gas turbine, called a combustion turbine, is a rotary engine that extracts energy from a flow of hot gas produced by combustion of gas or fuel oil in a stream of compressed air. It has an upstream air compressor with radial or axial flow mechanically coupled to a downstream turbine and a combustion chamber in between. Gas turbine may also refer to just the turbine element. Energy is released when compressed air is mixed with fuel and ignited in the combustor. The resulting gases are directed over the turbine blades, spinning the turbine, and mechanically powering the compressor. Finally, the gases are passed through a nozzle, generating additional thrust when accelerating the hot exhaust gases by expansion back to atmospheric pressure. Energy is extracted in the form of shaft power, compressed air and thrust, in any combination, and used to power aircraft, trains, ships, electrical generators, and even tanks. Gas turbines are always used if high power density, low weight and quick starting are required. As the moving parts of a gas turbine only perform rotary motion, almost vibration free running can be achieved if turbine is well balanced. [1]

Gas turbines are becoming increasingly used as power generations for a wide variety of applications around the world. Originally, they were developed solely for aircraft propulsion where their inherent low specific weight (i.e. mass/unit power) that made them essential for high-speed flight. For this particular purpose, they have been developed to a high degree of efficiency both thermodynamically and mechanically. [1]

1-2 <u>History of Gas Turbine</u>

1.2.1. <u>John Barber:</u>

In 1791, Barber took out a patent (UK patent no. 1833 – *Obtaining and Applying Motive Power, & c. A Method of Rising Inflammable Air for the Purposes of Procuring Motion, and Facilitating Metallurgical Operations*) which contained all of the important features of a successful gas turbine. Planned as a method of propelling a "horseless carriage", Barber's design included a chain-driven, reciprocating gas compressor, a combustion chamber, and a turbine. [2]

Barber's turbine was used to burn gas obtained from wood, coal, oil and substances, heated in a retort or producer, from where the gases were conveyed into a receiver and cooled. Air and gas were then to be compressed in different cylinders and pumped into an "exploder" (combustion chamber) where they were ignited, the mixture of hot gas then being played against the vanes of a paddle wheel. Water is injected into the explosive mixture to cool the mouth of the chamber and, by producing steam, to increase the volume of the charge. [3]

Barber's concept was sound, but given the technology of that day, it was not possible for the device to create sufficient power to both compress the air and the gas and produce useful work. Nevertheless, the credit for the idea that leads to the modern gas turbine can clearly be given to John Barber. [3]
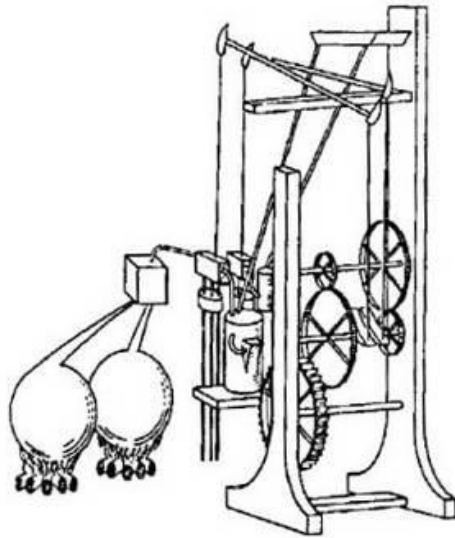
Fig 1.1: Early Design of Gas Turbine by John Barber [35]

1.2.2. <u>Franz Stolze:</u>

The gas turbine built in 1904 according to the plans of the Berlin engineer Franz Stolze must be recognised as the first attempt to produce such an engine. It remained unsuccessful however. [4]

Further attempts in Europe and America gradually produced useful technical results, but the plants remained fixed. Rudimentary theoretical knowledge and difficulties with materials and manufacturing procedures did not allow reliable and efficient gas turbines to be built. [4]
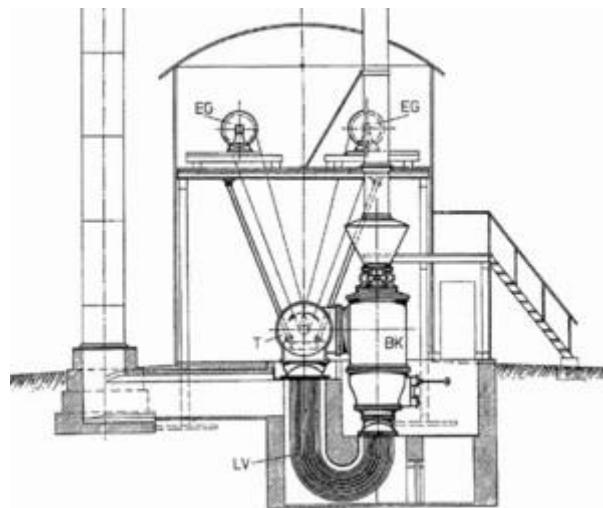
Fig 1.2: Franz Stole's Gas Turbine [36]

1.2.3. Charles Parsons:

Parsons was interested in marine applications and founded the Parsons Marine Steam Turbine Company in Newcastle. Famously, in June 1897, his turbine powered yacht, *Turbinia*, was exhibited moving at speed at Queen Victoria's Diamond Jubilee Fleet Review to demonstrate the great potential of the new technology. The *Turbinia* moved at 34 KN (63 km/h). The fastest Royal Navy ships using other technologies reached 27 KN (50 km/h). Part of the speed improvement was attributable to the slender hull of the *Turbinia*. [5]

Within two years, the destroyers HMS *Viper* and *Cobra* were launched with Parsons' turbines, soon followed by the first turbine powered passenger ship, Clyde steamer TS *King Edward* in 1901; the first turbine transatlantic liners RMS *Victorian* and *Virginian* in 1905, and the first turbine powered battleship, HMS *Dreadnought* in 1906, all of which were driven by Parsons' turbine engines. [5]
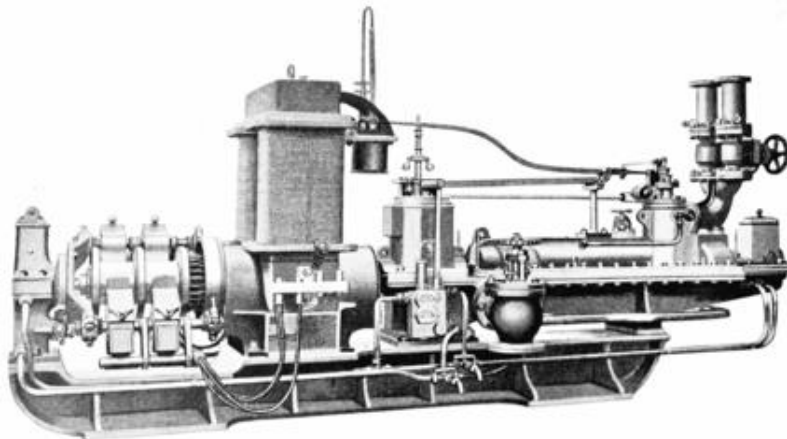
Fig 1.3: Charles Parson' Marine Steam Turbine [37]

1.2.4. Aegidius Elling:

His first gas turbine patent was granted in 1884. In 1903, he completed the first turbine that produced excess power; his original machine used both rotary compressors and turbines to produce 11 bhp (8 kW) net. He further developed the concept, and by 1912, he had developed a gas turbine system with separate turbine unit and compressor in series, a combination that is now common. [6]

One major challenge was to find materials that could withstand the high temperatures developed in the turbine to achieve high output powers. His 1903 turbine could withstand inlet temperatures up to 400° Celsius. Elling understood that if better materials could be found, the gas turbine would be an ideal power source for airplanes. [6]
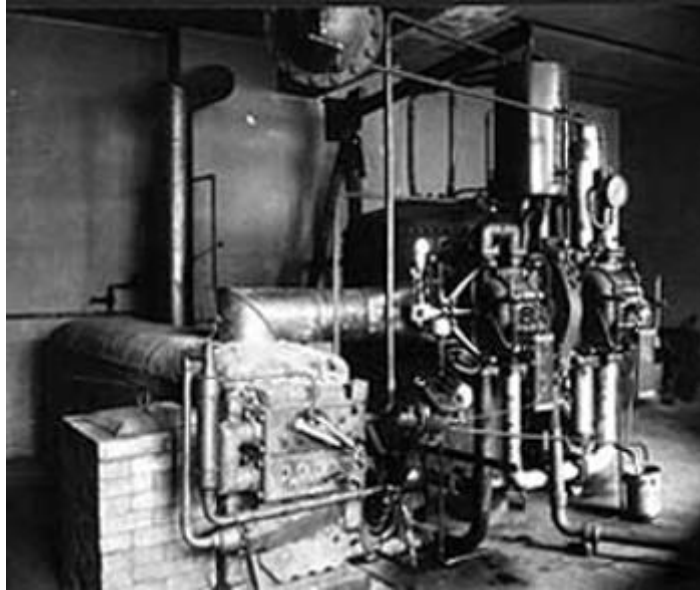
Fig 1.4: Aegidius Elling' Gas Turbine system [38]

1.2.5. <u>Armengaud-Lemale:</u>

The Armengaud-Lemale turbine engine in France, a first with a water-cooled combustion chamber. [7]

1.2.6. <u>Holzwarth impulse turbine:</u>

Hans Howarth developed the turbine from 1906 onwards for experimental purposes, it worked without a compressor and with periodic combustion, and separate reservoirs were filled by outside-driven fans with air or gas at low excess pressure. Via controlled inlet valves, firstly air and then gas flows from the reservoirs to the combustion chamber. [8]

The ignition of the mixture produces an abrupt increase in pressure which forces open a valve to the turbine. The combustion gases flow out and accelerate in the nozzle; they then give up their kinetic energy to the rotor and emerge through the exhaust into the atmosphere. [8]

The valve to the rotor closes so slowly that the air flowing in again can flush the combustion chamber and cool the rotor, the ignition of the mixture produces an abrupt increase in pressure which forces open a valve to the turbine. The combustion gases flow out and accelerate in the nozzle; they then give up their kinetic energy to the rotor and emerge through the exhaust into the atmosphere. [8]
The valve to the rotor closes so slowly that the air flowing in again can flush the combustion chamber and cool the rotor.
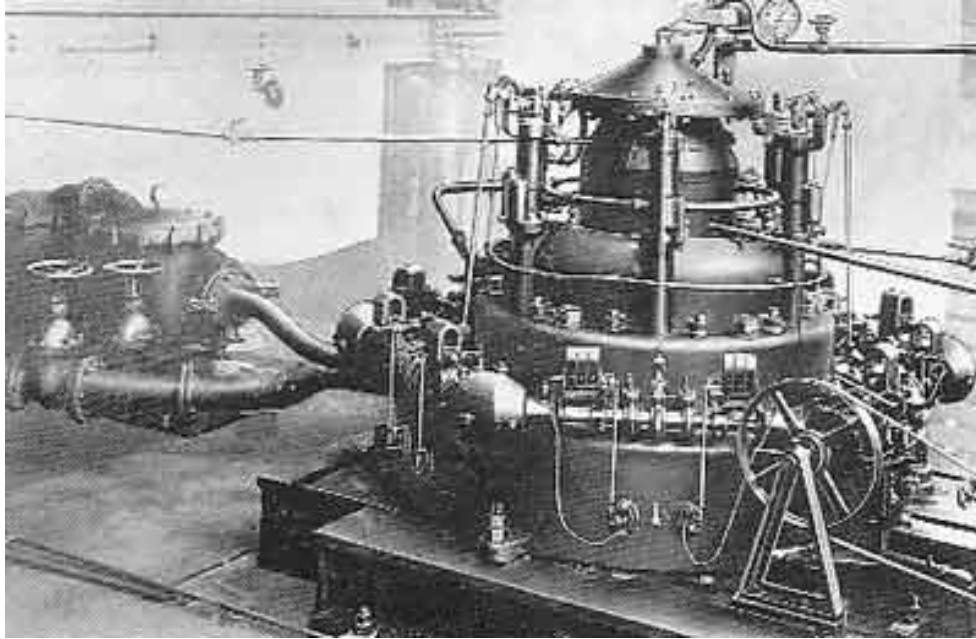
Fig 1.5: Holzwarth impulse turbine [39]

1.2.7. <u>Alan Arnold Griffith:</u>

In 1926, A.A. Griffith published a seminal paper, *An Aerodynamic Theory of Turbine Design*. He demonstrated that the woeful performance of existing turbines was due to a flaw in their design that meant the blades were "flying stalled", and proposed a modern airfoil shape for the blades that would dramatically improve their performance. The paper went on to describe an engine using an axial compressor and two-stage turbine, the first stage driving the compressor, the second a power-take-off shaft that would be used to power a propeller. This early design was a forerunner of the turboprop engine. Because of the paper, the Aeronautical Research Committee supported a small-scale experiment with a single-stage axial compressor and single-stage axial turbine. Work was completed in 1928 with a working tested design, and from this, a series of designs was built to test various concepts. [9]

1.2.8. <u>Brown, Boveri & Cie:</u>

Brown Boveri again took up the manufacture of a Holzwarth gas turbine and proposed a cycle, which might be called the two-chamber, two-stroke cycle. The first unit went into operation in 1933, at a German steel plant with blast furnace gas as fuel. [10]
This prophesy came true, but at a much later date due to the invention of the steam turbine which relegated the gas turbine to the background. They started selling axial compressor and turbine turbosets as part of the turbocharged steam generating Velox boiler. Following the gas turbine principle, the steam evaporation tubes are arranged within the gas turbine combustion chamber; the first Velox plant was erected in Mondeville, Calvados, France. [10]
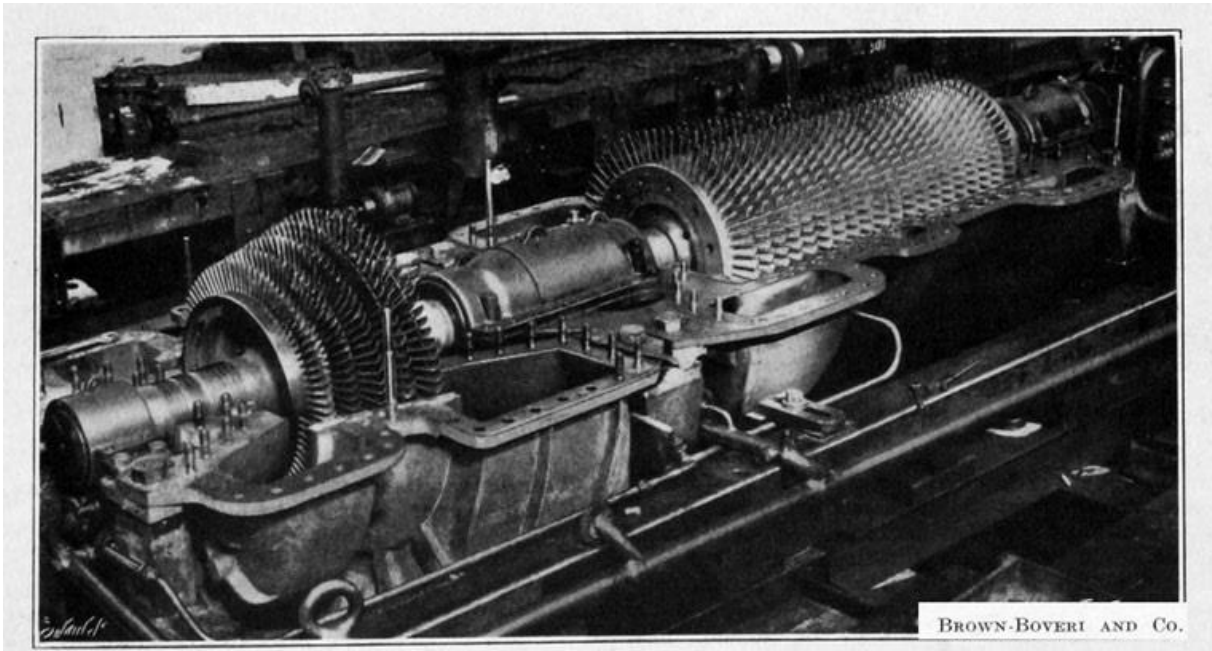
Fig 1.6: Brown, Boveri & Cie' Turbine [40]

2. <u>Basics of Thermodynamics and combustion kinetics</u>

2.1. <u>Definition of Thermodynamics</u>

Thermodynamics is a branch of physics that deals with heat, work, and temperature, and how they relate to energy, radiation, and other properties of matter. Thermodynamics has four laws that describe all interactions between these quantities, which convey a quantitative description using measurable macroscopic physical quantities. [11]

Thermodynamics applies to a wide variety of topics in science and engineering, especially physical chemistry, chemical engineering and mechanical engineering, but also in other complex fields such as meteorology. [12]

2.2. <u>State Equation</u>

An equation of state describes in a single equation the relation between the pressure, P, temperature, T, and volume V (or specific volume v) of a substance. For ideal-gas behaviour, i.e., a gas that is modelled by neglecting intermolecular forces and the volume of the molecules, the following equivalent forms of the equation of state apply: [12]

$$PV = NR_uT \tag{2.1}$$

$$PV = mRT \tag{2.2}$$

$$Pv = RT \tag{2.3}$$

$$P = \rho RT \tag{2.4}$$

2.3. <u>Ideal-Gas Mixtures</u>

Consider a multicomponent mixture of gases composed of N_1 moles of species 1, N_2 moles of species 2, etc. The mole fraction of species i, $\boldsymbol{\chi_i}$ is defined as the fraction of the total number of moles in the system that are species i: [12]

$$\chi_i = \frac{N_i}{N_1 + N_2 + \cdots + N_i + \cdots} = \frac{N_i}{N_{tot}} \tag{2.5}$$

2.4. <u>Stoichiometry</u>

The stoichiometric quantity is the exact amount of oxidizer required to burn a specific amount of fuel. If more than a stoichiometric quantity of oxidizer is supplied, the mixture is said to be fuel lean, while supplying less than the stoichiometric oxidizer results in a fuel-rich or rich mixture. The stoichiometric oxidizer (generally air) fuel ratio is determined by simply balancing the atoms on both sides of the chemical reaction equation, assuming a perfect

reaction. For a hydrocarbon fuel given by C_xH_y, the stoichiometric relation can be expressed as: [12]

$$C_xH_y + a(O_2 + 3.76N_2) \rightarrow xCO_2 + (y/2)H_2O + 3.76aN_2$$
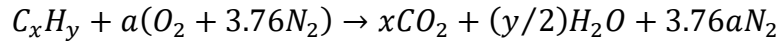
Where:

$$a = x + y/4$$

The **stoichiometric air–fuel ratio** can be found as:

$$(A/F)_{Stoic} = \left(\frac{m_{air}}{m_{fuel}}\right) \tag{2.6}$$

2.4.1. The equivalence ratio

The equivalence ratio, Φ, is commonly used to indicate quantitatively whether a fuel–oxidizer mixture is rich, lean, or stoichiometric. [12]

$$\boldsymbol{\Phi} = \frac{(A/F)_{Stoic}}{(A/F)} = \frac{(F/A)}{(F/A)_{Stoic}} \tag{2.7}$$

From this definition, we see that for fuel-rich mixtures, $\Phi > 1$, and for fuel-lean mixtures, $\Phi < 1$. For a stoichiometric mixture, Φ equals unity. [12]

In many combustion applications, the equivalence ratio is the single most important factor in determining a system's performance. [12]

Other parameters frequently used to define relative stoichiometry are **percent stoichiometric air,** which relates to the equivalence ratio as:

$$\% \; stoichiometric \; air = \frac{100\%}{\Phi} \tag{2.8}$$

2.4.2. Percent excess air

$$\% excess \; air = \frac{(1-\Phi)}{\Phi} 100\% \tag{2.9}$$

2.5. The laws of thermodynamics

2.5.1. The zeroth law of thermodynamics

If A is in thermal equilibrium with B and B is in thermal equilibrium with C, then C will be in thermal equilibrium with A. [13]

The zeroth law implies that just as the pressure is a physical property that enables us to anticipate when systems are in mechanical equilibrium when brought together regardless of their composition and size, then there exists a property that enables us to anticipate when two systems will be in thermal equilibrium regardless of their composition and size: we call this universal property the **temperature**. [13]

2.5.2. <u>The first law of thermodynamics</u>

The first law of thermodynamics is an extension of the law of conservation of energy, that energy can be neither created nor destroyed. That is, however much energy there was at the start of the universe, so there will be that amount at the end. [13]

For a fixed mass, i.e. a system, energy conservation is expressed for a finite change between two states, 1 and 2, as:

$$Q_{12} \quad - \quad W_{12} = \quad \Delta U_{1-2}$$

Q_{12} : Heat added to system in going from state 1 to state 2

W_{12} : Work done by system on surroundings in going from state 1 to state 2

ΔU_{1-2} : Change in total system energy in going from state 1 to state 2

2.5.1.1. <u>Path independence</u>

The dependency of a function or variable is that it may or may not relate to a specific path taken when going from a state 1 to a different state 2 [14]

Both 'Q' and 'W' are path functions and occur only at the system boundaries.

'ΔU' is the change in the total energy of the system, which is the sum of the internal, kinetic, and potential energies [12]

$$U = m(u + \frac{1}{2}v^2 + gz) \tag{2.10}$$

u : Mass-specific system internal energy

$\frac{1}{2}v^2$: Mass-specific system kinetic energy

gz : Mass-specific system potential energy
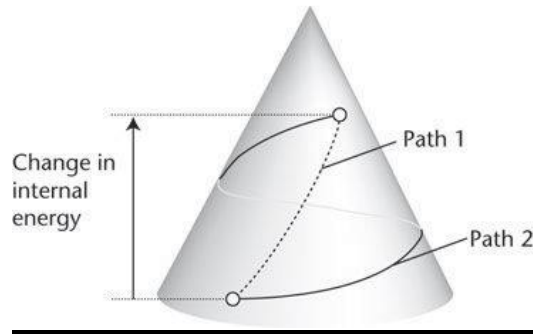
Fig 2.1: Path Dependency [14]

2.5.1.2. <u>Reversibility</u>

In thermodynamics, reversibility is a characteristic of certain processes (changes of a system from an initial state to a final state spontaneously or because of interactions with other systems) that is reversible, and restores the system to its initial state, without leaving net effects in any of the systems involved. [15]

2.5.3. <u>The Second law of thermodynamics</u>

The second law of thermodynamics states that the total entropy of an isolated system can never decrease over time, and is constant if and only if all processes are reversible.

Real life systems are subjected to friction, which make them a one directional process, meaning that entropy is always increasing [13]

2.5.3.1. <u>Reversible transformation</u>

$$\Delta S_{sys} = \frac{Q_{rev}}{T} \qquad\qquad (2.11)$$

2.5.3.2. <u>Irreversible transformation</u>

$$\Delta S_{sys} = \frac{Q_{rev}}{T} + \Delta S_{created} \qquad\qquad (2.12)$$

2.5.4. <u>Third law of thermodynamics</u>

The third law of thermodynamics states as follows, regarding the properties of closed systems in thermodynamic equilibrium:

The entropy of a system approaches a constant value as its temperature approaches absolute zero. [16]

This constant value is independent from any parameters characterizing the closed system. At absolute zero, the system will be in a state with the minimum possible energy. Entropy is related to the number of accessible microstates, and there is typically one unique state (called the ground state) with minimum energy. [16]

$$S - S_0 = K_B \ln \Omega \tag{2.13}$$

K_B :   The Boltzmann constant.

Ω :   The number of microstates consistent with the macroscopic configuration. The counting of states is from the reference state of absolute zero, which corresponds to the entropy of S_0.

The Boltzmann constant is the proportionality factor that relates the average relative kinetic energy of particles in a gas with the thermodynamic temperature of the gas. [17]

2.6. <u>Enthalpy</u>

It is defined as the sum of the system's internal energy and the product of its pressure and volume, deriving its formula can be done starting from the first law and using the defining equation of work done by the system at a constant pressure as follows: [18]

$$\Delta U = U_B - U_A = Q_p + W \tag{2.14}$$

At constant pressure:

$$W = -P\Delta V \tag{2.15}$$

From the previous equations, we derive the following:

$$U_B - U_A = Q_p - P(V_B - V_A) \tag{2.16}$$

Therefore:

$$Q_p = (U_B + PV_B) - (U_A + PV_A) \tag{2.17}$$

As stated before, Enthalpy is a function of the internal system energy, its pressure and its volume:

$$H(U, P, V) = U + PV \tag{2.18}$$

From that, we can write Q_p as follows:

$$Q_p = H_B - H_A = \Delta H \tag{2.19}$$

The U term is the energy required to create the system, and the PV term as the work that would be used to create space for the system if the pressure of the environment remained constant. When a system, for example, n moles of a gas of volume V at pressure p and temperature T, is created or brought to its present state from absolute zero, energy must be fed into it equal to its internal energy U plus PV, where PV is the work done in pushing against the ambient pressure. [19]

In basic chemistry, experiments are conducted at constant atmospheric pressure, and the pressure-volume work represents an energy exchange with the atmosphere that cannot be accessed or controlled, so that ΔH is the expression chosen for the heat of reaction. [20]

For a heat engine, a change in its internal energy is the difference between the heat input and the pressure-volume work done by the working substance while a change in its enthalpy is the difference between the heat input and the work done by the engine: [21]

$$dH = \delta Q - \delta W \tag{2.20}$$

2.7. <u>Gibbs Function:</u>

The use of an isolated system of fixed mass and fixed energy and volume is not particularly useful for many of the typical problems involving chemical equilibrium. There will always be a need to calculate the composition of a mixture at a given temperature, pressure, and stoichiometry. [12]

The **Gibbs free energy, G,** is a solution to that problem, by replacing the entropy as the main thermodynamic property. The Gibbs free energy is defined in terms of other thermodynamic properties as: [12]

$$G = H - TS \tag{2.21}$$

The second law can then be expressed as:

$$(dG)_{T,P,m} \leq 0 \tag{2.22}$$

Which states that the Gibbs function always decreases for a spontaneous, isothermal, isobaric change of a fixed-mass system in the absence of all work effects except boundary $(P - dV)$ work. This principle allows us to calculate the equilibrium composition of a mixture at a given temperature and pressure. This function attains a minimum in equilibrium, thus: [12]

$$(dG)_{T,P,m} = 0 \tag{2.23}$$

2.8. Equilibrium Constant:

For a mixture of ideal gases, the Gibbs function for species is given by:

$$G_{mix} = \sum N_i \bar{g}_{i,T} = \sum N_i \left[\bar{g}_{i,T}^0 + R_u T \ln(P_i/P^0) \right] \qquad (2.24)$$

Where $\bar{g}_{i,T}^0$ is the Gibbs is function of the pure species at the standard-state pressure, and P_i is the partial pressure, P^0 is the standard-state pressure (by convention taken to be 1 atm). [12]

For fixed temperature and pressure, the equilibrium condition becomes:

$$dG_{mix} = 0 \qquad (2.25)$$

Or

$$\sum dN_i \left[\bar{g}_{i,T}^0 + R_u T \ln(P_i/P^0) \right] + \sum N_i d \left[\bar{g}_{i,T}^0 + R_u T \ln(P_i/P^0) \right] = 0 \qquad (2.26)$$

The second term in the previous equation can be shown to be zero by recognizing that $dl\, n(P_i/P^0) = d\,pi/pi$ and that $\sum dP_i = 0$, since all changes in the partial pressures must sum to zero because the total pressure is constant. Thus: [12]

$$G_{mix} = \sum dN_i \left[\bar{g}_{i,T}^0 + R_u T \ln(P_i/P^0) \right] = 0 \qquad (2.27)$$

For the general system, where:

$$aA + bB +.. \rightarrow eE + fF + \cdots$$
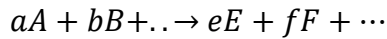
The change in the number of moles of each species is directly proportional to its stoichiometric coefficient:

$$dN_A = -\kappa a$$
$$dN_B = -\kappa b$$
$$.$$
$$.$$
$$dN_E = +\kappa e$$
$$dN_F = +\kappa f$$

By substituting and cancelling the proportionality constant, we obtain:

$$-a\left[\bar{g}_{A,T}^0 + R_u T \ln(P_A/P^0) \right] - b\left[\bar{g}_{B,T}^0 + R_u T \ln(P_B/P^0) \right] - \cdots + e\left[\bar{g}_{E,T}^0 + R_u T \ln(P_E/P^0) \right] + f\left[\bar{g}_{F,T}^0 + R_u T \ln(P_F/P^0) \right] + \cdots = 0 \qquad (2.28)$$

By rearranging and the log terms grouped together to yield:

$$-\left(e\bar{g}_{E,T}^0 + f\bar{g}_{F,T}^0 + \cdots - a\bar{g}_{A,T}^0 - b\bar{g}_{B,T}^0 - \cdots\right) = R_u T \, ln \frac{(P_E/P^0)^e (P_F/P^0)^f}{(P_A/P^0)^a (P_B/P^0)^b} \quad (2.29)$$

The term on the left-hand side of equation is called the **standard state Gibbs function change:**

$$\Delta \boldsymbol{G_T^0} = \left(e\bar{g}_{E,T}^0 + f\bar{g}_{F,T}^0 + \cdots - a\bar{g}_{A,T}^0 - b\bar{g}_{B,T}^0 - \cdots\right) \qquad (2.30)$$

The argument of the natural logarithm is defined as the **equilibrium constant:**

$$\boldsymbol{K_p} = \frac{(P_E/P^0)^e (P_F/P^0)^f}{(P_A/P^0)^a (P_B/P^0)^b} \qquad (2.31)$$

With these definitions, our statement of chemical equilibrium at constant temperature and pressure is given by:

$$\Delta \boldsymbol{G_T^0} = -R_u T \ln K_p \qquad (2.32)$$

With:

$$\boldsymbol{K_p} = \exp(-\Delta G_T^0 / R_u T) \qquad (2.33)$$

2.9. Standardized Enthalpy and Enthalpy of Formation

For any chemical species, the standardized enthalpy is defines as the sum of an enthalpy that takes into account the energy associated with chemical bonds forming the species themselves, called the enthalpy of formation h_f, and an enthalpy that is associated only with the temperature; a term describing the change in temperature from an initial state to another one, called the sensible enthalpy change Δh_s. Thus, we can write the molar standardized enthalpy for species as: [12]

$$\bar{h}_i(T) = \bar{h}_{f,i}^0(T_{ref}) + \Delta \bar{h}_{s,i}(T) \qquad (2.34)$$

$\bar{h}_i(T)$:   Standardized enthalpy at temperature T

$\bar{h}_{f,i}^0(T_{ref})$:   Enthalpy of formation at standard reference state (T_{ref}, P^0)

$\Delta \bar{h}_{s,i}(T)$:   Sensible enthalpy change in going from T_{ref} to T

The standard enthalpy of formation is a measure of the energy released or consumed when one mole of a substance is created under standard conditions from its pure elements. [22]

Thus, enthalpies of formation have a physical interpretation as the net change in enthalpy associated with breaking the chemical bonds of the standard-state elements and forming new bonds to create another compound of interest. [12]

Sensible enthalpy is a measure of the energy required when going from a reference temperature to a final temperature. [22]
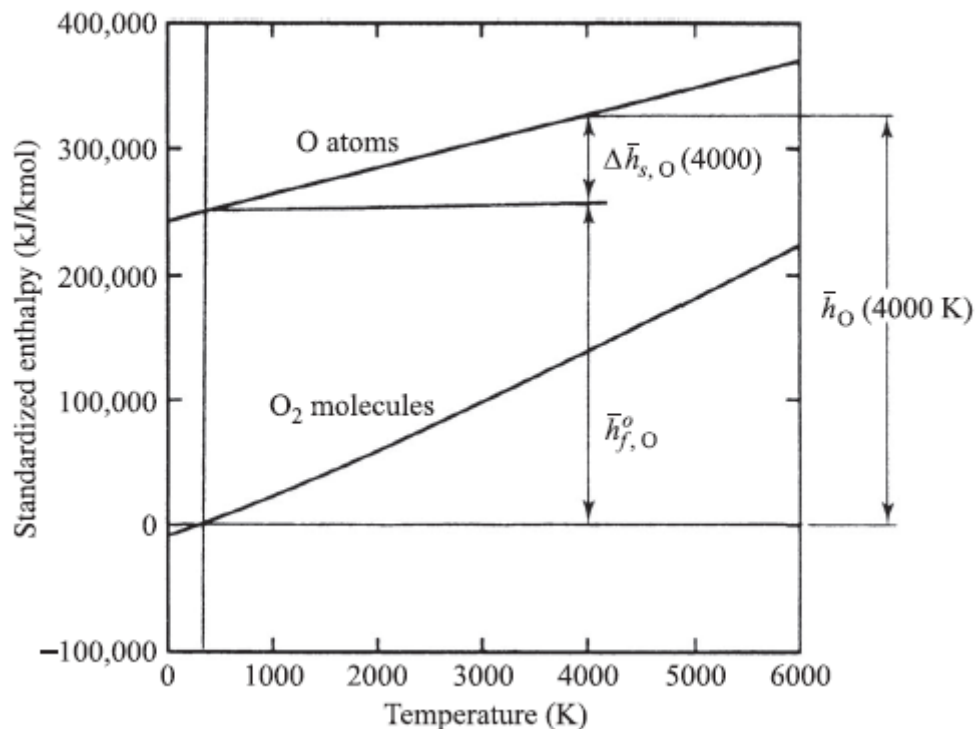
Fig 2.2: Standardized enthalpy, enthalpy of formation, and sensible enthalpy for Oxygen atom and molecules [12]

2.10. Calorific Equations of State

Expressions relating internal energy (or enthalpy) to pressure and temperature are called calorific equations of state:

$$u = u(T, v)$$

$$h = h(T, P)$$

The word "calorific" relates to expressing energy in units of calories, which has been superseded by the use of joules in the SI system.

General expressions for a differential change in *u* or *h* can be expressed by differentiating the previous equations:

$$du = \left(\frac{\partial u}{\partial T}\right)_v dT + \left(\frac{\partial u}{\partial v}\right)_T dv \qquad (2.35)$$

$$dh = \left(\frac{\partial h}{\partial T}\right)_P dT + \left(\frac{\partial h}{\partial P}\right)_T dP \qquad (2.36)$$

In the above, we recognize the partial derivatives with respect to temperature to be the **constant-volume** and **constant-pressure specific heats,** respectively

$$C_v = \left(\frac{\partial u}{\partial T}\right)_v \qquad (2.37)$$

$$C_p = \left(\frac{\partial h}{\partial T}\right)_P \qquad (2.38)$$

2.11.   Gas turbine cycle

Gas turbines usually operate on an open cycle

• A compressor takes in fresh ambient air (state 1), compresses it to a higher temperature and pressure (state 2).

• Fuel and the higher-pressure air from compressor are sent to a combustion chamber, where fuel is burned at constant pressure. The resulting high temperature gases are sent to a turbine (state 3).

• The high temperature gases expand to the ambient pressure (state 4) in the turbine and produce power.

• The exhaust gases leave the turbine. [34]
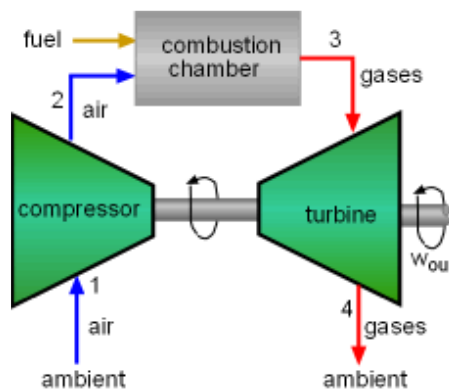
Fig 2.3: Open Gas Turbine Cycle [34]

By using the air-standard assumptions, replacing the combustion process by a constant pressure heat addition process, and replacing the exhaust discharging process by a constant pressure heat rejection process, the open cycle described above can be modelled as a closed cycle called ideal **Brayton cycle.** [34]
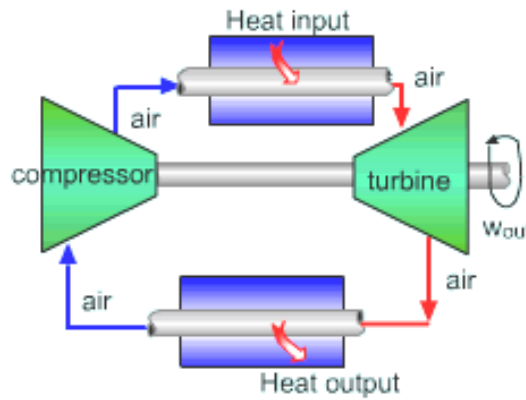
Fig 2.4: Closed Gas Turbine Cycle [34]

2.11.1. <u>Brayton cycle</u>

The ideal Brayton cycle is made up of four internally reversible processes.
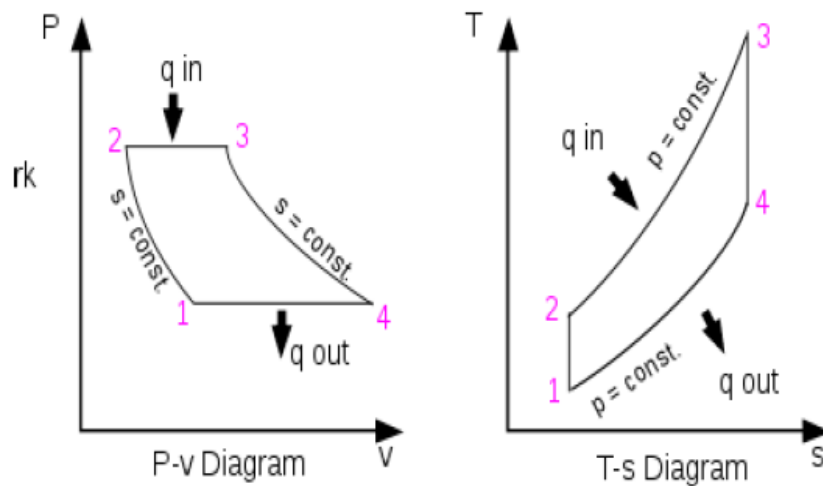
Fig 2.5: PV and TS diagrams for Bryton cycle [34]

1-2:   Isentropic compression

2-3:   Constant pressure heat addition

3- 4:   Isentropic expansion

4-1:   Constant pressure heat rejection

2.11.2. Efficiency of Brayton Cycle

The formula for the theoretical efficiency of this cycle goes as follow:

$$\eta_{th} = \frac{net\ work}{heat\ added} = \frac{q_{23} + q_{41}}{q_{23}} = 1 + \frac{q_{41}}{q_{23}} \qquad (2.39)$$

With:

$$q_{23} = q_{in} = h_3 - h_2 = C_p(T_3 - T_2) \qquad (2.40)$$

$$q_{41} = q_{out} = h_1 - h_4 = C_p(T_1 - T_4) \qquad (2.41)$$

By Replacing in the first equation, we get:

$$\eta_{th} = 1 - \frac{T_4 - T_1}{T_3 - T_2} = 1 - \left(\frac{T_1}{T_2}\right)\left(\frac{\frac{T_4}{T_1} - 1}{\frac{T_3}{T_2} - 1}\right) \qquad (2.42)$$

Consider process $1-2$, isentropic compression:

$$pV^\gamma = C = p\left(\frac{T}{p}\right)^\gamma = C \qquad (2.43)$$

$$\frac{T^\gamma}{p^\gamma} = C \qquad (2.44)$$

$$\frac{T}{p^{\frac{\gamma-1}{\gamma}}} = C \qquad (2.45)$$

$$\frac{T_1}{T_2} = \left(\frac{p_1}{p_2}\right)^{\frac{\gamma-1}{\gamma}} = \frac{1}{r_p^{\frac{\gamma-1}{\gamma}}} \qquad (2.46)$$

With:

$$r_p = \frac{p_2}{p_1} \qquad (2.47)$$

From the previous equations:

$$\frac{T_1}{T_2} = \frac{T_4}{T_3} \quad \Rightarrow \quad \frac{T_1}{T_4} = \frac{T_2}{T_3} \qquad (2.48)$$

Replacing in η_{th}:

$$\eta_{th} = 1 - \left(\frac{1}{r_p^{\frac{\gamma-1}{\gamma}}}\right)\left(\frac{\frac{T_3}{T_2} - 1}{\frac{T_3}{T_2} - 1}\right) \qquad (2.49)$$

After simplifying the previous equation, we get:

$$\eta_{th} = 1 - \frac{1}{r_p^{\frac{\gamma-1}{\gamma}}} \qquad (2.50)$$

Work ratio formula goes as follow:

$$r_w = \frac{net\ work}{work\ output} = \frac{w_{12}+w_{34}}{w_{34}} = \frac{-(T_2-T_1)-(T_4-T_3)}{-(T_4-T_3)} \qquad (2.51)$$

$$r_w = 1 - \frac{T_1}{T_3}\left(r_p\right)^{\frac{\gamma-1}{\gamma}} \qquad (2.52)$$

2.12.　　The Definition of Combustion

Combustion is a high-temperature exothermic redox chemical reaction between a fuel and an oxidant, usually atmospheric oxygen that produces oxidized, often gaseous products. [23]

2.13.　　Combustion conditions:

 Fuel must be continuously supplied; there must be oxygen present at all time and there must be heat to initiate the burning. The initial ignition energy does guarantee a passage into starting the flames, after that initial spark, the flame must feed enough energy to sustain the process at all time.

2.14.　　Types of fuels

A combustion reaction can be described by the following general equation:

$$Fuel + Combustion\ agent \rightarrow Products\ of\ combustion + Energy$$
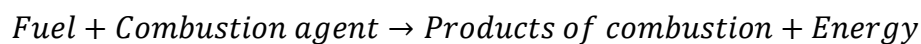
The fuel undergoes an oxidation reaction by the combustion-agent, which is therefore an oxidizing agent. [24]

There are mainly 2 types of fuels:

Fossil fuels: Petrol, carbon, gas…etc. These fuels come from pre-historical organic materials.

Biofuels: A biofuel is a fuel that is produced through contemporary processes from biomass, rather than a fuel produced by the very slow geological processes involved in the formation of fossil fuels. [24]

Fuels come in all three states of matter:

Gas: Such as Butane, Propane…etc.

Liquid: Like Gasoline, Kerosene, different oils…etc.

Solid: Like Wood, Charcoal, and Peat…etc.

2.15. Ergols

The term ergol stands for both the fuel and the combustion-agent used in ballistic missile launchers, earth satellites and spatial probes. The combination fuel/combustion agent is called **propergol.** Propergols can be in solid or liquid form. [24]

2.16. Kinetic model

In essentially all combustion processes, chemical reaction rates control the rate of combustion. Introducing **chemical kinetics**, the study of the elementary reactions and their rates. Much progress has been made in the few past decades in combustion because chemists have been able to define the detailed chemical pathways leading from reactants to products, and to measure or calculate their associated rates. With this knowledge, combustion scientists and engineers are able to construct computer models that simulate reacting systems. Although a tremendous amount of progress has been made, the problem of predicting the details of combustion in a complex flow field, the models created by these chemists are not absolute, they give a close enough result to the real reaction, but because fluid mechanics and chemistry are treated from first principles, this issue has not yet been solved. In general, the fluid mechanical problem alone still taxes the largest computers and the addition of detailed chemistry makes the solution nearly impossible, because the simulation of this kind of models to a near perfection will take a long time, and it is easily disturbed by exterior conditions. [12]

2.17. Global and Elementary reactions

The overall reaction of a mole of fuel with moles of an oxidizer to form b moles of combustion products can be expressed by the global reaction mechanism:

$$F + aO_x \rightarrow bPr$$
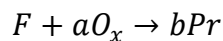
From experimental measurements, the rate at which the fuel is consumed can be expressed as:

$$\frac{d[X_F]}{dt} = -K_G(T)[X_F]^n[O_X]^m \tag{2.34}$$

Where the notation $[Xi]$ is used to denote the molar concentration of the ith species in the mixture. The rate of disappearance of the fuel is proportional to each of the reactants raised to Tapez une équation ici.a power. The constant of proportionality K_G, is called the **global rate coefficient,** and, in general, is not constant, but rather is a strong function of temperature. The minus sign indicates that the fuel concentration decreases with time. The exponents' n and m relate to the **reaction order.** [12]

2.18. A quick overview of reaction orders

There exist thee orders of reaction

Order zero: is when the rate is completely independent from the molar concentration of the reactant

$$v = -\frac{d[A]}{dt} = k[A]^0 = k$$

$$-\frac{d[A]}{dt} = k$$

$$d[A] = -k\,dt$$

$$\int_{[A]_0}^{[A]} d[A] = \int_0^t -k\,dt = -k\int_0^t dt$$

$$[A] - [A]_0 = -k(t - 0)$$

$$[A] = -kt + [A]_0 \tag{2.53}$$

We get the equation of a line with a slope –k and an intercept $[A]_0$.

First Order: The reaction speed is proportional to the molar concentration of the reactant

$$v = -\frac{d[A]}{dt} = -\frac{d[B]}{dt} = k[A] = k[B]$$

$$\int_{[A]_0}^{[A]} \frac{d[A]}{[A]} = \int_0^t -kdt = -k\int_0^t dt = ln[A] - ln[A]_0 = -kt$$

$$ln[A] = ln[A]_0 - kt \tag{2.54}$$

Second Order:

$$v = -\frac{d[A]}{dt} = -\frac{d[B]}{dt} = k[A]^2 = k[B]^2$$

$$-\frac{d[A]}{dt} = k[A]^2$$

$$-\frac{d[A]}{[A]^2} = kdt$$

$$\int_{[A]_0}^{[A]} -\frac{d[A]}{[A]^2} = \int_0^t k\,dt = k\int_0^t dt$$

$$\frac{1}{[A]} - \frac{1}{[A]_0} = kt$$

$$\frac{1}{[A]} = kt + \frac{1}{[A]_0} \tag{2.55}$$

2.19. Determination of the reaction order from experimental data

In the presence of experimental data, we start by tracing the values the concentration of the chemical reactant with respect to time, the order can be determined as follow: [25]

- If the resultant graph is a line, then the order of the reaction is zero

- If the resultant graph is a curve, we trace the natural log values of the concentration with respect to time, if it's a line, then it's a first order reaction

- If the resultant graph is not a line, we trace 1/[A] values with respect to time, if it's a line, then it's a second order reaction

The use of global reactions to express the chemistry in a specific problem is frequently referred to as the "black box" approach. Although this approach may be useful in solving some problems, it does not involve the real process of what is happening chemically in a system. It is very unrealistic to believe that oxidizer molecules simultaneously collide with a single fuel molecule to form product molecules, it is not an automated process, and since this would require breaking several bonds and subsequently forming many new bonds. In reality, many sequential processes can occur involving many **intermediat**e **species.** Let us consider the global reaction: [12]

$$2H_2 + O_2 \rightarrow 2H_2O$$
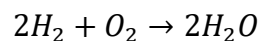
To effect this global conversion of hydrogen and oxygen to water, the following **elementary reactions** are important:

$$H_2 + O_2 \rightarrow HO_2 + H$$

$$H + O_2 \rightarrow OH + O$$

$$OH + H_2 \rightarrow H_2O + H$$

$$H + O_2 + M \rightarrow H_2O + M$$
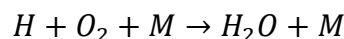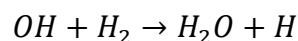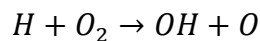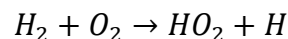
In this partial mechanism for hydrogen combustion, when oxygen and hydrogen molecules collide and react, instead of yielding water directly, they form the intermediate species HO2, the hydroperoxy radical, and a hydrogen atom, H, another radical. **Radicals** or **free radicals** are reactive molecules, or atoms, that have unpaired electrons. The hydrogen atom created then reacts with O2 to form two additional radicals, OH and O. It is the subsequent reaction of the hydroxyl radical (OH) with molecular hydrogen, that forms water. [12]

To have a complete picture of the combustion of H2 and O2, more than 20 elementary reactions can be considered. [12]

The collection of elementary reactions necessary to describe an overall reaction is called a reaction **mechanism.** Reaction mechanisms may involve only a few steps or as many as several hundred. A field of active research involves selecting the minimum number of elementary steps necessary to describe a particular global reaction. [12]

3. Gas turbine Main Parts and their performances
3.1. General description of the gas turbine working process

Gas turbine engines derive their power from burning fuel in a combustion chamber and using the fast-flowing combustion gases to drive a turbine in much the same way as the high-pressure steam drives a steam turbine. The gas turbine operates on the principle of the Brayton cycle, where compressed air is mixed with fuel and burned under constant pressure conditions. The resulting hot gas is allowed to expand through a turbine to perform work. [26]

A gas turbine essentially brings together air that it compresses in its compressor module, and fuel, which are then ignited. Resulting gases are expanded through a turbine.

That turbine's shaft continues to rotate and drive the compressor, which is on the same shaft, and operation continues. A separate starter unit is used to provide the first rotor motion, until the turbine's rotation is up to design speed and can keep the entire unit running. [26]

The compressor module, combustor module, and turbine module connected by one or more shafts are collectively called the gas generator.

The figures down below shows the schematic for a typical gas generator.
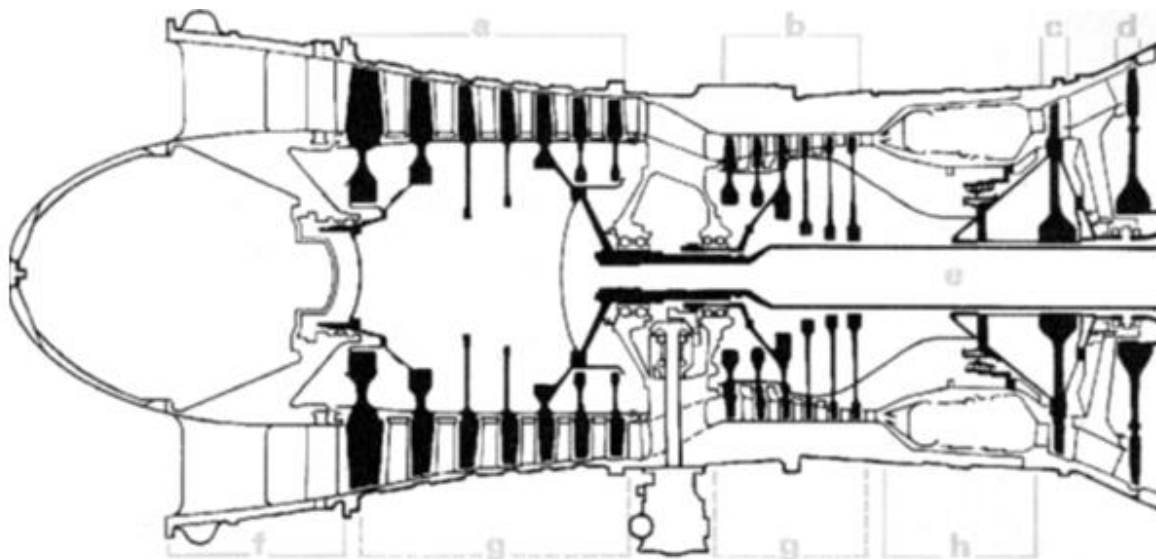
Fig 3.1: Rolls Royce rb211 industrial gas turbine [44]

The gas generator works in a similar way to a Four-Stroke classical engine following the same basic steps that are the intake, compression, combustion and exhaust.
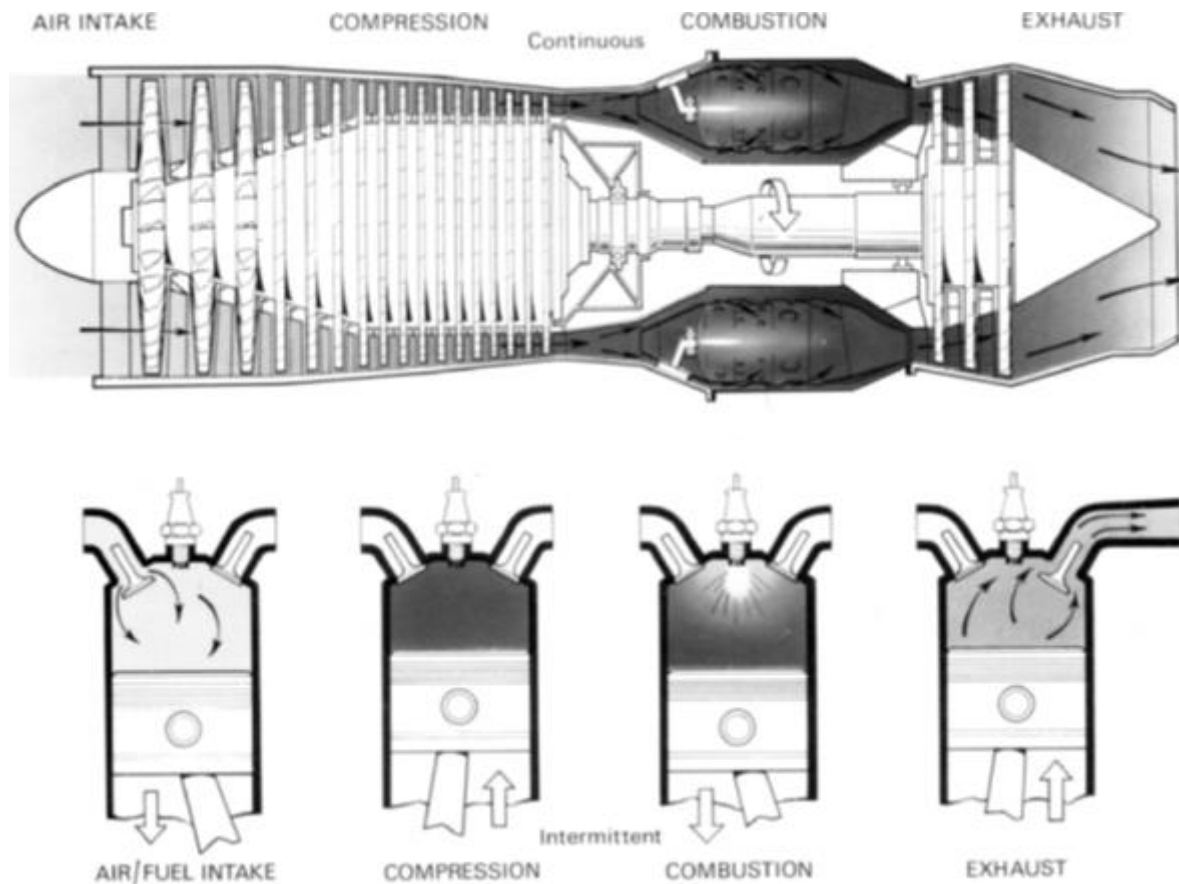
Fig 3.2: Comparison Between Gas Turbine Cycle/4 strokes engine cycle [45]

3.2. Primary Module Basics

The primary modules in a gas turbine are the

1. Compressor module.
2. Combustion module.
3. Turbine module.

A gas turbine also has an inlet section/module and an exhaust section/module. [27]

3.2.1. Compressors

In the gas turbine engine, compression of the air before expansion through the turbine is done by one of two basic types of compressor, one giving centrifugal flow and the other axial flow. Both types are driven by the engine turbine and are usually coupled direct to the turbine shaft. [27]

Most advanced and large gas turbines have compressors that are of the axial design type. Some of the earlier, smaller, or deliberately compact gas turbines have centrifugal compressors. [28]

Each compressor stage plays a role for stepping up the overall compressor pressure ratio (PR), so although an axial stage may not offer as much of a PR as a centrifugal stage of the same diameter, a multistage axial compressor offers far higher PR (and therefore mass flow rates and resultant power) than a centrifugal design. [27]

3.2.1.1. <u>Centrifugal Compressor</u>

3.2.1.1.1. <u>Operation Principle</u>

The centrifugal compressor consists essentially of a stationary casing, hosting a rotating **impeller**, and a number of fixed diverging passages in which the air is decelerated with a consequent rise in static pressure. The latter process is one of diffusion, the part of the compressor containing the diverging passages is known as the **diffuser.** [28]

Fig 3.3: Typical impellers for centrifugal compressors [27]

The impeller may be single- or double-sided but the fundamental theory is the same for both. The double-sided impeller was required in early aero engines because of the relatively small flow capacity of the centrifugal compressor for a given overall diameter. [27]

Air enters the impeller eye gaining whirl speed by the vanes on the impeller disc. The centripetal acceleration is obtained by a pressure head, so that the static pressure of the air increases from the eye to the tip of the impeller. The rest of the static pressure rise is obtained in the diffuser, where the very high velocity of the air leaving the impeller tip is reduced to approximately the same velocity with which the air enters the impeller eye, it should be appreciated that friction in the diffuser will cause some loss in **stagnation** pressure. [28]
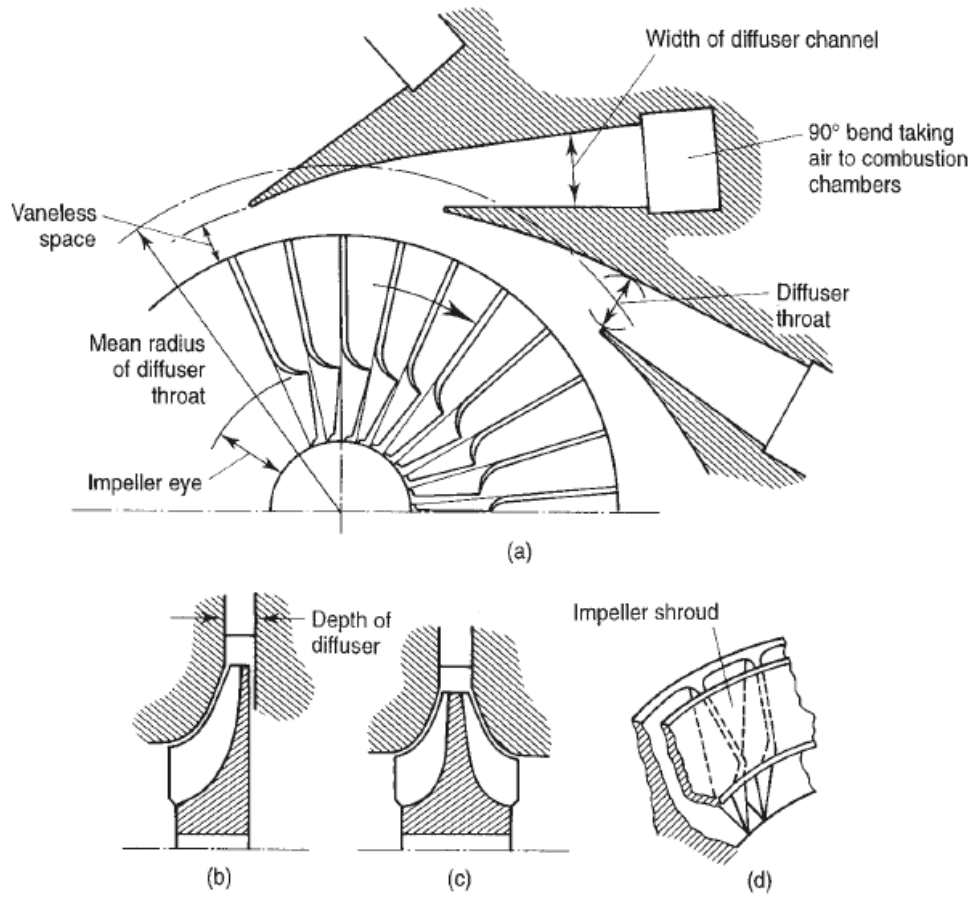
Fig 3.4: Diagrammatic sketches of centrifugal compressors [28]
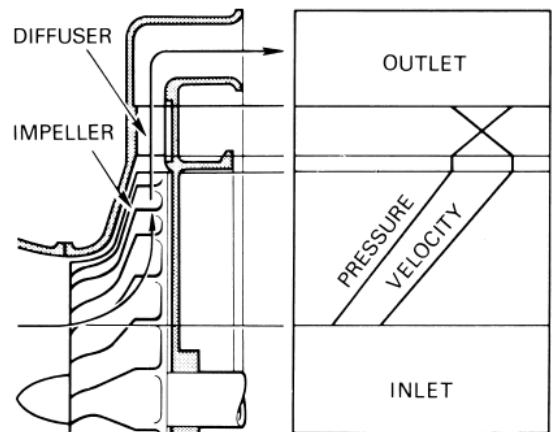
Fig 3.5: Pressure/velocity changes through a centrifugal compressor [27]

To maximize the airflow and pressure rise through the compressor requires the impeller to be rotated at high speed; therefore, impellers are designed to operate at high speed.
By operating at such high tip speeds, the air velocity from the impeller is increased so that greater energy is available for conversion to pressure. [27]

3.2.1.1.2. <u>Work done and pressure rise</u>

The diffuser applies no work on the air; the energy absorbed by the compressor will be determined by the conditions of the air at the inlet and outlet of the impeller.

The air enters the impeller eye in the axial direction, so the initial angular momentum of the air is zero. The axial portion of the vanes must be curved so that the air can pass into the eye. The angle that the leading edge of a vane makes with the tangential direction $\boldsymbol{\alpha}$ will be given by the direction of the relative velocity of the air at inlet, $\boldsymbol{V_1}$

If the air leaves the impeller tip with an absolute velocity $\boldsymbol{C_2}$, it will have a tangential or whirl component $\boldsymbol{C_{w2}}$ and a comparatively small radial component $\boldsymbol{C_{r2}}$. Under ideal conditions $\boldsymbol{C_2}$ would be such that the whirl component is equal to the impeller tip speed **U**. [28]
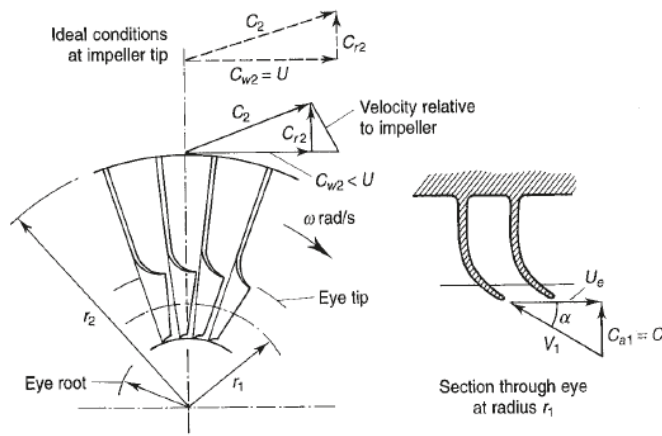
Fig 3.6: Nomenclature, Velocity Diagram for Centrifugal Impeller [28]

Obeying its inertia, the air trapped between the impeller vanes will move around with the impeller, and we have already noted that this results in a higher static pressure on the leading face of a vane than on the trailing face. [28]
This is known as the **Slip**. How far the whirl velocity at the impeller tip falls short of the tip speed depends largely upon the number of vanes on the impeller. [28]
The greater the number of vanes, the smaller the slip, i.e. the more nearly C_{w2} approaches U. It is necessary in design to assume a value for the **Slip factor σ**, where s is defined as the ratio $\boldsymbol{C_{w2}}$/**U**. Various approximate analyses of the flow in an impeller channel have led to formulae for **σ :**

$$\sigma = 1 - \frac{0.63\,\pi}{n} \tag{3.1}$$

Where *n* is the number of vanes.
The theoretical torque in the impeller; will be equal to the rate of change of angular momentum experienced by the air. Considering unit mass flow of air, this torque is given by:

$$Theoretical\ torque = C_{w2}r_2 \tag{3.2}$$

$$Theoretical\ work = C_{w2}r_2\omega = C_{w2}U \tag{3.3}$$

Where ω is the angular velocity.

Or, introducing the slip factor:

$$Theoretical\ work\ done = \sigma U^2 \tag{3.4}$$

Taking account of the friction between the casing and the air carried by the vanes and the disc friction also known as 'Windage', the actual work is greater than the theoretical value, so we are due to introduce a **power factor ψ**, therefore the actual work becomes:

$$Work\ done = \psi \sigma U^2 \tag{3.5}$$

If $(T_{03} - T_{01})$ is the stagnation temperature rise across the whole compressor then, since no energy is added in the diffuser, this must be equal to the stagnation temperature rise $(T_{02} - T_{01})$ Across the impeller alone.
It will therefore be equal to the temperature equivalent of the work done on the air given by the following equation:

$$T_{03} - T_{01} = \frac{\psi \sigma U^2}{C_p} \tag{3.6}$$

Where C_p is the mean specific heat over this temperature range.

If a value for the *overall* isentropic efficiency η_c is assumed, then it is known how much of the work is usefully employed in raising the pressure of the air. The overall stagnation pressure ratio follows as: [28]

$$\frac{P_{03}}{P_{01}} = \left(\frac{T\prime_{03}}{T_{01}}\right)^{\gamma/(\gamma-1)} = \left[1 + \frac{\eta_c(T_{03}-T_{01})}{T_{01}}\right]^{\gamma/(\gamma-1)} = \left[1 + \frac{\eta_c \psi U^2}{C_p T_{01}}\right]^{\gamma/(\gamma-1)} \tag{3.7}$$

3.2.1.1.3. <u>The Diffuser</u>

It is much more difficult to arrange for an efficient deceleration of flow than it is to obtain an efficient acceleration because of the natural tendency in a diffusing process for the air to break away from the walls of the diverging passage, reverse its direction, and flow back in the direction of the pressure gradient.
If the divergence is too rapid, this may result in the formation of eddies with consequent transfer of some kinetic energy into internal energy and a reduction in useful pressure rise. A small angle of divergence, however, implies a long diffuser and a high value of skin friction loss. Experiments show that the optimum included angle of divergence is about 7°, which can be up to double with diffusers of low length/width ratio without incurring a serious increase in stagnation pressure loss. [28]
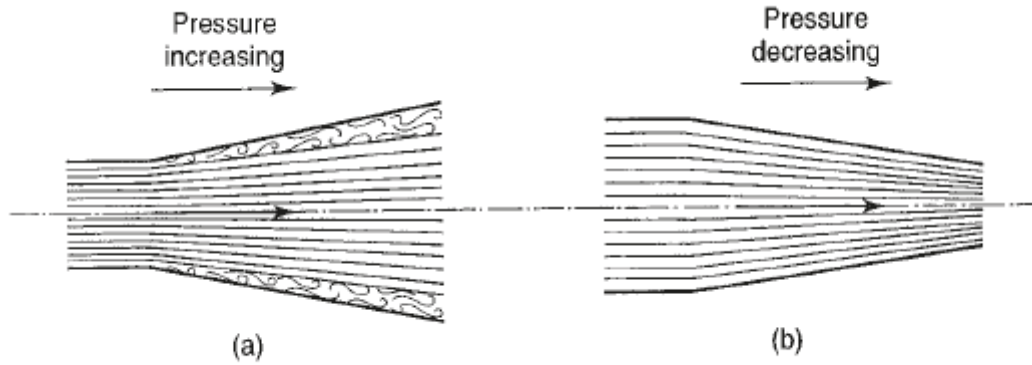
Fig 3.7: Diffusing and accelerating flow [28]

The airflow can be controlled effectively in the shortest length possible by dividing it into a number of separate streams by fixed diffuser vanes when leaving the impeller, the passages formed by the vanes have a constant depth, the width diverging in accordance with the shape of the vanes. The angle of the diffuser vanes at the leading edge must be designed to suit the direction of the absolute velocity of the air at the radius of the leading edges, so that the air will flow smoothly over the vanes. [28]

3.2.1.2. The Axial Compressor

An axial flow compressor consists of one or more rotor assemblies that carry blades of airfoil section. These assemblies are mounted between bearings in the casings called the stator vanes. The compressor is a multistage unit as the amount of pressure increase by each stage is small; a stage consists of a row of rotating blades followed by a row of stator vanes.
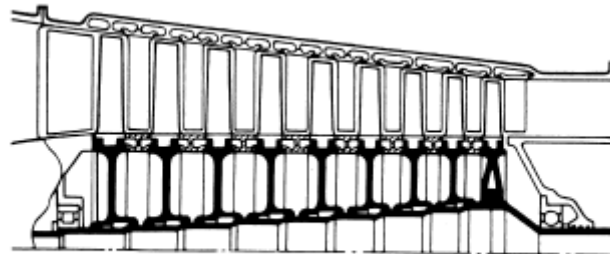
Fig 3.8: Multi-stage high-pressure ratio compressor [27]

Where several stages of compression operate in series on one shaft, it becomes necessary to vary the stator vane angle to enable the compressor to operate effectively at speeds below the design condition. [27]
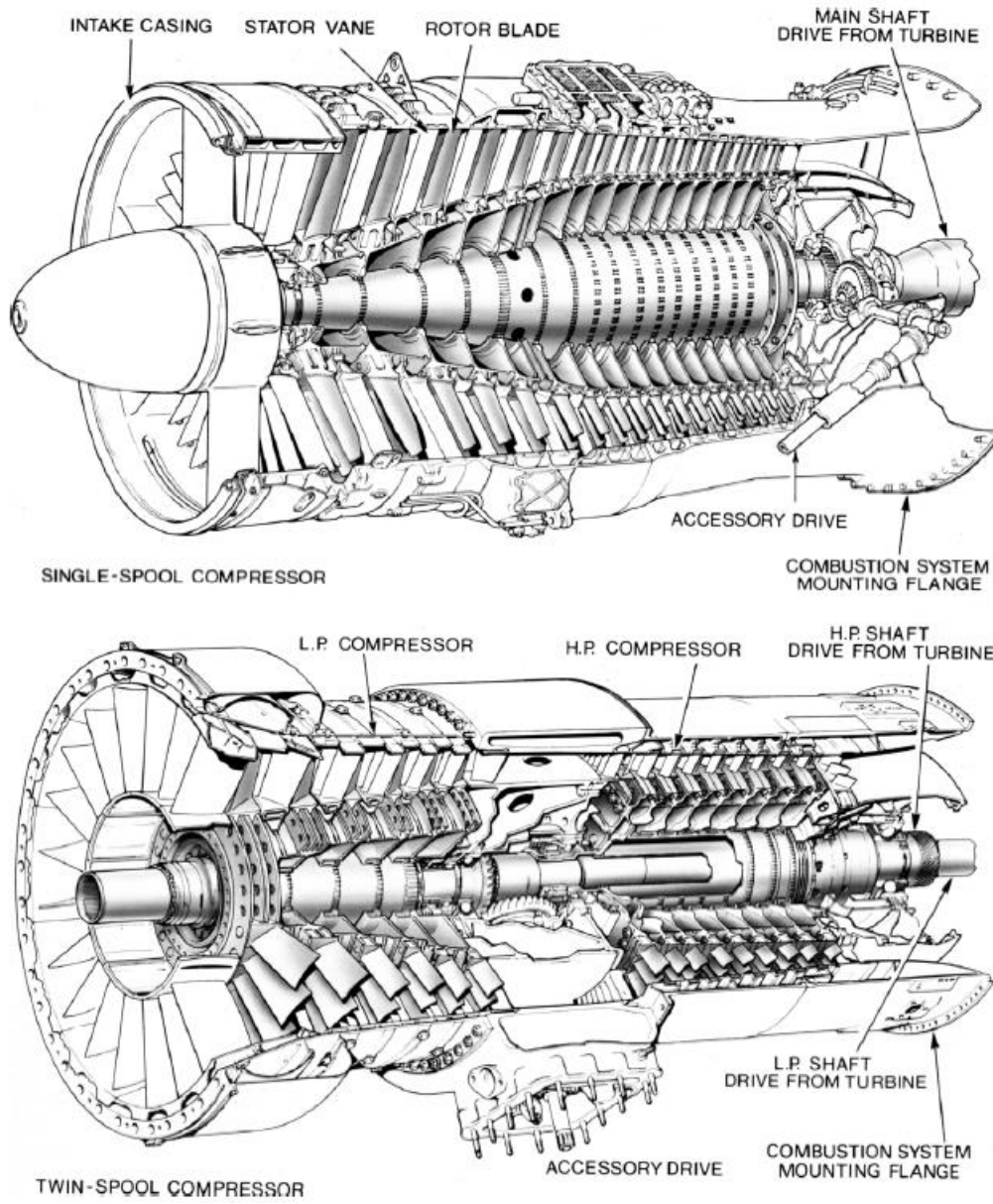
Fig 3.9: Typical axial flow compressors [27]

Since the early history of the gas turbine, the axial flow compressor had the potential for both higher-pressure ratio and higher efficiency than the centrifugal one. A main advantage for jet engines; was the larger flow rate possible for a given frontal area. These potential gains were realized as the result of intensive research into the aerodynamics of axial compressors. [28]

Early axial flow units had pressure ratios of 5:1 and required about 10 stages. Over the years, the overall pressure ratios available have risen dramatically, and some turbofan engines have pressure ratios exceeding 40:1. With the result that the number of stages for a given overall pressure ratio has been greatly reduced, there has been in consequence a reduction in engine weight for a specified level of performance, which is important for aircraft engines. [28]

3.2.1.2.1.   Operation Principle

The working fluid is initially accelerated by the rotor blades, and then decelerated in the stator blade passages wherein the kinetic energy transferred in the rotor is converted to static pressure. The process is repeated in as many stages as are necessary to yield the required overall pressure ratio. [28]
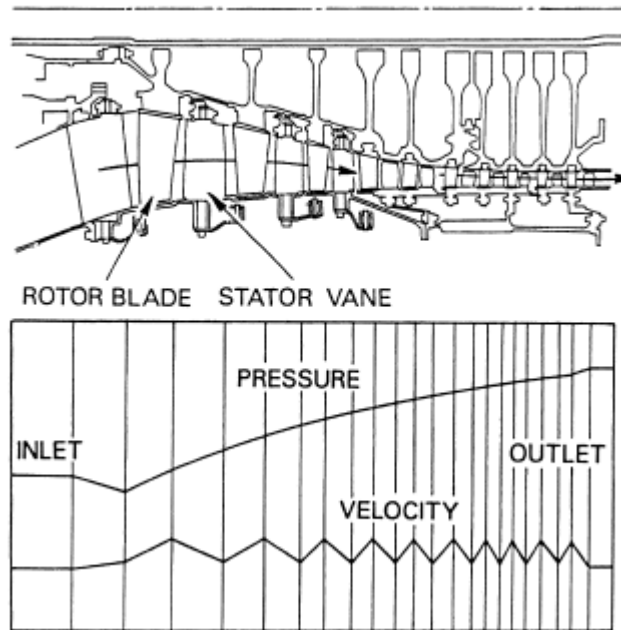
Fig 3.10: Pressure and velocity changes through an axial compressor [27]

The design of compressor blading is based on both aerodynamic theory and experiment is necessary, not only to prevent wasteful losses, but also to ensure a minimum of stalling troubles which are all too prevalent in axial compressors, especially if the pressure ratio is high. Stalling arises when the difference between the flow direction and the blade angle of incidence becomes excessive. The fact that the pressure gradient is acting against the flow direction is always a danger to the stability of the flow. [28]
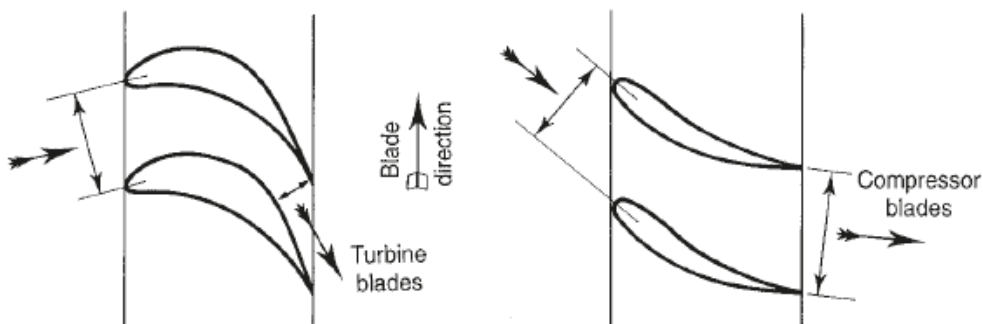
Fig 3.11: Comparison of typical forms of turbine and compressor rotor blades [28]

3.2.1.2.2. <u>Elementary theory</u>

Applying a steady flow energy equation to the rotor, and recognizing that the process can be assumed adiabatic, it can readily be seen that the power input is given by:

$$W = mC_p(T_{02} - T_{01})$$

Repeating with the stator, where the process can again be assumed adiabatic and there is zero work input, it follows that $T_{02} = T_{03}$. All the power is absorbed in the rotor, and the stator merely transforms kinetic energy to an increase in static pressure with the stagnation temperature remaining constant. The increase in stagnation pressure is accomplished wholly within the rotor and, in practice; there will be some decrease in stagnation pressure in the stator due to fluid friction. Losses will also occur in the rotor and the stagnation pressure rise will be less than would be obtained with an isentropic compression and the same power input. [28]
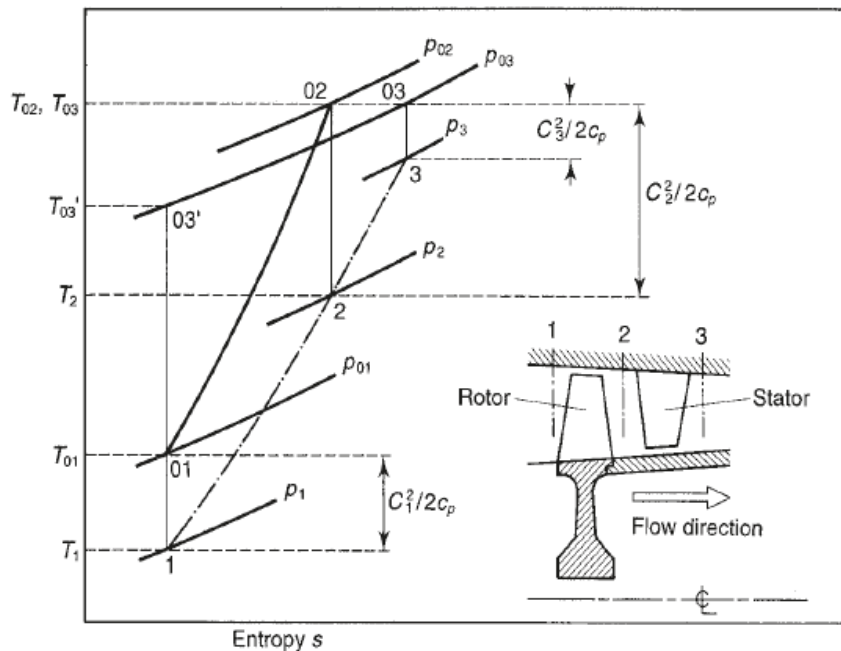
Fig 3.12: Compressor stage and T–s diagram [28]

The velocity vectors and associated velocity diagram for a typical stage are as follow:
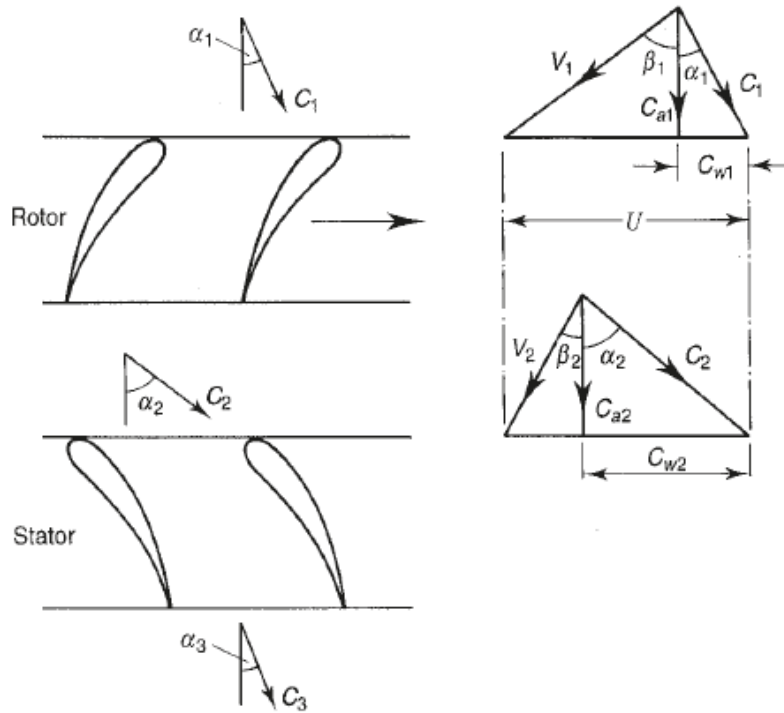
Fig 3.13: Velocity triangles for one stage [28]

The air approaches the rotor with a velocity C_1 at an angle α_1 from the axial direction; combining C_1 vectorially with the blade speed U gives the velocity relative to the blade V_1 at an angle β_1 from the axial direction.

After passing through the rotor, which increases the absolute velocity of the air, the fluid leaves the rotor with a relative velocity V_2 at an angle β_2 determined by the rotor blade outlet angle.

Assuming that the design is such that the axial velocity C_a is kept constant, the value of V_2 can be obtained and the outlet velocity triangle constructed by combining V_2 and U vectorially to give C_2 at angle α_2.

The air leaving the rotor at α_2 then passes to the stator where it is diffused to a velocity C_3 at angle α_3, typically the design is such that $C_3 \approx C_1$ and $\alpha_3 \approx \alpha_1$ so that the air is prepared for entry to another similar stage. [28]

Assuming that $C_{a1} = C_{a2} = C_{a3}$, two basic equations follow immediately from the geometry of the velocity triangles. These are:

$$\frac{U}{C_a} = \tan \alpha_1 + \tan \beta_1 \tag{3.8}$$

$$\frac{U}{C_a} = \tan \alpha_2 + \tan \beta_2 \tag{3.9}$$

By considering the change in angular momentum of the air in passing through the rotor, the following expression for the power input to the stage can be deduced:

$$W = mU(C_{w2} - C_{w1}) \tag{3.10}$$

Where C_{w1} and C_{w2} are the tangential components of fluid velocity before and after the rotor. This expression can be put in terms of the axial velocity and air angles to give:

$$W = mUC_a(\tan \alpha_2 - \tan \alpha_1) \tag{3.11}$$

It is more useful, however, to express the power in terms of the rotor blade air angles, b1 and b2. It can readily be seen that $(\tan \alpha_2 - \tan \alpha_1) = (\tan \beta_1 - \tan \beta_2)$. Thus, the power input is given by:

$$W = mUC_a(\tan \beta_1 - \tan \beta_2) \tag{3.12}$$

This input energy will be absorbed usefully in raising the pressure of the air and wastefully in overcoming various frictional losses. But regardless of the losses, or in other words of the efficiency of compression, the whole of this input will reveal itself as a rise in stagnation temperature of the air ΔT_{0s} [28]

$$\Delta T_{0s} = T_{03} - T_{01} = T_{02} - T_{01} = \frac{UC_a}{C_P}(\tan \beta_1 - \tan \beta_2) \tag{3.13}$$

The pressure rise obtained will be strongly dependent on the efficiency of the compression process. Denoting the isentropic efficiency of the stage by η_s, where $\eta_s = (T'_{03} - T_{01})/(T_{03} - T_{01})$, the stage pressure ratio is then given by: [28]

$$R_s = \frac{P_{03}}{P_{01}} = \left[1 + \frac{\eta_s \Delta T_{0s}}{T_{01}}\right]^{\gamma/(\gamma-1)} \tag{3.14}$$

3.2.2. The Combustion System

In the early days of gas turbines, the basic goals were high combustion efficiency, flame stability and the reduction of visible smoke; these goals were achieved by the early 1970s, with visible smoke virtually eliminated. [28]
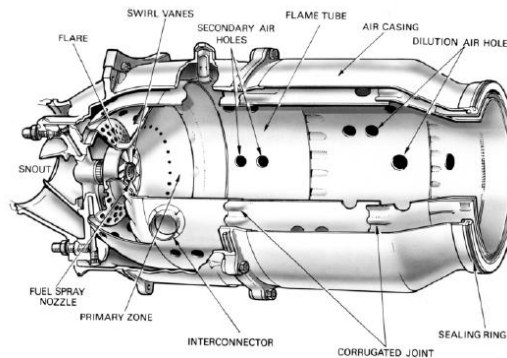
Fig 3.14: An early combustion chamber [28]

Combustion in the normal, open-cycle, gas turbine is a continuous process in which fuel is burned in the air supplied by the compressor; after the initial electrical spark that starts the process, the flame must be self-sustaining to keep the burning going. The designer has considerable latitude in choosing a combustor configuration, and the different requirements of aircraft and ground-based units with respect to weight, volume and frontal area can result in widely different solutions. In recent years, the effect of stringent restrictions on emissions of oxides of nitrogen (NO_x) has been the only major impact on combustion design, for both industrial and aircraft applications. [28]

3.2.2.1. Types of Combustors

3.2.2.1.1. Tubular Combustors

The earliest aircraft engines made use of can combustors, in which the air leaving the compressor is split into a number of separate streams, each supplying a separate chamber. These chambers are spaced around the shaft connecting the compressor and turbine, each chamber having its own fuel jet fed from a common supply line. This arrangement was well suited to engines with centrifugal compressors, where the flow was divided into separate streams in the diffuser. [28]
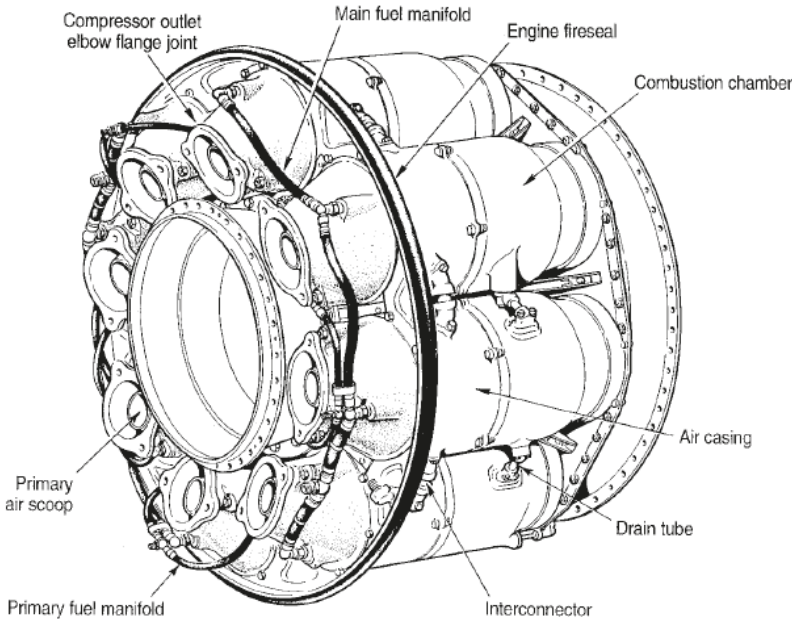
Fig 3.15: Can-type combustor [courtesy Rolls-Royce] [44]

3.2.2.1.2.   Annular Combustor

An annular combustion chamber is in the shape of a ring or a cylinder and where the entire space between the compressor and the turbine is used for combustion, the fuel is fed inside the tube with multiple fuel jet pumps spread in a ring shape around the entrance of the tube. [28]
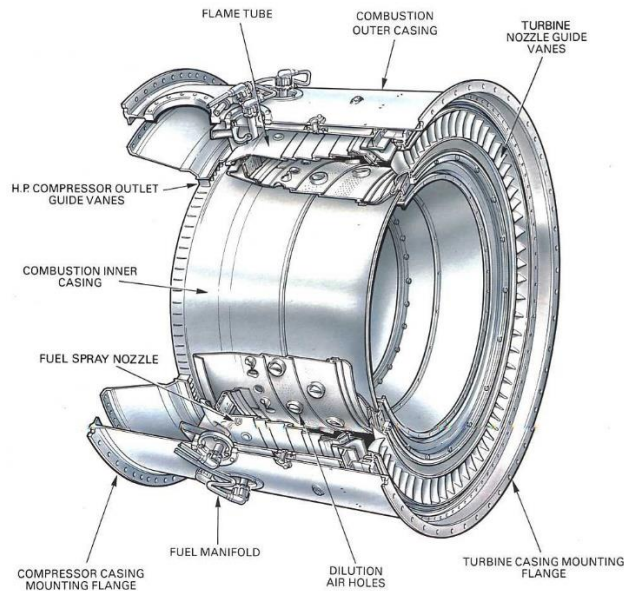
Fig 3.16: Annular-type combustor [44]

3.2.2.1.3.   Cannular Combustor

Separate combustion cans are still widely used in industrial engines, but recent designs make use of a **cannular** system, where individual flame tubes are uniformly spaced around an annular casing. [28]
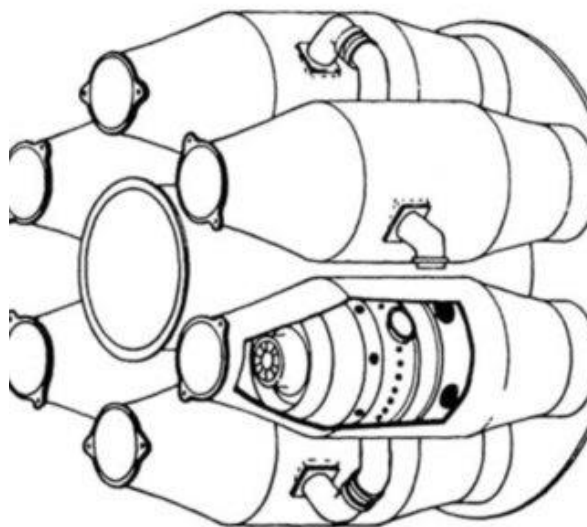
Fig 3.17: Cannular Combustor [44]
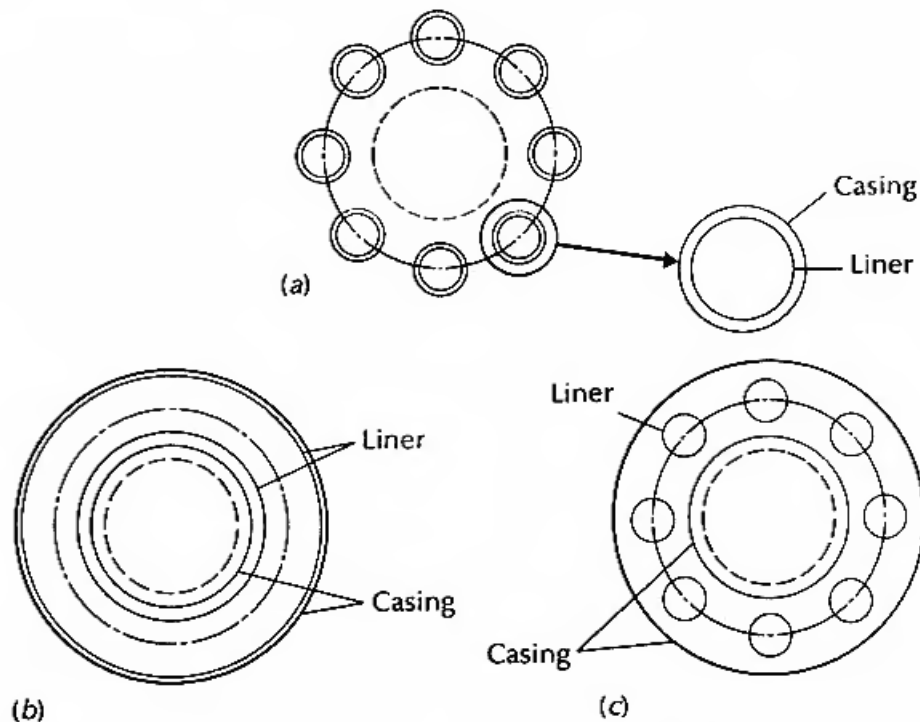
Fig 3.18: All Combustors types, (a) Can type (b) annular type (c) cannular type [44]

3.2.2.2. Important factors affecting combustor design

The temperature of the gases after combustion must be comparatively low to suit the highly stressed turbine materials and methods of blade cooling.

At the end of the combustion space, the temperature distribution must be of known form if the turbine blades are not to suffer from local overheating.

Combustion must be maintained in a stream of air moving with a high velocity in the region of 30~60 m/s, and stable operation is required over a wide range of air/fuel ratio from full load to idling conditions.

The formation of carbon deposits must be avoided, particularly the hard brittle variety. Small particles carried into the turbine in the high velocity gas stream can erode the blades and block cooling air passages.

In aircraft gas turbines, combustion must also be stable over a wide range of chamber pressure because of the substantial change in this parameter with altitude and forward speed.

Avoidance of smoke in the exhaust is of major importance for all types of gas turbine.

Although gas turbine combustion systems operate at extremely high efficiencies, they produce pollutants such as carbon monoxide (CO) and UHC and these must be controlled to very low levels. [28]

3.2.2.3. Combustion Process

Combustion of a liquid fuel occurs by mixing a spray of droplets with air, vaporization of the droplets, the breaking down of heavy hydrocarbons into lighter fractions, the intimate mixing of molecules of these hydrocarbons with oxygen molecules, and finally the chemical reactions themselves. A high temperature, such as is provided by the combustion of an approximately stoichiometric mixture, is necessary if all these processes are to occur sufficiently rapidly for combustion in a moving air stream to be completed in a small space. [28]

The overall air/fuel ratio is in the region of 100:1, while the stoichiometric ratio is approximately 15:1; the air should be introduced in three stages.
About 15–20 per cent of the air is introduced around the jet of fuel in the **primary zone** to provide the necessary high temperature for rapid combustion.
30 per cent of the total air is then introduced through holes in the flame tube in the **secondary zone** to complete the combustion. For high combustion efficiency, this air must be injected carefully at the right points in the process, to avoid chilling the flame locally and drastically reducing the reaction rate in that neighbourhood.
Finally, in the tertiary or **dilution zone** the remaining air is mixed with the products of combustion to cool them down to the temperature required at inlet to the turbine. Sufficient turbulence must be promoted so that the hot and cold streams are thoroughly mixed to give the desired outlet temperature distribution, with no hot streaks, which would damage the turbine blades. [28]

The zonal method of introducing the air cannot give a self-piloting flame in an air stream by itself, which is moving an order of magnitude faster than the flame speed in a burning mixture.
The second essential feature is therefore a recirculating flow pattern, which directs some of the burning mixture in the primary zone back onto the incoming fuel and air.
One way of achieving this for the fuel is injected in the same direction as the air stream, and the primary air is introduced through twisted radial vanes, known as **swirl vanes**, so that the resulting vortex motion will induce a region of low pressure along the axis of the chamber.
This vortex motion is sometimes enhanced by injecting the secondary air through short tangential chutes in the flame tube, instead of through plain holes. The net result is that the burning gases tend to flow towards the region of low pressure, and some portion of them is swept round towards the jet of fuel. [28]
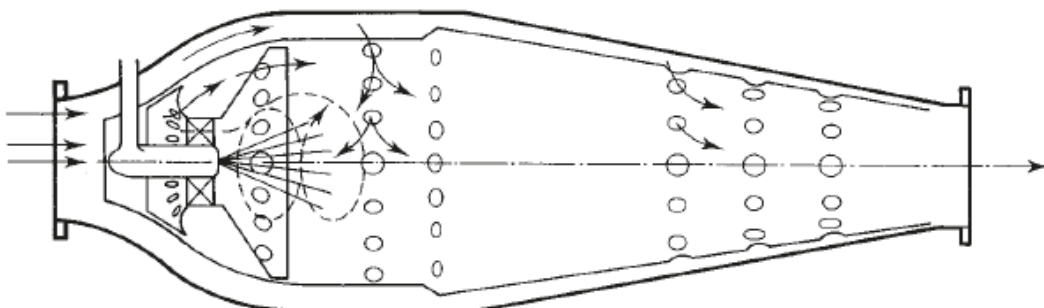
Fig 3.19: Combustion chamber with swirl vanes [28]
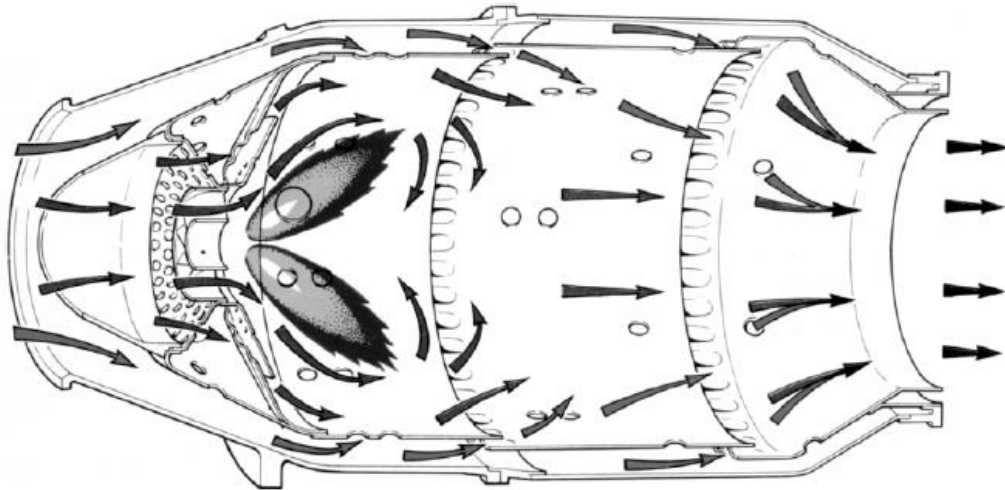
Fig 3.20: Flame stabilizing and general airflow pattern [28]

Many other solutions to the problem of obtaining a stable flame are possible. One is to dispense with the swirl vanes and achieve the recirculation by a careful positioning of holes in the flame tube downstream of a hemispherical baffle.

Another possible solution is using upstream injection that gives good mixing of the fuel and primary air. It is difficult to avoid overheating the fuel injector, however, and upstream injection is employed more for afterburners in the jet pipe of aircraft engines than in main combustion systems.

A third solution is that a vaporizer system wherein the fuel is injected at low pressure into walking-stick-shaped tubes placed in the primary zone. A rich mixture of fuel vapour and air issues from the vaporizer tubes in the upstream direction to mix with the remaining primary air passing through holes in a baffle around the fuel supply pipes. [28]
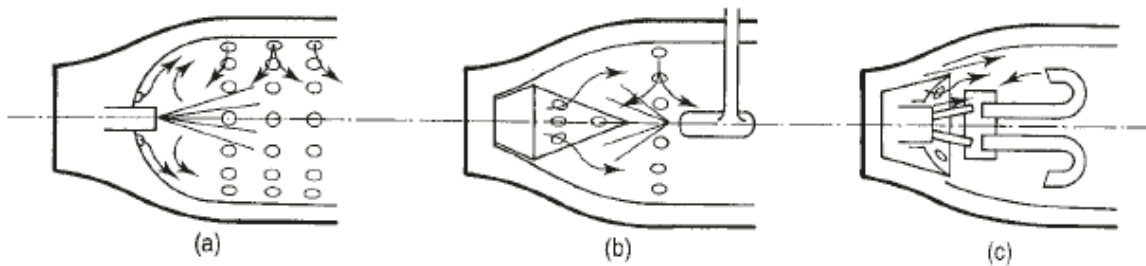
Fig 3.21: Methods of flame stabilization [28]

3.2.3. Turbines

As with the compressor, there are two basic types of turbine: axial flow and radial flow. The vast majority of gas turbines use the axial flow turbine so most of following study is devoted to the theory of this type. [28]
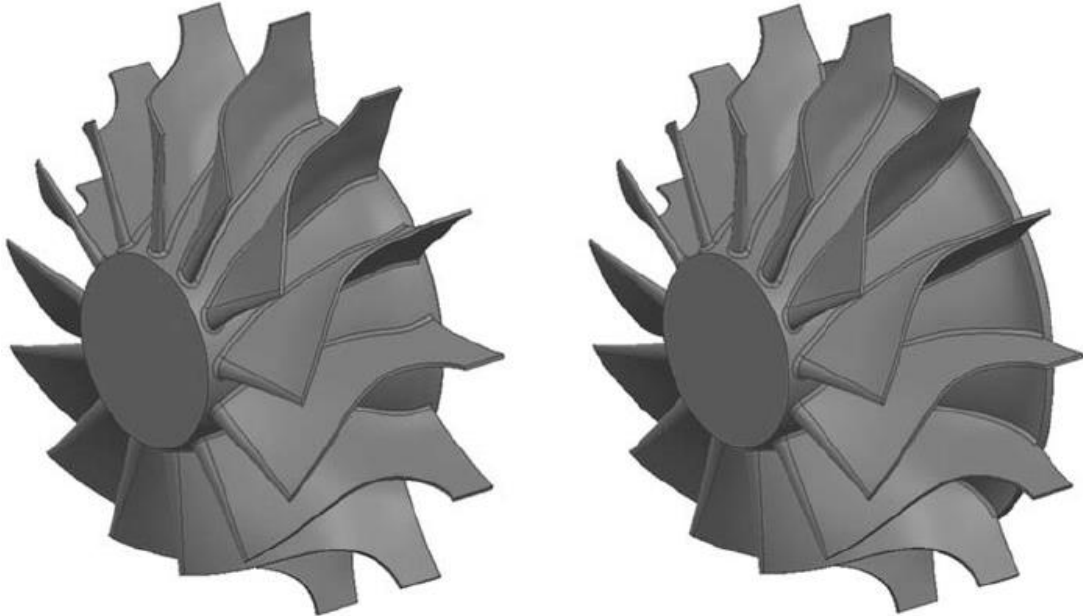
Fig 3.22: Typical Radial Turbine [48]
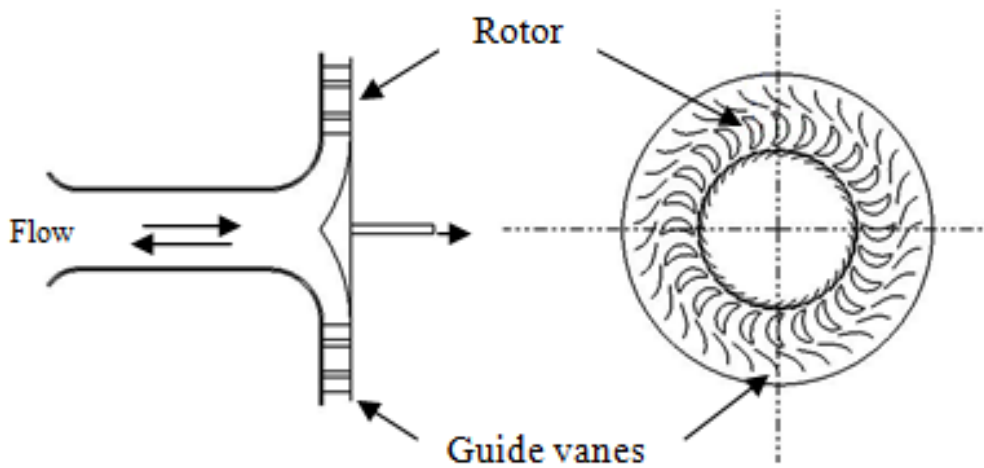
Fig 3.23: Radial Turbine schematic [49]
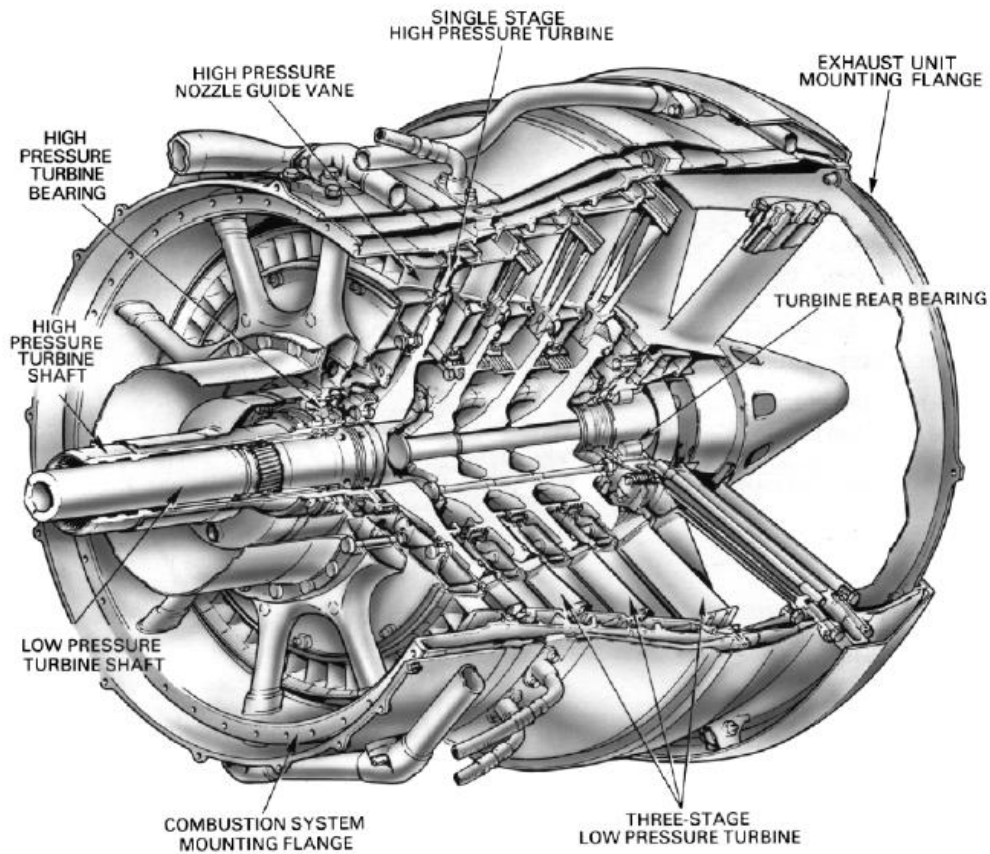
Fig 3.24: A twin turbine and shaft arrangement [44]
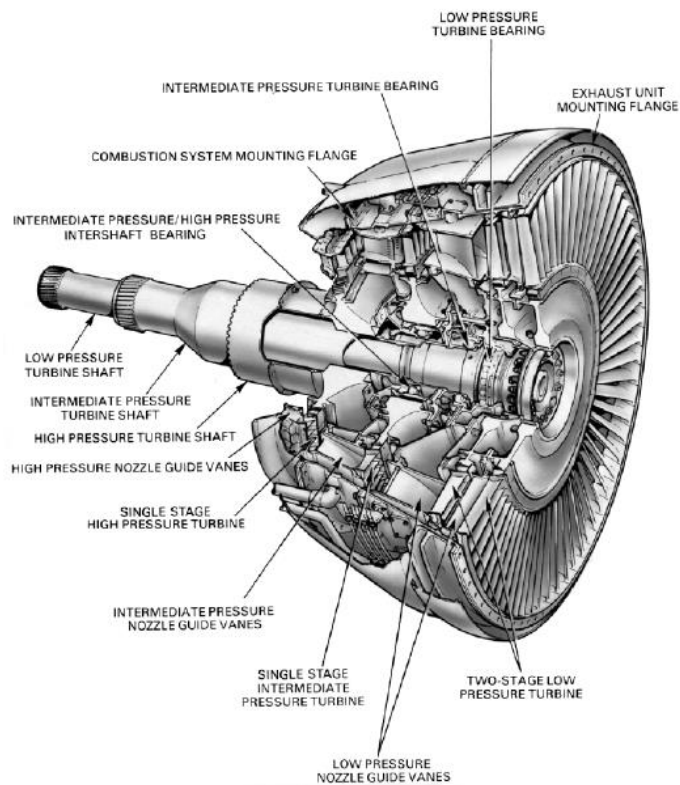
Fig 3.25: A triple turbine and shaft arrangement. [44]

The turbine depends for its operation on the transfer of energy between the combustion gases and the turbine. This transfer is never per cent because of thermodynamic and mechanical losses. [27]

The gas is expanded by the combustion process, forcing its way into the converging shaped discharge nozzles of the turbine, where it will be accelerated. At the same time, the gas flow is given a "spin" or in the direction of rotation of the turbine blades by the nozzle guide vanes. On impact with the blades, energy is absorbed which causes the turbine to rotate at high speed and so provide the power for driving the turbine shaft and compressor.
The rate of gas flow and the energy change of the gas between the inlet and the outlet of the turbine blades controls the torque applied to the turbine. The design of the turbine is such that the flow will lose its spin at exit from the turbine and will be straightened out to give an axial flow into the exhaust system. Excessive residual whirl reduces the efficiency of the exhaust system and tends to produce jet pipe vibration, which has a detrimental effect on the exhaust cone supports and struts. [27]

3.2.3.1. **Elementary theory of axial flow turbine**

The gas enters the row of nozzle blades with a static pressure and temperature P_1, T_1 and a velocity C_1, is expanded to P_2, T_2 and leaves with an increased velocity C_2 at an angle α_2. The rotor blade inlet angle will be chosen to suit the direction β_2 of the gas velocity V_2 relative to the blade at the inlet. β_2 And V_2 are found by vectorial subtraction of the blade speed U from the absolute velocity C_2. After being deflected and usually further expanded in the rotor blade passages, the gas leaves at P_3, T_3 with relative velocity C_3 at angle β_3. Vectorial addition of U yields the magnitude and direction of the gas velocity at exit from the stage, C_3 and α_3. α_3 is known as the **swirl angle**.
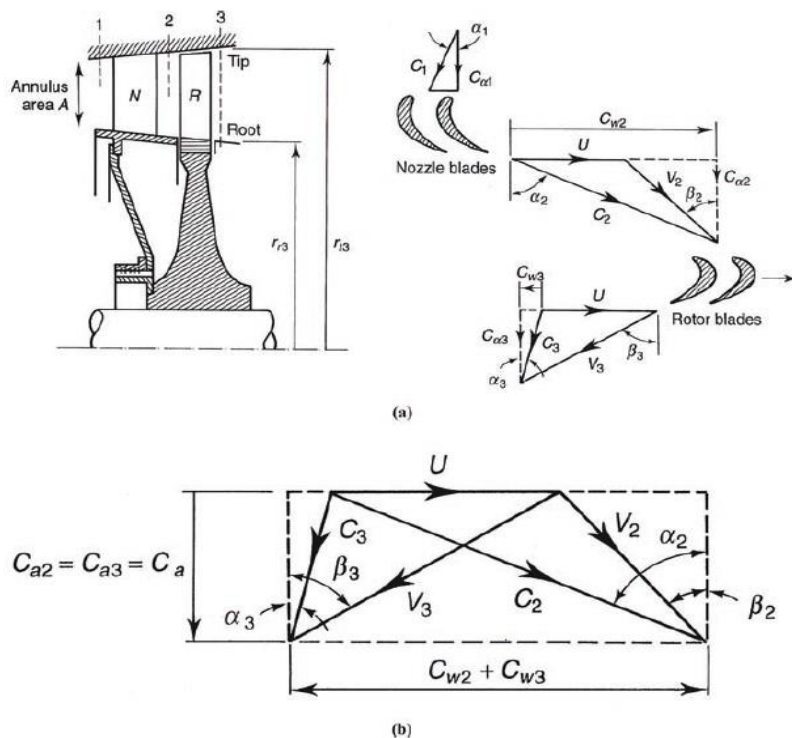
Fig 3.26: (a) Axial flow turbine stage; (b) Velocity diagram [28]

When the velocity triangles are superimposed in the usual way, we have the velocity diagram for the stage as shown previously.

The geometry of the diagram gives immediately the relations

$$\frac{U}{C_a} = \tan \alpha_2 - \tan \beta_2 = \tan \beta_3 - \tan \alpha_3 \tag{3.15}$$

Applying the principle of angular momentum to the rotor, the stage work output per unit mass flow is:

$$W_s = U(C_{w2} + C_{w3}) = UC_a(\tan \alpha_2 + \tan \alpha_3) \tag{3.16}$$

The Work in terms of the gas angles associated with the rotor blade will be expressed as:

$$W_s = UC_a(\tan \beta_2 + \tan \beta_3) \tag{3.17}$$

Note that the 'work-done factor' required in the case of the axial compressor is unnecessary here. This is because in an accelerating flow the effect of the growth of the boundary layer along the annulus walls is much less than when there is a decelerating flow with an adverse pressure gradient.

From the steady flow energy equation, we have $W_s = C_p \Delta T_{0s}$ where the gradient ΔT_{0s} is the stagnation temperature drop in the stage, and hence:

$$C_p \Delta T_{0s} = UC_a(\tan \beta_2 + \tan \beta_3) \tag{3.18}$$

When the stage inlet and outlet velocities are equal, i.e. $C_1 = C_3$, the previous equation also gives the static temperature drop in the stage ΔT_s.

$$\Delta T_{0s} = 8.71 \left(\frac{U}{100}\right)\left(\frac{C_a}{100}\right)(\tan \beta_2 + \tan \beta_3) \tag{3.19}$$

$$\Delta T_{0s} = \eta_s T_{01} \left[1 - \left(\frac{1}{P_{01}/P_{03}}\right)^{(\gamma-1)/\gamma}\right] \tag{3.20}$$

The loss coefficient for the nozzle blades may be defined by:

$$\lambda_N = \frac{p_{01} - p_{02}}{p_{02} - p_2} = \frac{(p_{01}/p_{02}) - 1}{1 - (p_2/p_{02})} \tag{3.21}$$

Now:

$$\frac{p_{01}}{p_{02}} = \frac{p_{01}}{p_2}\frac{p_2}{p_{02}} = \left(\frac{T_{01}}{T'_2}\right)^{\gamma/(\gamma-1)}\left(\frac{T_2}{T_{02}}\right)^{\gamma/(\gamma-1)} = \left(\frac{T_2}{T'_2}\right)^{\gamma/(\gamma-1)} \tag{3.22}$$

Hence:

$$\lambda_N = \frac{(T_2/T'_2)^{\gamma/(\gamma-1)} - 1}{1 - (T_2/T_{02})^{\gamma/(\gamma-1)}} \tag{3.23}$$

And Finally:

$$\lambda_N = \frac{\left[1+\frac{T_2-T\prime_2}{T\prime_2}\right]^{\gamma/(\gamma-1)}-1}{1-\left[1+\frac{T_2-T_{02}}{T_{02}}\right]^{\gamma/(\gamma-1)}}$$

(3.24)
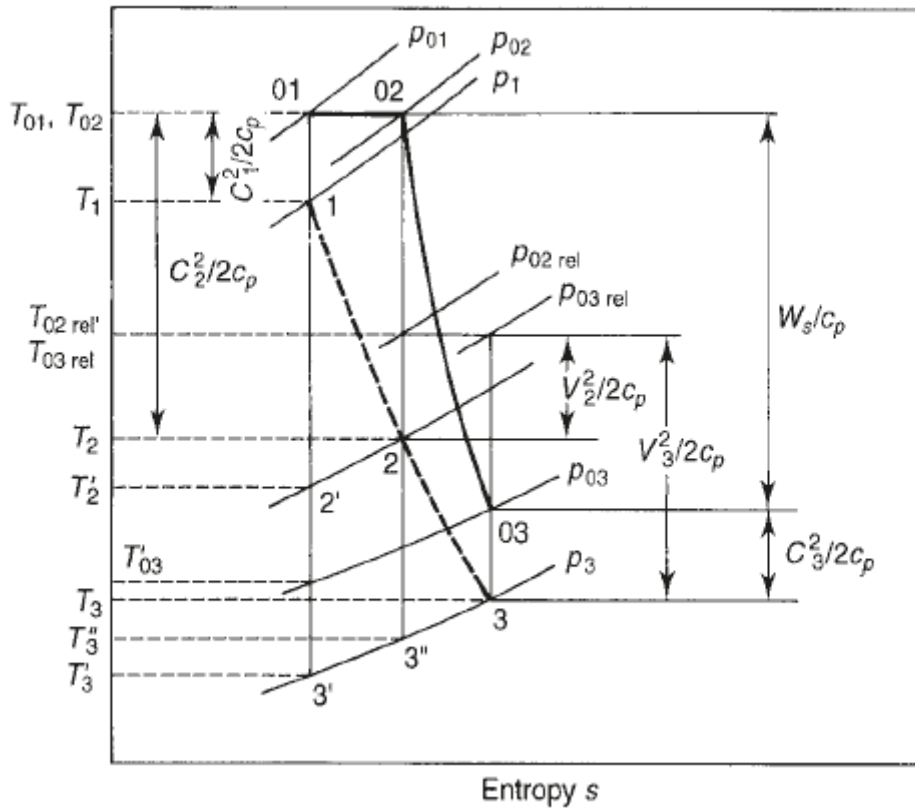
3.27: T-S Diagram [28]

3.3. Cussons P9005
Introduction

Gas turbines are becoming increasingly used as power plants for a wide variety of applications around the world. Cussons have designed and manufactured educational gas turbines since 1970 and the latest version incorporates many improvements. Cussons P9005 Gas Turbine Unit is now offered as a full two-shaft machine with built in starting equipment, power absorption system and data logging option. It provides the means for carrying out an extensive programme of experiments in gas turbine technology using only the instrumentation provided. [29]

Particular features of the Two Shaft Gas Turbine Unit are its versatility, ease of operation, safety and low noise level. All instrumentation and controls are carried on the panel, which displays the flow diagram with a clear indication of all measurements identified, by symbols and illuminated tell-tales. Measurement of power turbine torque is by calibrated electrical dynamometer. [29]

Fig 3.28: Cussons Technology - P9005 - Two-Shaft Gas Turbine [29]

The Two Shaft Gas Turbine employs a centrifugal compressor and a radial turbine, arranged back to back on a common shaft, which together with a gas-fuelled combustion chamber operating on propane or butane, form the gas generator. [29]

The complete unit is built on a robust steel chassis mounted on castors, carrying a melamine laminate instrument panel and steel cladded panels. The overall dimensions permit the unit to pass through any normal doorway and special attention has been paid to the requirements of easy installation, low noise level, convenience of operation and safety. [29]

3.3.1. General Description

Cussons P9005 Two Shaft Gas Turbine Unit is a self-contained equipment with the gas generator , power turbine, loading unit, instrumentation and controls all housed on a castor mounted framework, giving a degree of mobility. Thus, the Unit can be tidily stored when not in use and then readily positioned near the required services, when it has to run. The services required are: [29]

a) The Unit requires to be positioned under an exhaust duct so that the gas turbine exhaust products can be extracted if prolonged running is contemplated.

b) A cooling water supply is required for the oil cooler.

c) A drain is required to cater for the oil cooling water.

d) A single-phase electrical power supply.

e) A suitable gaseous fuel supply.

The Gas Turbine Unit has been tropicalized and is generally suitable for use in ambient temperatures of up to 40ºC and ambient conditions of up to 80% relative humidity. [29]

3.3.2. Gas Generator

The single shaft gas generator comprises a centrifugal compressor, a tubular combustion chamber and a radial turbine (Fig. 2, Refs. B, C and D). The compressor and gas generator turbine are close coupled with the shaft located in a central housing by hydrodynamic bearings. The gas generator consists of a single stage centrifugal compressor, a single gaseous-fuelled combustion chamber and a single stage radial turbine. The compressor and turbine are mounted back to back on a short shaft supported in a journal bearing. [29]

3.3.2.1. Compressor

The compressor is a single sided centrifugal type with a multi-bladed aluminium alloy impeller, and an unbladed diffuser volute casing with tangential exit. [29]

3.3.2.2. Combustion Chamber

The single vertical combustion chamber is of conventional design, incorporating a flame tube with central fuel injector for gaseous fuels. The combustion chamber is shown in Fig. 4 Inner Combustion Chamber. The flame tube divides the incoming airflow into 'primary' and 'secondary' air, with a stabilised combustion zone and tertiary dilute ion air. A spark igniter is mounted in the side of the combustion chamber for starting purposes.

To allow a compressor air bleed to be taken from the chamber an air valve is incorporated in the top of the combustion chamber outer casing.

The combustion chamber and the associated instrumentation are designed for use with propane C_3H_8 but may be used with a mixture of propane and butane C_4H_{10} if the pressure in the supply bottle is sufficient to inject the fuel into the combustion chamber. [29]

3.3.2.3. Turbine

The gas generator turbine is a single inward flow radial design with a 90mm diameter and a volute type inlet casing operating over the range 170 to 600 rps and developing a maximum power of approximately 4 kW. [29]

3.3.3. Power Turbine

The power turbine is also, as with the gas generator, based on an automotive turbocharger, but in this case, the compressor has been replaced with a toothed pinion to provide a belt drive to the electric generator. [29]
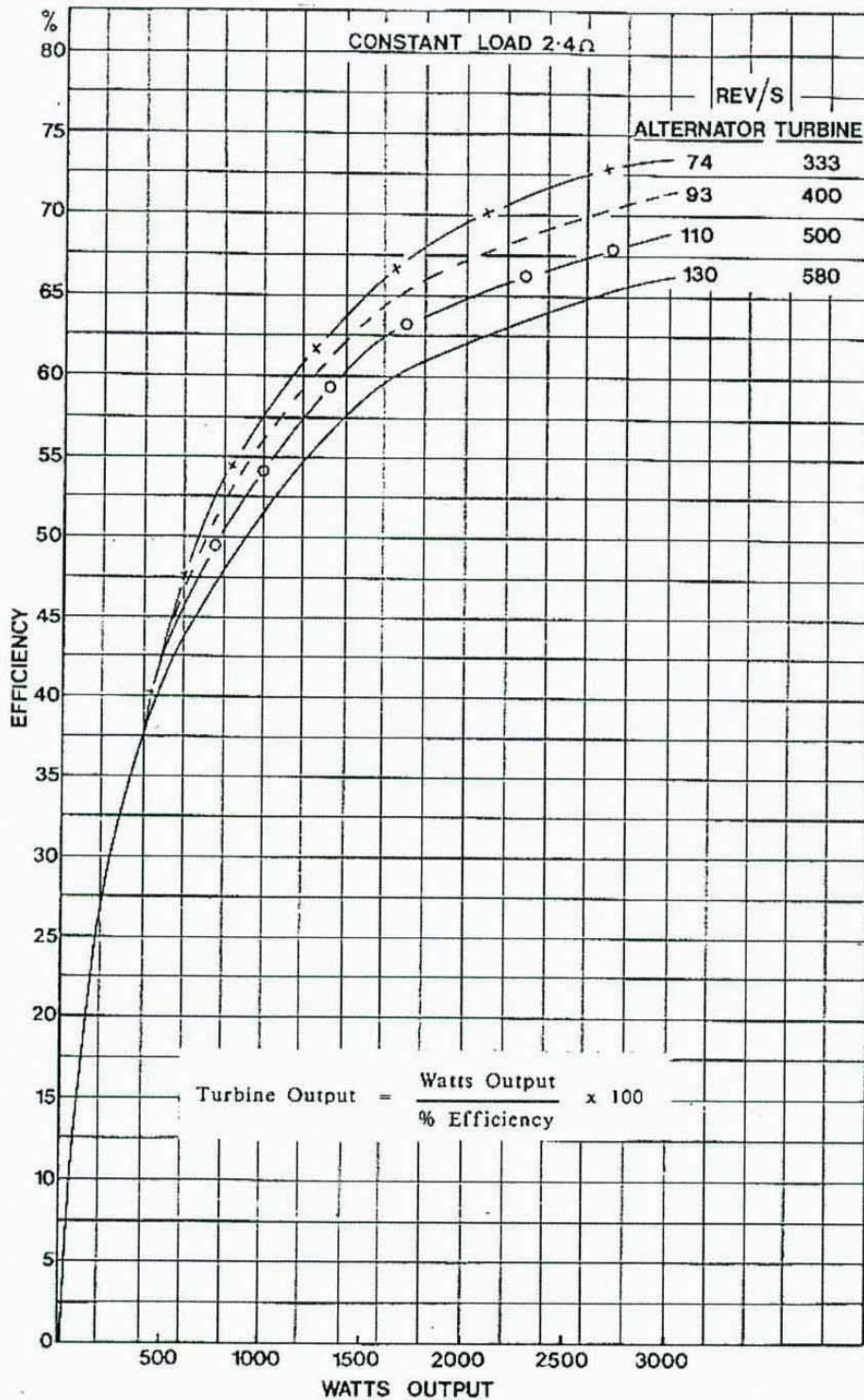
Fig 3.29: Efficiency graph P9005 [29]
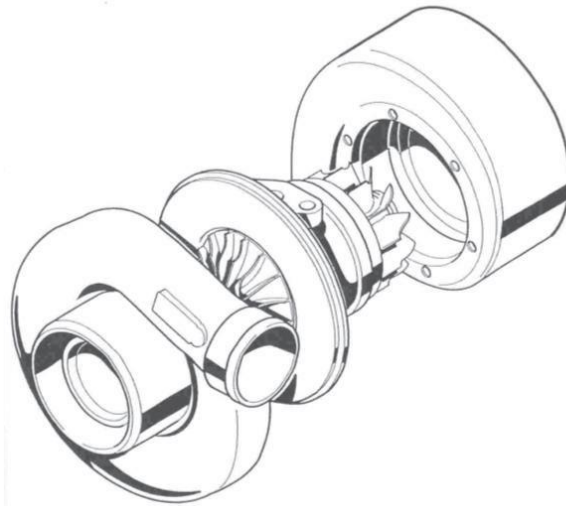
Fig 3.30: Compressor and gas generator turbine unit [51]
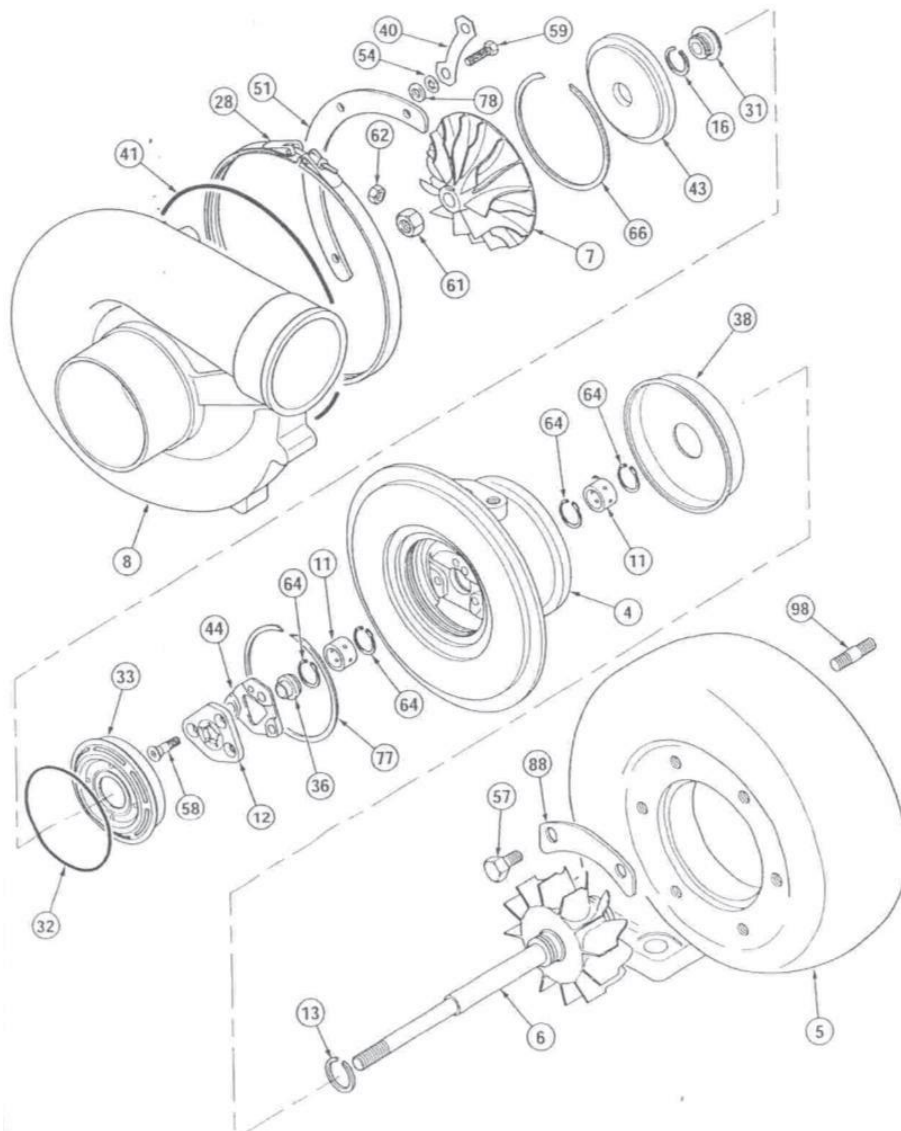
Fig 3.31: Exploded view of compressor and gas generator turbine unit [51]

3.3.4. Instrumentation

Instrumentation for both operational and experimental measurement is integrated into the coloured schematic diagram on the instrument and control panel. [29]

3.3.4.1. Temperature

All temperatures are measured using NiCr/NiAl type K thermocouples. The seven temperature channels are: [29]

T1 Air inlet temperature
T2 Gas generator compressor exit temperature
T3 Gas generators turbine inlet temperature
T4 Power turbine inlet temperature
T5 Power turbine exit temperature
Tg Gas (fuel) temperature
To Oil (lubricant) temperature

3.3.4.2. Pressure

Conventional Bourdon tube pressure gauges are used to measure all pressures other than the combustion chamber pressure loss (p2 – p3) which is obtained from a differential mercury manometer. Snubbers are fitted in the P2, P3 and P4 pressure lines. [29]

3.3.4.3. Airflow Rate

The airflow is measured a t the inlet to the gas generator compressor by a Pitot-reverse Pitot tube connected to a differential manometer on the front panel. [29]

3.3.4.4. Fuel Flow Rate

A conventional tapered tube and float flow meter calibrated for gaseous propane at 150 Kpa.g and 15°C, is used to measure the fuel flow rate. If a butane-propane fuel mixture is used then the flow meter readings can be corrected by multiplying by the square root of the quotient of the densities of propane and the mixture of propane/butane: [29]

$$\dot{m}_{mixture} = \dot{m}_{reading}\sqrt{\frac{\rho_{propane}}{\rho_{mixture}}} \qquad (3.25)$$

If the readings are taken at a pressure of 150 Kpa (1.5 bar) and a temperature of 15°C (which are the calibration conditions for the flow meter) then the multiplicative correction factor is:

$$\sqrt{\left[\frac{\rho_{propane}}{\rho_{mixture}}\right]} = \sqrt{\left[\frac{44}{44P+58B}\right]} \qquad (3.26)$$

Where P is fraction of propane in mixture and B is fraction of butane in mixture

P	B	Correction Factor
1.0	0.0	1.000
0.9	0.1	0.984
0.8	0.2	0.970
0.7	0.3	0.955
0.6	0.4	0.942
0.5	0.5	0.929
0.4	0.6	0.916
0.3	0.7	0.904
0.2	0.8	0.893
0.1	0.9	0.882

Two Shaft Gas Turbine Test Results

FUEL FLOW			AIR FLOW		OIL	PRESSURES			TEMPERATURES					SPEEDS		POWER OUTPUT			
Mf	Tg	Pg		P-RP	Toil	P3	P4	P2-P3	T1	T2	T3	T4	T5	G.G	P.T	Voltage	Current	Correct	Power
gram/sec	°C	KPa	g/sec	mm H₂O	°C	bar	bar	mm Hg	°C	°C	°C	°C	°C	rev/sec	rev/sec	V	A	Factor	WATTS
2.34	18.26	154	148.72		64.40	0.69	0.15		18.99	93.98	726.07	624.76	501.95	1514.16	612.11	64.50	29.80		1922.0
2.12	18.47	148	134.45		65.63	0.58	0.13		18.77	83.59	713.38	622.31	505.86	1398.44	608.59	54.69	25.62		1401.2
1.87	19.06	150	120.53		62.89	0.48	0.10		19.17	74.45	699.71	615.97	500.73	1281.25	602.73	44.78	21.28		952.7
1.69	19.56	152	107.92		60.50	0.40	0.09		19.31	67.07	700.20	618.65	501.95	1179.69	611.33	35.84	17.26		618.6
1.54	19.92	154	96.51		58.64	0.33	0.08		19.25	60.94	712.16	630.13	511.23	1085.45	608.01	27.42	13.35		366.1
1.43	21.09	150	83.91		56.45	0.27	0.06		19.54	55.27	747.31	656.25	529.05	977.05	608.59	14.92	7.30		108.9

T3 OVER TEMPERATURE SETTING   900°C

BELT TENSIONING RAM PRESSURE   KPa

PITOT - REVERSE PITOT CONSTANT

AIR FLOW CALIBRATION EQUATION:-

$M_{air} = 11.51\{h\}^{0.5}$

DATE TEST COMPLETED

TEST ENGINEERS SIGNATURE

Remarks

4. The final state of combustion and numerical analysis of the chemical reaction

4.1. The Global Equation of Combustion:

Considering all chemical substances appear in the reaction the equation can we written as follow:

$$r_c C_n H_m + \left(n + \frac{m}{4}\right)(O_2 + 3.76N_2) \xrightarrow{yields} n_1 CO_2 + n_2 H_2O + n_3 O_2 + n_4 N_2 + n_5 NO + n_6 OH$$
$$+ n_7 CO + n_8 H_2 + n_9 O + n_{10} H + n_{11} N$$
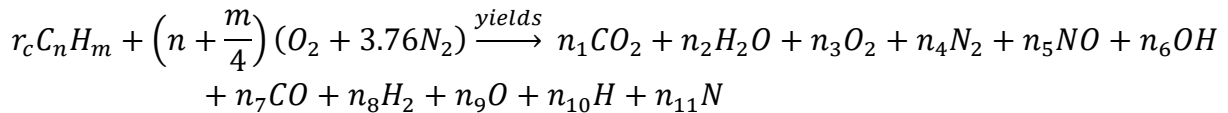
4.2. Calculating the number of moles of combustion products:

To calculate the number of moles of the reaction product, we use a set of equations as follow:

4.2.1. Conservation of chemical species:

Carbone conservation:

$$n \times r_c = n_1 + n_7$$

Hydrogen conservation:

$$m \times r_c = 2n_2 + n_6 + 2n_8 + n_{10}$$

Oxygen conservation:

$$2 \times \left(n + \frac{m}{4}\right) = 2n_1 + n_2 + 2n_3 + n_5 + n_6 + n_7 + n_9$$

Nitrogen conservation:

$$7.52 \times \left(n + \frac{m}{4}\right) = 2n_4 + n_5 + n_{11}$$

Additionally there are 7 dissociation equations:
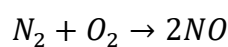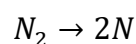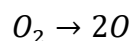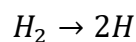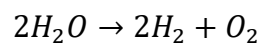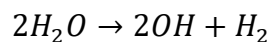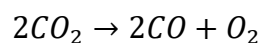
$$2CO_2 \rightarrow 2CO + O_2$$
$$2H_2O \rightarrow 2OH + H_2$$
$$2H_2O \rightarrow 2H_2 + O_2$$
$$H_2 \rightarrow 2H$$
$$O_2 \rightarrow 2O$$
$$N_2 \rightarrow 2N$$
$$N_2 + O_2 \rightarrow 2NO$$

To calculate the equilibrium constant for these elementary reactions we use the following set of equations:

$$K_p[17] = \frac{P_{CO}^2 \times P_{O_2}}{P_{CO_2}{}^2} \tag{4.1}$$

With the partial pressure for each chemical species being:

$$P_i = \frac{n_i}{\sum n_i} \times P \tag{4.2}$$

Where P is the total pressure, and N_t defined as:

$$N_t = \sum n_i \tag{4.3}$$

By combining the previous equations with the global equation, we get:

$$K_p[17] = \frac{n_7{}^2 \times n_3}{n_1{}^2} \times \frac{P}{N_t} \tag{4.4}$$

The same goes for the 6 other equations:

$$K_p(14) = \frac{n_6{}^2 \times n_8}{n_2{}^2} \times \frac{P}{N_t} \tag{4.5}$$

$$K_p(15) = \frac{n_8{}^2 \times n_3}{n_2{}^2} \times \frac{P}{N_t} \tag{4.6}$$

$$K_p(16) = \frac{n_{10}{}^2}{n_8} \times \frac{P}{N_t} \tag{4.7}$$

$$K_p(17) = \frac{n_9{}^2}{n_3} \times \frac{P}{N_t} \tag{4.8}$$

$$K_p(18) = \frac{n_{11}{}^2}{n_4} \times \frac{P}{N_t} \tag{4.9}$$

$$K_p(19) = \frac{n_5{}^2}{n_3 \times n_4} \times \frac{P}{N_t} \tag{4.10}$$

For a Constant value of T, we obtain the following set of 12 equations with 12 unknowns

$$f_1 = n_1 + n_7 - (n \times r_c)$$

$$f_2 = 2n_2 + n_6 + 2n_8 + n_{10} - (m \times r_c)$$

$$f_3 = 2n_1 + n_2 + 2n_3 + n_5 + n_6 + n_7 + n_9 - \left(2 \times \left(n + \frac{m}{4}\right)\right)$$

$$f_4 = 2n_4 + n_5 + n_{11} - \left(7.52 \times \left(n + \frac{m}{4}\right)\right)$$

$$f_5 = (n_7{}^2 \times n_3) - \left(\frac{K_p[17]}{P} \times N_t \times n_1{}^2\right)$$

$$f_6 = (n_6{}^2 \times n_8) - \left(\frac{K_p[23]}{P} \times N_t \times n_2{}^2\right)$$

56

$$f_7 = (n_8{}^2 \times n_3) - \left(\frac{K_p[1]}{P} \times N_t \times n_2{}^2\right)$$

$$f_8 = n_{10}^2 - \left(\frac{K_p[31]}{P} \times N_t \times n_8\right)$$

$$f_9 = n_9^2 - \left(\frac{K_p[32]}{P} \times N_t \times n_3\right)$$

$$f_{10} = n_9^2 - \left(\frac{K_p[32]}{P} \times N_t \times n_3\right)$$

$$f_{11} = n_{11}^2 - \left(\frac{K_p[33]}{P} \times N_t \times n_4\right)$$

$$f_{12} = n_5^2 - \left(\frac{K_p[30]}{P} \times n_3 \times n_4\right)$$

In order to solve this system we will be using numerical methods like 'Newton-Raphson'
We will first need to linearize our equations for that method to work.

4.3. <u>Enthalpy of the chemical reaction</u>

For an adiabatic reaction, the following is true:

$$Q = 0 \tag{4.11}$$

Because the combustion occurs at a constant pressure, then:

$$W = 0 \tag{4.12}$$

For the case of an open system, we have:

$$W + Q = \Delta H \tag{4.13}$$

Which is why, for an adiabatic and isobar reaction:

$$\Delta H = 0 \tag{4.14}$$

From the previous equations, we can get the adiabatic temperature of combustion T_{ad} as follow:

$$f(T) = \Delta H = H_P(T_{ad}) - H_R(T_i) \tag{4.15}$$

4.3.1. Calculating the reactants enthalpy

The reactant enthalpy can be calculated as follow:

$$H_r = r_c\left(H_{fuel}\right) + \left(n + \frac{m}{4}\right) H_a \tag{4.16}$$

And H_{fuel} is the enthalpy of the fuel at the initial temperature and can be calculated as follow:

$$H_{fuel} = \Delta H_f^0 + H_{fuel,S}(T) \tag{4.17}$$

And H_a is the air enthalpy.

4.3.2. Calculating the reaction products enthalpy

Once the number of moles is determined with the previous method the product enthalpy can be calculated as follow:

$$H_p = n_1 \times H_{CO_2} + n_2 \times H_{H_2O} + n_3 \times H_{O_2} + n_4 \times H_{N_2} + n_5 \times H_{NO} + n_6 \times H_{OH} + n_7 \times H_{CO} + n_8 \times H_{H_2} + n_9 \times H_O + n_{10} \times H_H + n_{11} \times H_N \tag{4.18}$$

4.4. Calculating the adiabatic combustion temperature

Using bisection method, we can find the adiabatic temperature of combustion by following these steps:

For a T_{ad} we chose a temperature interval $[T_1, T_2]$

We calculate this set of equations:

$$\begin{cases} f(T_1) = H_P(T_1) - H_R(T_i) \\ f(T_2) = H_P(T_2) - H_R(T_i) \end{cases}$$

We verify the following conditions:

If $f(T_1) \times f(T_2) > 0$ then we need to change the interval $[T_1, T_2]$.

If $f(T_1) \times f(T_2) < 0$ then T_{ad} is in the interval $[T_1, T_2]$.

We then calculate:

$$T_{ad}^0 = \frac{T_1 + T_2}{2}$$

We calculate:

$$f(T_{ad}^0) = H_P(T_{ad}^0) - H_R(T_i)$$

We then verify the following conditions:

If $f(T_{ad}^0) \times f(T_2) < 0$ then T_{ad}^1 is in the interval $[T_1, T_{ad}^0]$.

And $T_{ad}^1 = \frac{T_{ad}^0 + T_1}{2}$

Else T_{ad}^1 is in the interval $[T_{ad}^0, T_2]$.

And $T_{ad}^1 = \frac{T_{ad}^0 + T_2}{2}$

We repeat the previous steps until we get:

$\left| T_{ad}^i T_{ad}^{i-1} \right| \leq \varepsilon$

Where ε is the tolerated error.

And finally, we get:

$T_{ad} \approx T_{ad}^i$

4.5. Numerical Methods
4.5.1. Gauss-Seidel Method
4.5.1.1. General Introduction:

In certain cases, such as when a system of equations is large, iterative methods of solving equations are more advantageous. Elimination methods, such as Gaussian elimination, are prone to large round-off errors for a large set of equations. Iterative methods, such as the Gauss-Seidel method, give the user control of the round-off error. In addition, if the physics of the problem are well known, initial guesses needed in iterative methods can be made more judiciously leading to faster convergence. [31]

4.5.1.2. The algorithm for the Gauss-Seidel method:

Given a general set of **n** equations and **n** unknowns, we have:

$$a_{11}x_1 + a_{12}x_2 + a_{13}x_3 + \cdots + a_{1n}x_n = c_1$$

$$a_{21}x_1 + a_{22}x_2 + a_{23}x_3 + \cdots + a_{2n}x_n = c_2$$

$$a_{31}x_1 + a_{32}x_2 + a_{33}x_3 + \cdots + a_{3n}x_n = c_3$$

$$.\qquad\qquad.$$

$$.\qquad\qquad.$$

$$.\qquad\qquad.$$

$$a_{n1}x_1 + a_{n2}x_2 + a_{n3}x_3 + \cdots + a_{nn}x_n = c_n$$

If the diagonal elements are non-zero, each equation is rewritten for the corresponding unknown, that is, the first equation is rewritten with x_1 on the left hand side, and the second equation is rewritten with x_2 on the left hand side and so on as follows: [31]

$$x_1 = \frac{c_1 - a_{12}x_2 - a_{13}x_3 - \cdots - a_{1n}x_n}{a_{11}}$$

$$x_2 = \frac{c_2 - a_{21}x_1 - a_{23}x_3 - \cdots - a_{2n}x_n}{a_{22}}$$

$$.$$
$$.$$
$$.$$

$$x_{n-1} = \frac{c_{n-1} - a_{n-1,1}x_1 - a_{n-1,2}x_2 - \cdots - a_{n-1,n-2}x_{n-2} - a_{n-1,n}x_n}{a_{n-1,n-1}}$$

$$x_n = \frac{c_n - a_{n1}x_1 - a_{n2}x_2 - \cdots - a_{n,n-1}x_{n-1}}{a_{nn}}$$

These equations can be rewritten in a summation form as

$$x_1 = \frac{c_1 - \sum_{\substack{i=1 \\ j\neq 1}}^{n} a_{1,i}x_j}{a_{11}}$$

$$x_2 = \frac{c_2 - \sum_{\substack{i=1 \\ j\neq 2}}^{n} a_{2,i}x_j}{a_{22}}$$

$$x_{n-1} = \frac{c_{n-1} - \sum_{\substack{i=1 \\ j\neq n-1}}^{n} a_{n-1,i}x_j}{a_{n-1,n-1}}$$

$$x_n = \frac{c_n - \sum_{\substack{i=1 \\ j\neq n}}^{n} a_{n,i}x_j}{a_{nn}}$$

Hence for any row, i

$$x_i = \frac{c_i - \sum_{\substack{i=1 \\ j \neq i}}^{n} a_{ij}x_j}{a_{ii}}, i = 1,2,3,\dots,n$$

Now to find x_i, one assumes an initial guess for the values of x_i and then uses the rewritten equations to calculate the new estimates. Remember, one always uses the most recent estimates to calculate the next estimates x_i . At the end of each iteration, one calculates the absolute relative approximate error for each x_i as [31]

$$|\mathcal{E}_a|_i = \left|\frac{x_i^{new} - x_i^{old}}{x_i^{new}}\right|$$

Where x_i^{new} is the recently obtained value of x_i, and x_i^{old} is the previous value of x_i

When the absolute relative approximate error for each x_i is less than the pre-specified tolerance, the iterations are stopped.

4.5.2. Newton-Raphson Method
4.5.2.1. General Introduction:

The Newton-Raphson method, or Newton Method, is a powerful technique for solving equations numerically. Like so much of the differential calculus, it is based on the simple idea of linear approximation. The Newton Method, properly used, usually homes in on a root with devastating efficiency. [32]

4.5.2.2. Using Linear Approximations to Solve Equations:

Let $f(x)$ be a well-behaved function, and let r be a root of the equation $f(x) = 0$.

We start with an estimate x_0 of r. From x_0, we produce an improved estimate x_1.   From x_1, we produce a new estimate x_2. We go on until we are close enough to r. [33]

4.5.2.3. The Newton-Raphson Iteration:

Let x_0 be a good estimate of r and let $r = x_0 + h$. Since the true root is r, and $h = r - x_0$, the number h measures how far the estimate x_0 is from the truth.

Since h is small, we can use the linear (tangent line) approximation to conclude that: [33]

$$0 = f(r) = f(x_0 + h) \approx f(x_0) + hf'(x_0)$$

And therefore, unless $f'(x_0)$ is close to 0,

$$h \approx -\frac{f(x_0)}{f'(x_0)}$$

It follows that:

$$r = x_0 + h \approx x_0 - \frac{f(x_0)}{f'(x_0)}$$

Our new improved estimate x_1 of r is therefore given by:

$$x_1 = x_0 - \frac{f(x_0)}{f'(x_0)}$$

The next estimate x_2 is obtained from x_1 in exactly the same way as x_1 was obtained from the point x_0:

$$x_2 = x_1 - \frac{f(x_1)}{f'(x_1)}$$

Continuing in this way. If x_n is the current estimate, then the next estimate x_{n+1} is given by

$$x_{n+1} = x_n - \frac{f(x_n)}{f'(x_n)}$$

4.5.2.4. Geometric Interpretation of the Newton-Raphson Iteration:

The curve $y = f(x)$ meets the x-axis at the root r. Let a be the current estimate of the root r. The tangent line to $y = f(x)$ at the point $(a, f(a))$ has equation:

$$y = f(a) + (x - a)f'(a)$$

Let b be the x-intercept of the tangent line. Then: [32]

$$b = a - \frac{f(a)}{f'(a)}$$
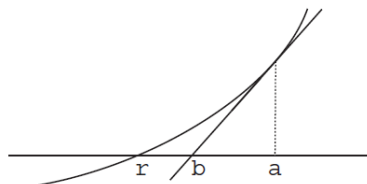
Fig 4.1: Geometric Interpretation of the Newton-Raphson [32]

Comparing with Equation 1: b is the next Newton-Raphson estimate of the root r. The new estimate b is obtained by drawing the tangent line at $x = a$, and then sliding to the x-axis along this tangent line.

4.6. The reduced global mechanism for ethylene combustion

For our case, we are going to be studying the kinetic model for Ethylene.

A 10-step global reaction scheme has been tailored, containing 11 of the most important species for ethylene oxidation in air (H, O, OH, CO, CO2, H2, H2O, O2, C2H2, C2H4, and N2), hereafter denoted G11. [30]

The global reaction is as follow:

$$r_c C_2 H_4 + \left(n + \frac{m}{4}\right)(O_2 + 3.76 N_2) \xrightarrow{yields} n_1 CO_2 + n_2 H_2 O + n_3 O_2 + n_4 N_2 + n_5 OH + n_6 CO$$
$$+ n_7 H_2 + n_8 O + n_9 H + n_{10} C_2 H_2$$
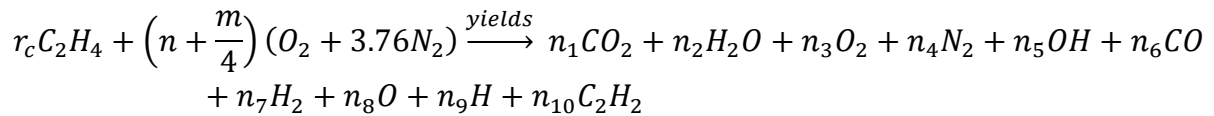
To calculate the number of moles of the reaction product, we use a set of equations as follow:

1-conservation of chemical species:

1-1 Carbone conservation:

$$r_c \times 2 = n_1 + n_6 + 2n_{10}$$

1-2 Hydrogen conservation:

$$r_c \times 4 = 2n_2 + n_5 + 2n_7 + n_9 + 2n_{10}$$

1-3 Oxygen conservation:

$$2 \times \left(n + \frac{m}{4}\right) = 2n_1 + n_2 + 2n_3 + n_5 + n_6 + n_8$$

1-4 Nitrogen conservation:

$$7.52 \times \left(n + \frac{m}{4}\right) = 2n_4$$

In addition to 10 elementary reactions:

$$O_2 + C_2 H_4 \rightarrow 2CO + 2H_2$$

$$O + CO \rightarrow CO_2$$

$$OH + CO \rightarrow H + CO_2$$

$$O_2 + H_2 \rightarrow OH + OH$$

$$O_2 + H \rightarrow OH + O$$

$$OH + H_2 \rightarrow H + H_2 O$$

$$O + H_2 + M \rightarrow H_2 O + M$$

$$2H + M \rightarrow H_2 + M$$

$$C_2 H_4 \rightarrow C_2 H_2 + H_2$$

$$C_2 H_2 + OH \rightarrow 2H_2 + 2CO$$
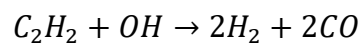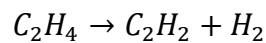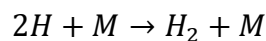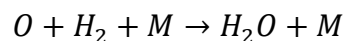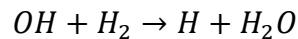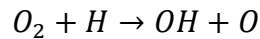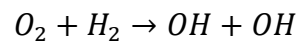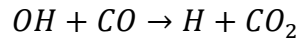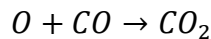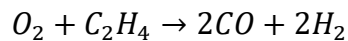
Table 1 G11 global reaction mechanism: Third body efficiencies for $H_2 = 2.5$ and for $H_2O = 16.0$

Reaction	A	n	E_a (cal)
I. $O2 + C2H4 <=> 2CO+2H2$	7.800E+23	.000	35500.00
II. $O + CO(+M) <=> CO2(+M)$	5.300E+13	.000	−4540.00
III. $OH + CO <=> H + CO2$	4.400E+06	1.500	−740.00
IV. $O2 + H2 <=> OH + OH$	1.700E+20	.000	48000.00
V. $O2 + H <=> OH + O$	2.600E+14	.000	16800.00
VI. $OH + H2 <=> H + H2O$	2.200E+17	.000	5150.00
VII. $O + H2 + M <=> H2O + M$	1.100E+20	−2.000	.00
VIII. $2H + M <=> H2 + M$	2.400E+19	−1.000	.00
IX. $C2H4 <=> C2H2 + H2$	2.500E+12	.000	71530.00
X. $C2H2 + 2OH <=> 2H2 + 2CO$	5.380E+22	.000	14000.00

To calculate the equilibrium constant for these elementary reactions we use the following set of equations:

$$K_p(1) = \frac{P_{CO}^2 \times P_{H_2}^2}{P_{O_2} \times P_{C_2H_4}}$$

With the partial pressure for each chemical species being:

$$P_i = \frac{n_i}{\sum n_i} \times P$$

Where P is the total pressure, and N_t defined as:

$$N_t = \sum n_i$$

By combining the previous equations with the global equation, we get:

$$K_p(1) = \frac{n_6^2 \times n_7^2}{n_3 \times r_c} \times \frac{P}{N_t}$$

The same goes for the other equations:

$$K_p(2) = \frac{n_1}{n_6 \times n_8} \times \frac{P}{N_t}$$

$$K_p(3) = \frac{n_1 \times n_9}{n_5 \times n_6} \times \frac{P}{N_t}$$

$$K_p(4) = \frac{n_5^2}{n_3 \times n_7} \times \frac{P}{N_t}$$

$$K_p(5) = \frac{n_5 \times n_8}{n_3 \times n_9} \times \frac{P}{N_t}$$

$$K_p(6) = \frac{n_2 \times n_9}{n_5 \times n_7} \times \frac{P}{N_t}$$

$$K_p(7) = \frac{n_2}{n_7 \times n_8} \times \frac{P}{N_t}$$

$$K_p(8) = \frac{n_7}{n^2{}_9} \times \frac{P}{N_t}$$

$$K_p(9) = \frac{r_c}{n_7 \times n_{10}} \times \frac{P}{N_t}$$

$$K_p(10) = \frac{n^2{}_6 \times n^2{}_7}{n^2{}_5 \times n_{10}} \times \frac{P}{N_t}$$

For a Constant value of T, we obtain the following set of equations:

$$f_1 = 2r_c - n_1 - n_6 - 2n_{10}$$

$$f_2 = r_c - 2n_2 - n_5 - n_7 - n_9 - 2n_{10}$$

$$f_3 = 2n_1 + n_2 + 2n_3 + n_5 + n_6 + n_8 - 6$$

$$f_4 = 2n_4 - 45.12$$

$$f_5 = (n^2{}_6 \times n^2{}_7) - \left(\frac{K_p(1)}{P} \times N_t \times n_3 \times r_c \right)$$

$$f_6 = n_1 - \left(\frac{K_p(2)}{P} \times N_t \times n_6 \times n_8 \right)$$

$$f_7 = (n_1 \times n_9) - \left(\frac{K_p(3)}{P} \times N_t \times n_5 \times n_6 \right)$$

$$f_8 = n^2{}_5 - \left(\frac{K_p(4)}{P} \times N_t \times n_3 \times n_7 \right)$$

$$f_9 = (n_5 \times n_8) - \left(\frac{K_p(5)}{P} \times N_t \times n_3 \times n_9 \right)$$

$$f_{10} = (n_2 \times n_9) - \left(\frac{K_p(6)}{P} \times N_t \times n_5 \times n_7 \right)$$

$$f_{11} = n_2 - \left(\frac{K_p(7)}{P} \times N_t \times n_7 \times n_8 \right)$$

$$f_{12} = n_7 - \left(\frac{K_p(8)}{P} \times N_t \times n^2_9 \right)$$

$$f_{13} = r_c - \left(\frac{K_p(9)}{P} \times N_t \times n_7 \times n_{10} \right)$$

$$f_{14} = (n^2_6 \times n^2_7) - \left(\frac{K_p(10)}{P} \times N_t \times n^2_5 \times n_{10} \right)$$

This set of equations will be solved using the previously explained numerical methods. The numerical model and the results will be discussed in the next chapter.

5. Results and Duscission
5.1. Turbulence Models

Turbulence refers to the state of the flow of a fluid in which the velocity exhibits at all points a vortex character, the size, location and orientation of which vary constantly.

Navier-Stokes equations are nonlinear partial differential equations that describe the motion of fluids.

The mathematical existence of solutions to the Navier-Stokes equations is not demonstrated, but they often allow, by an approximate resolution, to propose a modelling of many phenomena.

Reynolds used the Navier-Stokes equations to simplify the turbulence problem, by using the resulting equations he was able to model the turbulent flow in order to determine its properties.

5.1.1. Fundamental Equations

Continuity equation:

$$\frac{\partial \rho}{\partial t} + \frac{\partial v}{\partial xj} = 0$$

For $\rho_t = 0$

$$\frac{\partial v}{\partial xj} = 0$$

We replace the following $v = \bar{v} + v'$

$$\frac{\partial(\bar{v} + v')}{\partial xj} = 0$$

We take the average of the previous equation:

$$\frac{\overline{\partial(\bar{v} + v')}}{\partial xJ} = 0$$

The Equation becomes :

$$\frac{\partial \bar{v}}{\partial xj} = 0 \qquad (5.1)$$

The momentum conservation equation:

$$\rho \left[\frac{\partial u}{\partial t} + v \frac{\partial u}{\partial xj} \right] = -\frac{\partial p}{\partial xi} + \frac{\partial}{\partial xj} \left(\mu \frac{\partial u}{\partial xj} \right)$$

We replace the following:

$$u = \bar{u} + u'$$

$$v = \bar{v} + v'$$

$$p = \bar{p} + p'$$

$$\rho \left[\frac{\partial(\bar{u} + u')}{\partial t} + \frac{\partial}{\partial xj} [(\bar{v} + v')(\bar{u} + u')] \right] = -\frac{\partial(\bar{p} + p')}{\partial xi} + \frac{\partial}{\partial xj} \left(\mu \frac{\partial(\bar{u} + u')}{\partial xj} \right)$$

We take the average of the previous equation:

$$\rho \left[\overline{\frac{\partial(\bar{u} + u')}{\partial t}} + \overline{\frac{\partial}{\partial xj} [(\bar{v} + v')(\bar{u} + u')]} \right] = -\overline{\frac{\partial(\bar{p} + p')}{\partial xi}} + \overline{\frac{\partial}{\partial xj} \left(\mu \frac{\partial(\bar{u} + u')}{\partial xj} \right)}$$

By expanding we get :

$$\rho \left[\overline{\frac{\partial(\bar{u}+u')}{\partial t}} + \overline{\frac{\partial}{\partial xj} [\bar{u}\bar{v} + \bar{u}v' + \bar{v}u' + v'u']} \right] = -\overline{\frac{\partial(\bar{p}+p')}{\partial xi}} +$$

$$\overline{\frac{\partial}{\partial xj} \left(\mu \frac{\partial(\bar{u}+u')}{\partial xj} \right)} \tag{5.2}$$

The equation becomes:

$$\rho \left[\frac{\partial \bar{u}}{\partial t} + \frac{\partial \overline{uv}}{\partial xj} \right] = -\frac{\partial \bar{p}}{\partial xi} + \frac{\partial}{\partial xi} \left(\mu \frac{\partial \bar{u}}{\partial xi} \right) - \rho \overline{u'v'} \tag{5.3}$$

The term $\rho \overline{u'v'}$ is called Reynolds Tensor.

The Reynolds Tensor can be written in the following matrix form:

$$\rho\overline{u'v'} = \rho \begin{bmatrix} \overline{u'^2_1} & \overline{u'_1 u'_2} & \overline{u'_1 u'_3} \\ \overline{u'_2 u'_1} & \overline{u'^2_2} & \overline{u'_2 u'_3} \\ \overline{u'_3 u'_1} & \overline{u'_3 u'_2} & \overline{u'^2_3} \end{bmatrix}$$

Equations 5.3 in (3D) are called RANS Equations.

The number of equations in the system is 4 (1 continuity and 3 Conservation of Q.d.Mvt) and the number of unknowns in the system is 10 (u, v, w, p, and 6 in the Reynolds tensor).

Since the number of unknowns is greater than the number of equations so we have what is called "a closure problem". To close the system we need additional equations, which will be filled by using the turbulence models.

The turbulence models are additional equations that must be solved with the RANS equations to find all the unknowns of the system. The number of equations to add depends on the model used. The models are generally based on 2 approaches:

-Eddy's Viscosity approach.

-The Reynolds tensor equations.

5.1.2. **Eddy's viscosity**

In Eddy's model we must change the additional term $\rho\overline{u'v'}$ by the following equation:

$$\rho\overline{u'v'} = \rho \frac{\overline{u'^2_1} + \overline{u'^2_2} + \overline{u'^2_3}}{3} + \mu_t \left[\frac{\partial u}{\partial xi} + \frac{\partial u}{\partial xj} \right]$$

This equality contains two terms:

$$\rho \frac{\overline{u'^2_1} + \overline{u'^2_2} + \overline{u'^2_3}}{3} \quad \text{Isotropic}$$

$$\mu_t \left[\frac{\partial u}{\partial xi} + \frac{\partial u}{\partial xj} \right] \qquad \text{Anisotropic}$$

The isotropic term can be modified as follows:

$$\rho\overline{u'v'} = \frac{2}{3}\rho\frac{\overline{u'^2}_1 + \overline{u'^2}_2 + \overline{u'^2}_3}{2} + \mu_t\left[\frac{\partial u}{\partial xi} + \frac{\partial u}{\partial xj}\right]$$

$$\rho\overline{u'v'} = \frac{2}{3}\rho k\delta_{ij} + \mu_t\left[\frac{\partial u}{\partial xi} + \frac{\partial u}{\partial xj}\right]$$

Where k is the kinetic energy of the turbulent flow:

This approach consists in finding the turbulent viscosity μ_t, by finding μ_t we can replace the term $\rho\overline{u'v'}$ in the RANS equations and the system will become closed.

The k-Epsilon and k-Omega models are based on this approach.

5.1.3. The kinetic energy transport equation
The kinetic energy transport equation can be found as follows:

-First we subtract equation (2) from equation (a):

$$\rho\left[\frac{\partial(\bar{u}+u')}{\partial t} + \frac{\partial}{\partial xj}[\bar{u}\bar{v} + \bar{u}v' + \bar{v}u' + v'u']\right] = -\frac{\partial(\bar{p}+p')}{\partial xi} + \frac{\partial}{\partial xj}\left(\mu\frac{\partial(\bar{u}+u')}{\partial xj}\right) \quad (5.2)$$

$$\rho\left[\frac{\partial\bar{u}}{\partial t} + \frac{\partial\overline{uv}}{\partial xj}\right] = -\frac{\partial\bar{p}}{\partial xi} + \frac{\partial}{\partial xj}\left(\mu\frac{\partial\bar{u}}{\partial xj}\right) - \rho\overline{u'v'} \quad (5.3)$$

We find the conservation equation of momentum as a function of fluctuations:

$$\rho\left[\frac{\partial u'}{\partial t} + \frac{\partial}{\partial xj}[\bar{u}v' + \bar{v}u' + v'u' - \overline{u'v'}]\right] = -\frac{\partial p'}{\partial xi} + \frac{\partial}{\partial xj}\left(\mu\frac{\partial u'}{\partial xj}\right) \quad (5.4)$$

-By multiplying by u' we find:

$$u'\frac{\partial u'}{\partial t} + u'\frac{\partial}{\partial x_j}(\bar{u}v') + u'\frac{\partial}{\partial x_j}(\bar{v}u') + u'\frac{\partial}{\partial x_j}(u'v') - u'\frac{\partial}{\partial x_j}(\overline{u'v'})$$

$$= -u'\frac{1}{\rho}\frac{\partial p'}{\partial xi} + u'\frac{\partial}{\partial xj}\left(\frac{\partial u'}{\partial xj}\right) \quad (5.5)$$

Each term in this equation will undergo a mathematical modification as follows:

Term 1 : $u'\dfrac{\partial u'}{\partial t} = \dfrac{\partial}{\partial t}\left(\dfrac{1}{2}u'^2\right)$

Term 2 : $u'\dfrac{\partial}{\partial x_j}(\bar{u}v') = u'v'\dfrac{\partial}{\partial x_j}\bar{u}$

Term 3 : $u'\dfrac{\partial}{\partial x_j}(\bar{v}u') = \bar{v}\dfrac{\partial}{\partial x_j}\left(\dfrac{1}{2}u'^2\right)$

Term 4 : $u' \frac{\partial}{\partial x_j}(u'v') = \frac{\partial}{\partial x_j}\left(v' \frac{1}{2}u'^2\right)$

Terme 5 : $u' \frac{\partial}{\partial x_j}(\overline{u'v'}) = u' \frac{\partial}{\partial x_j}(\overline{u'v'})$

Terme 6 : $u' \frac{1}{\rho}\frac{\partial p'}{\partial xi} = \frac{1}{\rho}\left(\frac{\partial}{\partial x_i}u'p'\right)$

Terme 7 : $u' \frac{\partial}{\partial xj}\left(\frac{\partial u'}{\partial xj}\right) = \frac{\partial}{\partial x_j}\left(vu' \frac{\partial u'}{\partial x_j}\right) - \frac{\partial u'}{\partial x_j}\frac{\partial u'}{\partial x_j}$

By replacing in the equation (5.5) we find:

$$\frac{\partial}{\partial t}\left(\frac{1}{2}u'^2\right) + u'v' \frac{\partial}{\partial x_j}\bar{u} + \bar{v}\frac{\partial}{\partial x_j}\left(\frac{1}{2}u'^2\right) + \frac{\partial}{\partial x_j}\left(v' \frac{1}{2}u'^2\right)$$
$$- u' \frac{\partial}{\partial x_j}(\overline{u'v'}) = -\frac{1}{\rho}\left(\frac{\partial}{\partial x_i}u'p'\right)\frac{\partial}{\partial x_j}\left(vu' \frac{\partial u'}{\partial x_j}\right) - \frac{\partial u'}{\partial x_j}\frac{\partial u'}{\partial x_j}$$

-Then we take the average of this equation:

$$\frac{\partial}{\partial t}\left(\frac{1}{2}u'^2\right) + \overline{u'v'^{\frac{\partial}{\partial x_j}}\bar{u}} + \overline{\bar{v}\frac{\partial}{\partial x_j}\left(\frac{1}{2}u'^2\right)} + \overline{\frac{\partial}{\partial x_j}\left(v'^{\frac{1}{2}}u'^2\right)}$$
$$- \overline{u'^{\frac{\partial}{\partial x_j}}(\overline{u'v'})} = -\overline{\frac{1}{\rho}\left(\frac{\partial}{\partial x_\iota}u'p'\right)} + \overline{\frac{\partial}{\partial x_j}\left(vu'^{\frac{\partial u'}{\partial x_j}}\right)} - v\overline{\frac{\partial u'}{\partial x_j}\frac{\partial u'}{\partial x_j}}$$

$$\frac{\partial}{\partial t}\left(\frac{1}{2}\bar{u}'^2\right) + \overline{u'v'}\frac{\partial}{\partial x_j}\bar{u} + \bar{v}\frac{\partial}{\partial x_j}\left(\frac{1}{2}\bar{u}'^2\right) + \frac{\partial}{\partial x_j}\left(\frac{1}{2}\overline{u'u'v'}\right)$$
$$= -\frac{1}{\rho}\left(\frac{\partial}{\partial x_i}\overline{u'p'}\right) + \frac{\partial}{\partial x_j}\left(\overline{vu' \frac{\partial u'}{\partial x_j}}\right) - v\overline{\frac{\partial u'}{\partial x_j}\frac{\partial u'}{\partial x_j}}$$

- We rearrange the equation:

$$\frac{\partial}{\partial t}\left(\frac{1}{2}\bar{u}'^2\right) + \bar{v}\frac{\partial}{\partial x_j}\left(\frac{1}{2}\bar{u}'^2\right) = -\frac{\partial}{\partial x_j}\left(\frac{1}{2}\overline{u'u'v'} + \frac{1}{\rho}\overline{v'p'} - \overline{vu' \frac{\partial u'}{\partial x_j}}\right) - \overline{u'v'}\frac{\partial}{\partial x_j}\bar{u} - v\overline{\frac{\partial u'}{\partial x_j}\frac{\partial u'}{\partial x_j}} \quad (5.6)$$

With: $\frac{1}{2}\bar{u}'^2 = k$

The equation becomes :

$$\frac{\partial}{\partial t} k + \bar{v} \frac{\partial}{\partial x_j} k = -\frac{\partial}{\partial x_j} \left(\frac{1}{2} \overline{u'u'v'} + \frac{1}{\rho} \overline{v'p'} - \overline{vu' \frac{\partial u'}{\partial x_J}} \right) - \overline{u'v'} \frac{\partial}{\partial x_j} \bar{u} - \overline{\frac{\partial u'}{\partial x_J} \frac{\partial u'}{\partial x_J}} \quad (5.7)$$

The latter represents the transport equation of the kinetic energy k. By Using a Benchmark we can do the following modeling of the equation of k:

$$\frac{Dk}{Dt} = \frac{\partial k}{\partial t} + \bar{v} \frac{\partial k}{\partial x_j} = \frac{\partial}{\partial x_j} \left[\frac{v_t}{\sigma_k} \frac{\partial k}{\partial x_j} \right] + P - \varepsilon \qquad (5.8)$$

With : $\sigma_k = 1$

And: $V \sim k^{1/2} \qquad l \sim \frac{k^{3/2}}{\varepsilon} \qquad v_t \sim Vl$

5.1.4. The K-Epsilon Model

The model k epsilon introduces to the RANS equation two unknowns instead of 6, the two unknowns are:

k: kinetic energy

Epsilon: dissipation of this kinetic energy

These two unknowns will be introduced as boundary conditions with U the input speed.

By analogy we can find the transport equation of epsilon as follows:

$$\frac{\partial(\rho\varepsilon)}{\partial t} + \bar{v} \frac{\partial(\rho\varepsilon)}{\partial x_j} = \frac{\partial}{\partial x_j} \left[\left(\frac{v_t}{\sigma_k} \right) \frac{\partial \varepsilon}{\partial x_j} \right] + C_{1\varepsilon} P_k \frac{\varepsilon}{k} - C_{2\varepsilon} \rho \frac{\varepsilon^2}{k} \qquad (5.9)$$

$C_{1\varepsilon}$ and $C_{2\varepsilon}$ are constants.

The k is the Epsilons will be replaced in the following equation:

$$\mu_t = \rho C_\mu \frac{k^2}{\varepsilon} \qquad (5.10)$$

μ_t is determined from this equation and replaced in the Modified Reynolds tensorand with that the system is closed.

5.1.5. The K-Omega Model

Similarly we can find the transport equation of Omega:

$$\frac{\partial(\rho\omega)}{\partial t} + \bar{v}\frac{\partial(\rho\omega)}{\partial x_j} = \frac{\partial}{\partial x_j}\left[\left(\frac{v_t}{\sigma_k}\right)\frac{\partial\omega}{\partial x_j}\right] + \frac{\gamma}{v_t}P_k - \beta\rho\frac{\omega^2}{k} \tag{5.11}$$

γ , σ_k , β are constants.

k and Omega will be replaced in the following equation:

$$\mu_t = \rho\frac{k}{\omega}$$

μ_t is determined from this equation and replaced in the Modified Reynolds tensorand with that the system is closed.

5.1.6. The K-Omega SST Model

For the mixed model k omega SST we use the following transition

-From the transport equation of epsilon we replace epsilon by:

$$\varepsilon = C_\mu k\omega$$

We find the same omega equation but with an additional term:

$$\frac{\partial(\rho\omega)}{\partial t} + \bar{v}\frac{\partial(\rho\omega)}{\partial x_j} = \frac{\partial}{\partial x_j}\left[\left(\frac{v_t}{\sigma_k}\right)\frac{\partial\omega}{\partial x_j}\right] + \frac{\gamma}{v_t}P_k - \beta\rho\frac{\omega^2}{k} + 2\frac{\rho\sigma_{\omega2}}{\omega}\nabla k\nabla\omega \tag{5.12}$$

So we can change between the Epsilon and Omega equations by adding or canceling this term.

For that we will introduce the following function F1 to the additional term:

$$2(1 - F_1)\frac{\rho\sigma_{\omega2}}{\omega}\nabla k\nabla\omega$$

The F1 function is called the mix function.

The transition between the two equations is done as follows:

-The function is chosen so as to appear near the obstacle which will cancel the additional term

$F_1 = 1$ So

$$2(1 - F_1)\frac{\rho\sigma_{\omega 2}}{\omega}\nabla k\nabla\omega = 0$$

So the Solver will use the Omega transport equation.

The function will disappear far from the obstacle which will leave the additional term

$F_1 = 0$ So

$$2(1 - F_1)\frac{\rho\sigma_{\omega 2}}{\omega}\nabla k\nabla\omega = 2\frac{\rho\sigma_{\omega 2}}{\omega}\nabla k\nabla\omega$$

The Solver will use the transport equation of Epsilon.
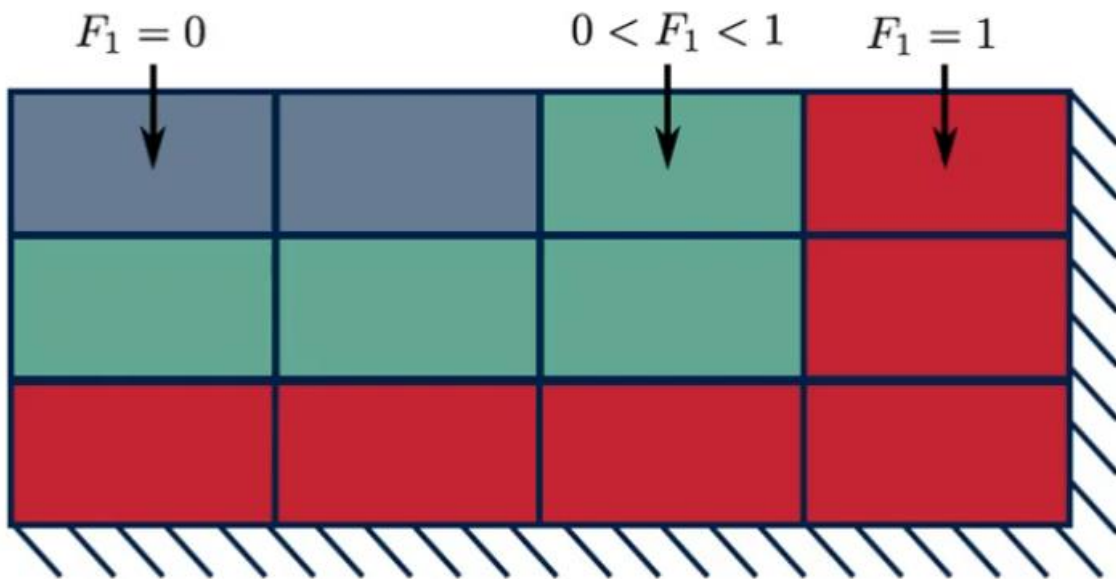
Fig 5.1: The Variation of F the Blending Function With Respect to the distance to the wall [53]

F_1 takes the following form :

$$F_1 = Tanh(arg_1^4)$$
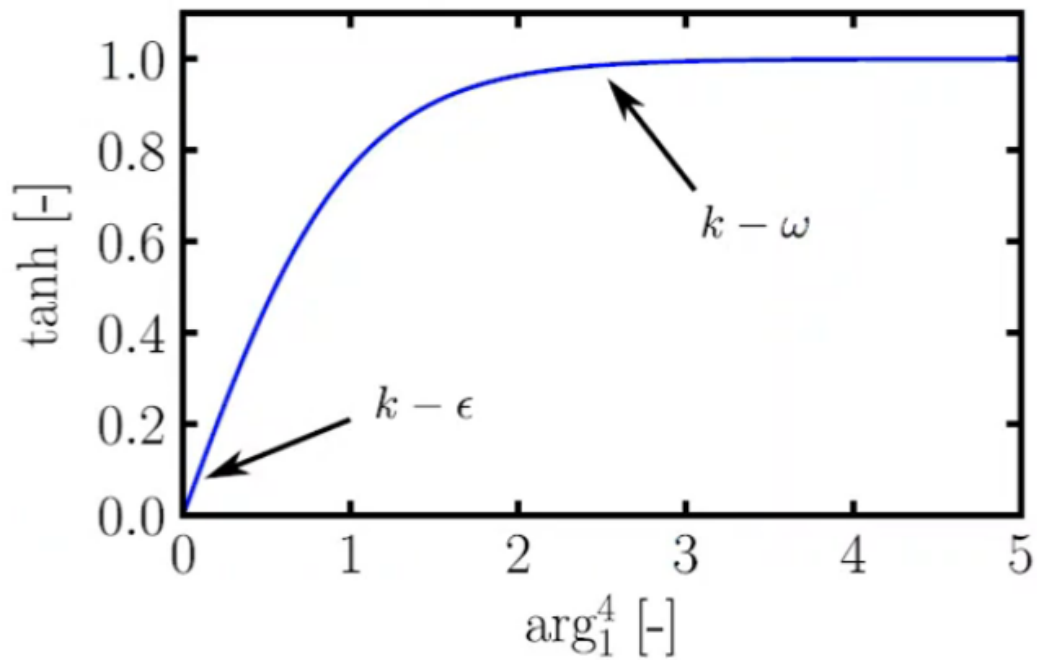
$$arg_1 = \min \left[\max \left(\frac{\sqrt{k}}{\beta^\star \omega d}, \frac{500\nu}{d^2\omega} \right), \frac{4\rho\sigma_{w2}k}{CD_{kw}d^2} \right]$$
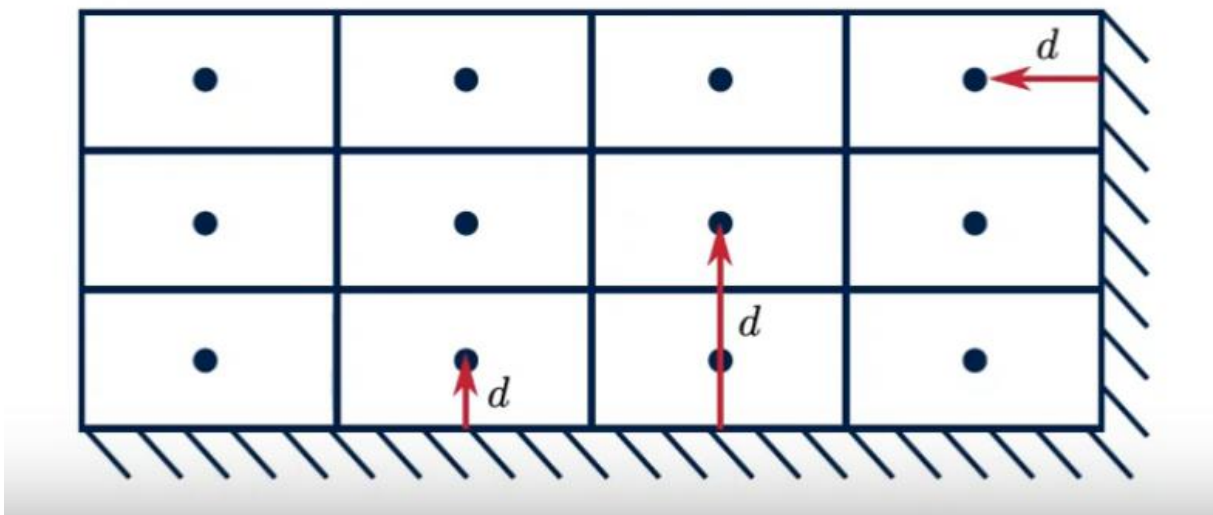
Fig 5.2: Blending function F1' Plot [53]

-The CFD Code will calculate the distance to the nearest obstacle before calculating the other parameters, the code will then evaluate the value of the argument and F1 is calculated for all grid grid. The Solver will assume which grid is to calculate using k-epsilon or k-omega.

In the k-omega SST model a viscosity limiter is introduced, in the case of the k-omega model μ_t is calculated directly by the following equation:

$$\mu_t = \rho \frac{k}{\omega}$$

In the case of the model k-omega SST, μ_t is calculated with this equation:

$$\mu_t = \frac{a_1 \rho k}{\max(a_1 \omega, SF_2)}$$

Where F_2 is also a function of mixture. If SF_2 is larger then the viscosity will be limited.

The limiter gives more accurate results and closer to experimental measurements.

$$F_2 = \tanh\left(\mathrm{arg}_2^2\right)$$

$$\mathrm{arg}_2 = \max\left(\frac{2\sqrt{k}}{\beta^\star \omega d}, \frac{500\nu}{\omega d^2}\right)$$

5.1.7. The Near-wall Treatment

-This treatment is necessary to properly capture the speed profile near the obstacle. We therefore need a large number of grids close to our geometry.

This approach used in this case is the linear fragments approach. In each grid we put a function that describes a small portion of the profile, this function is linear (it gives a straight line) and several lines will be mounted to build the profile.
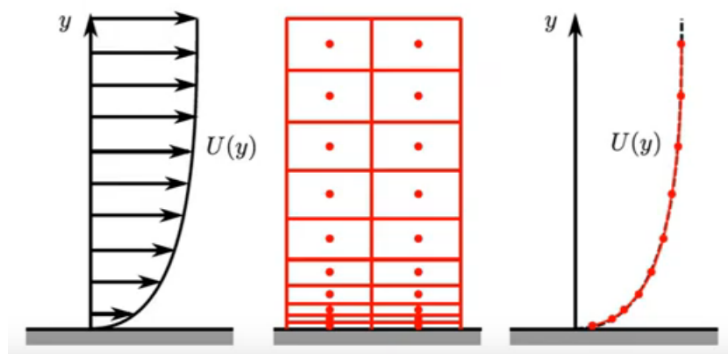
Fig 5.3: The Grid Size Variation [53]

Another approach will be to use a single grid which will have a nonlinear function describing the profile throughout the region, this will make the calculation easier and help the stability of the digital diagram.
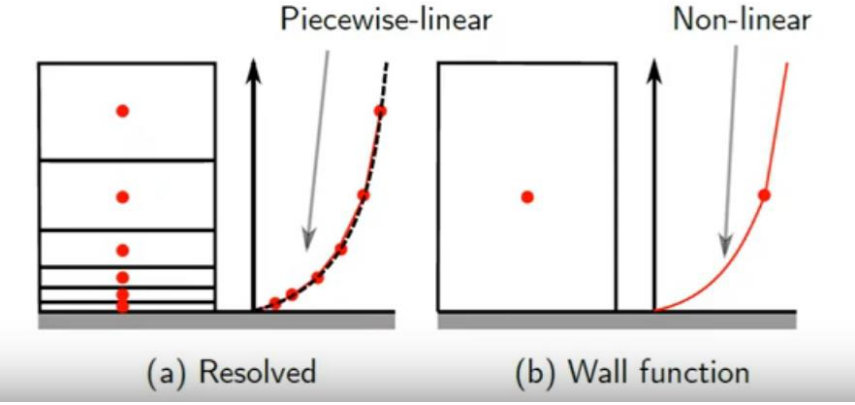
Fig 5.4: Large Grid Method [53]

This non-linear function is determined from the experimental results or from the results of the DNS.
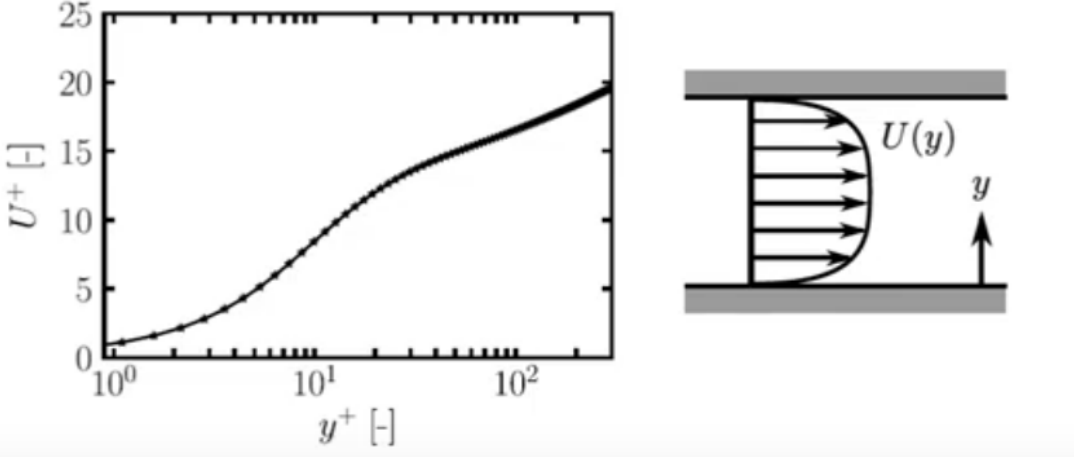
Fig 5.5: The tangential velocity as a function of the vertical distance to the obstacle [53]

The graph is divided as follows:
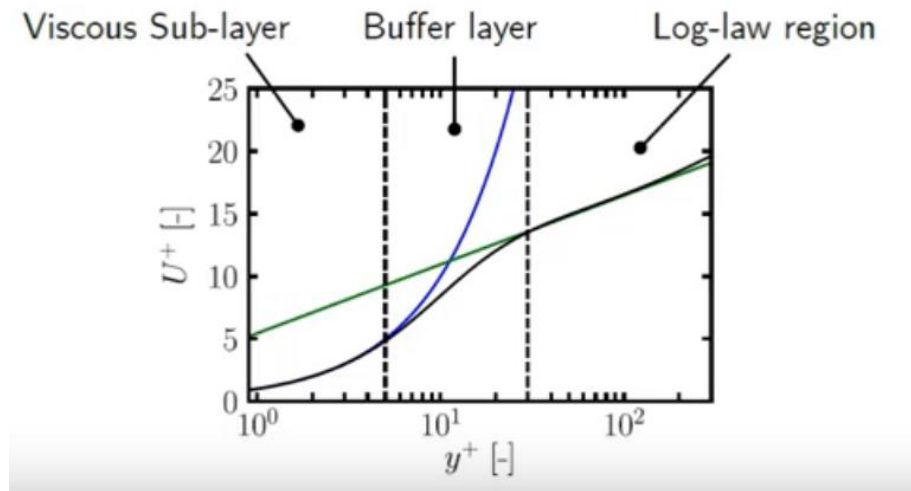
Fig 5.6: Variation of Velocity Function With respect to y+ [53]

-The graph in black is the function we must use, and the blue and green graph correspond to empirical functions which are measured in their respected regions.

In the left region; the blue graph is closer to the black graph. So for y + <5 we can use the corresponding function:

$$U^+ = y^+$$

In the right region; the green graph is closer to the black graph. So for y +> 30 we can use the corresponding function:

$$U^+ = \frac{1}{\kappa}\log(Ey^+)$$

Where Kappa and E are empirical coefficients (0.4187 and 9.793 respectively)

y + and U + are the vertical distance to the obstacle and the dimensionless velocity.

$$y^+ = \frac{yu_\tau}{\nu}$$

$$U^+ = \frac{U}{u_\tau}$$

And $u_\tau = \sqrt{\tau/\rho}$ is a referential velocity.

In order not to use several functions to describe the development of the velocity profile, we can use another approach, This approach is the function of Spalding:

$$y^+ = U^+ + 0.1108 \left[e^{U^+} - 1 - 0.4U^+ - \frac{1}{2}(U^+)^2 - \frac{1}{6}(U^+)^3 \right]$$

This function is continuous valid for y + <300
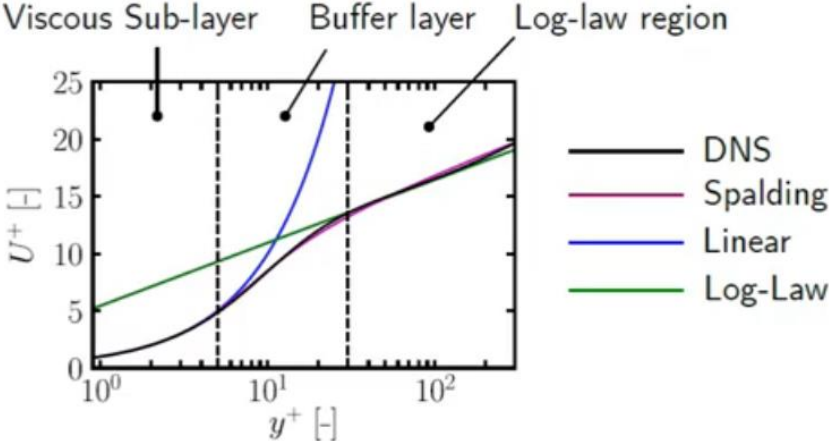
Fig 5.7: The Spalding Equation Variation [53]

5.1.8. The Advantages and Disadvantages of each model

The k-epsilon Model:

-It predicts well far from obstacles, it is used for turbulent flow only so epsilon well describes the evolution of Eddy dissipation.

-It lacks sensitivity to unfavorable pressure gradients, because of the modeling of the diffusive term.

$$\frac{\partial}{\partial x_j}\left[\left(\frac{v_t}{\sigma_k}\right)\frac{\partial \varepsilon}{\partial x_j}\right]$$

The k-Omega Model:

-Predicted close to the wall, Omega controls flow dissipation better than epsilon, so boundary layer detachment (separation) will be detected more precisely.

-The separation may be excessive, because the model is very sensitive to the value of omega.

The k-omega SST Model:

-It offers similar benefits to k-omega and k-epsilon.

-It gives very accurate predictions of the onset and amount of flow separation.

-It is recommended for high precision boundary layer simulations.

-Dependence on distance from wall makes it less suitable for free shear fluxes, and it requires mesh resolution near wall.

To calculate the number of moles of the reaction products we used a Matlab based program code that uses the Newton-Raphson method to calculated the solution of a non-linear set of equations, without passing by the gaussian elimination method, because in Matlab's data base they run multiple codes that can calculate the inverse of a nxn matrix, as long as the matrix is not singular.

The gaussian elimination is used in fortran based codes because we would have to introduce the calculation of the matrix inverse, which will make the calculation direct, without passing by the inverse of the matrix but it would still require a stabilization method presented as a re-arangement of the equations to make the final matrix diagonally dominant, else the solutions will fluctuate out of bounce within the first 50 iterations.

We are capable of studying any type of hydrocarbon, all we need is the composition of the latter as well as the equivalence ratio of the equation and also the set of dissosiation equations which is included in the kinetic model of the hydrocarbon we're studying with their respective equilibrium constants.

Some kinetic models include up to hundreds of sub equations, in our case the model contained a set of 10 equations that describes the process of the reaction.

We will be using some equations from "Temperature dependence of gas properties in polynomial form By J.R. Andrews Naval Postgraduate School Monterey, California" to get the polynomial form of Heat capacity for different species.

We will be using the results we obtained from out program, and try to compare them to the results we obtained from both the experimental data found in the gas turbine guide pre-tests, aswell as the simulation we ran for the combustion in a nearly identical combustor model that 5was made in SolidWorks based on the measures we found in the guide.

We will be using some data from the "study on the effects of air preheat on the combustion and heat transfer characteristics of Bunsen flames by H.S. Zhen, J. Miao, C.W. Leung, C.S. Cheung, Z.H. Huang Department of Mechanical Engineering, The Hong Kong Polytechnic University, Hong Kong, China" as well as " The Effect of Inlet Air Preheat on CO And NO Production in the Combustion in Canister Burner by Ishak M. s. a., Mohammad Nazri Mohd Jaafar and Wan Zaidi Wan Omar" and "Study on Direct Flame Oxide Fuel Cell Using Flat Burner and Ethylene Flame by Md. Moinul Hossain and Rong Lan, University of Kent" to compare it with our results for more accuracy.

Speaking of the simulation, the physical domains was done with a hexahedral structured grid. The geometry meshing was done to have a variable density distribution by mean of small mesh sizes which were incorporated in high gradient zone and bigger sizes in low gradient zone. The resulting base mesh contains approximately 6 million cells, which were then applied in this simulation work and presented in this paper.

5.2. Ansys Simulation

First we created a model similar to the combustor of the P9005 gas turbine using real time measures and the guide's included measures.
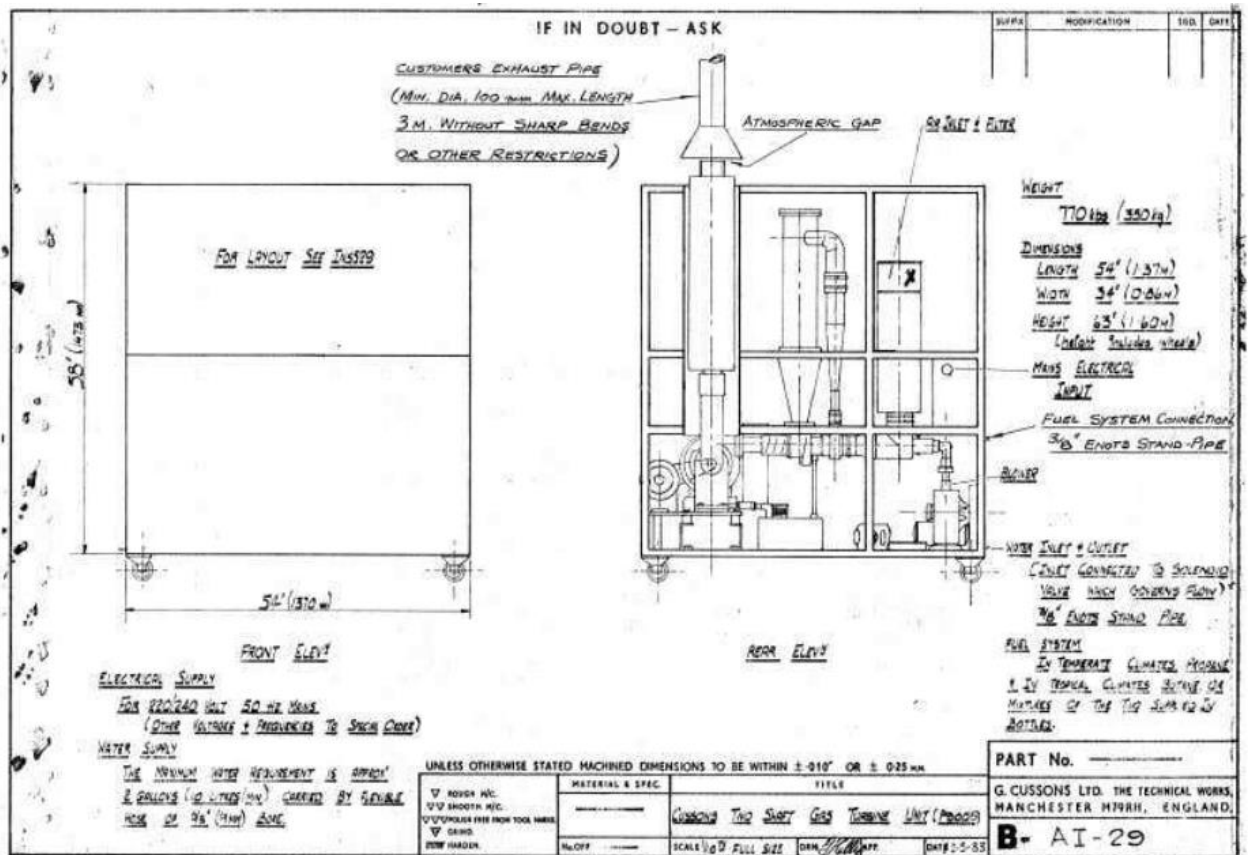
Fig 5.8: P9005 Measures [29]

We couldent rely solely on the exterior measures due to the combustor having an interior flame tube

Fig 5.9: Interior flame Tube [54]
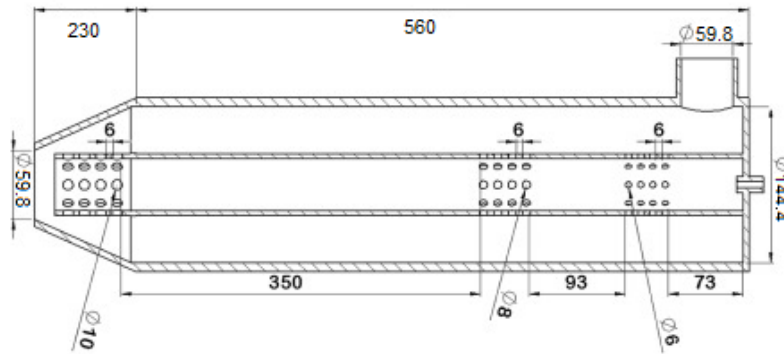
Fig 5.10: Flame Tube Measures [54]

The model was made in Solidworks and then using the Import function in ansys we get the following.
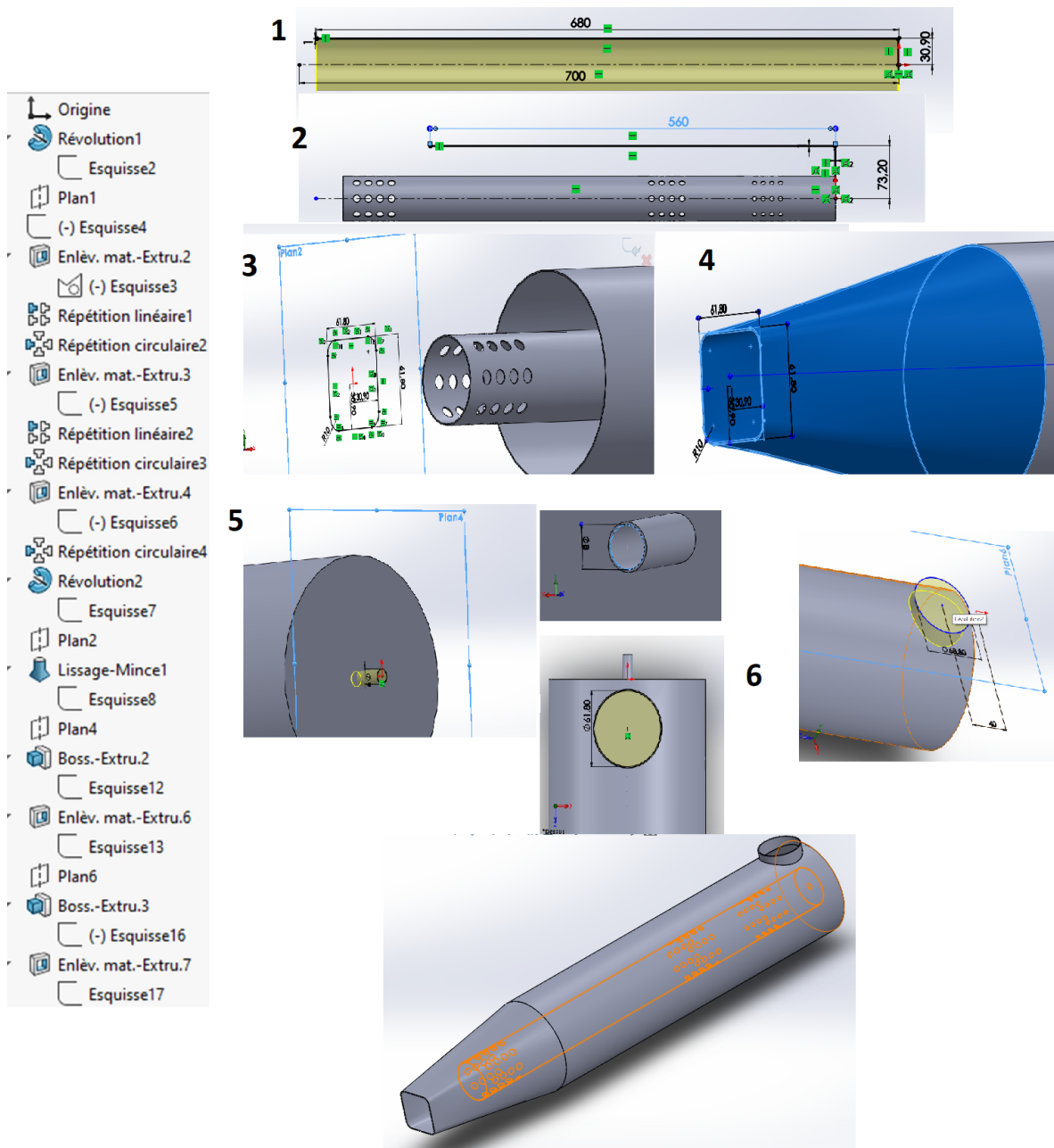
Fig 5.11: SolidWorks Steps
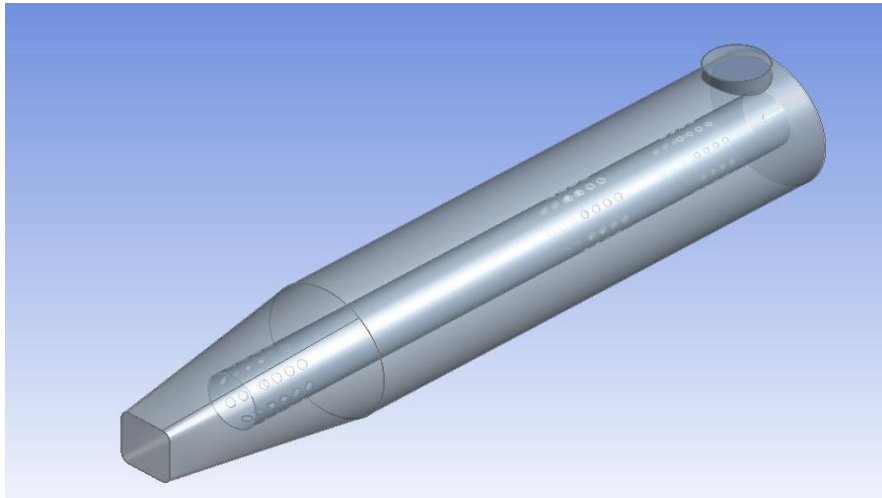
Fig5.12: The SolidWorks Model

We have 2 main flow entrences and 1 exit: Air inlet, Fuel Inlet, and Gas Outlet.
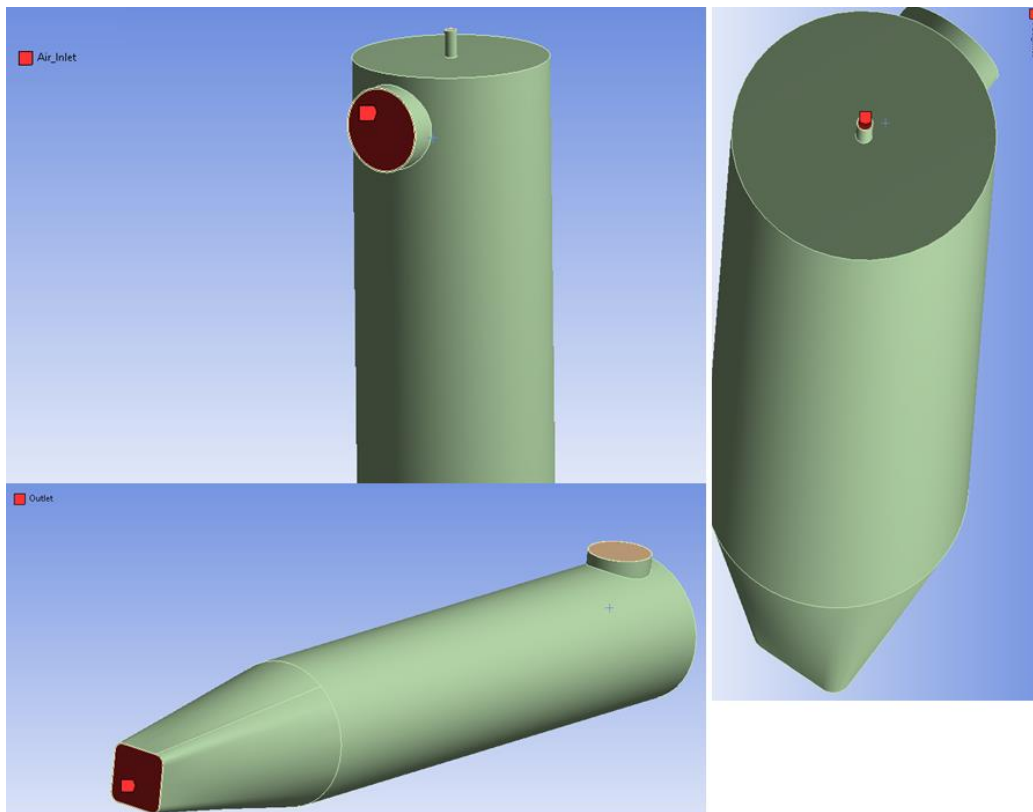
Fig 5.13: Fuel/Air Inlets, Oulet

Before jumping to the meshing step, we first separated the solid and fluid parts using the fill option in Ansys Design Modeler

For the meshing we used refinement methods specially for the areas near the inlets and outlet

We also minimized the element size to 4.10^{-3}

Fig 5.14: Overall meshing of the combustor model

5.2.1. <u>Mesh Quality Metric</u>

Commercial software codes tend to quantify the mesh quality in terms of criteria that can measure the element quality and the gradation in mesh element size such that at the very least, it will allow one to identify "bad" quality locations and thus decide where a careful visual inspection maybe needed. Such quantification is presented in the form of mesh quality metrics.

This post has no intention of presenting an exhaustive list of metrics, but to name a few (orthogonality, skewness, aspect-ratio) as conceptual means in the evaluation of mesh quality and its impact on obtaining an accurate solution.

<u>Orthogonality</u>

The concept of mesh orthogonality relates to how close the angles between adjacent element faces (or adjacent element edges) are to some optimal angle (depending on the relevant topology). An example for orthogonality is presented as in ANSYS Fluent in the figure below.

The orthogonality measure ranges from 0 (bad) to 1 (good).
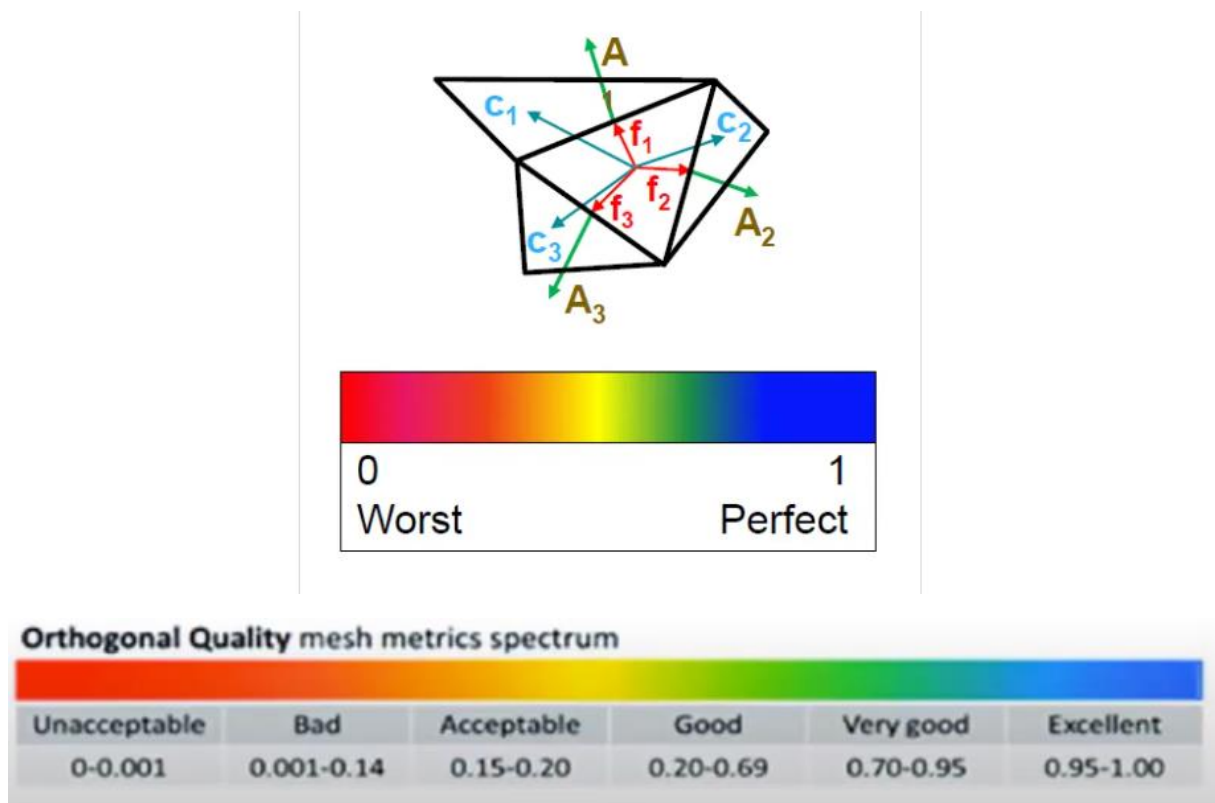
Fig 5.15: Orthogonal quality metrics [59]

Now we take a look at the Quality of our meshing

Paramètres de maillage	Qualité orthogonale
☐ Min	6.0467e-002
☐ Max	1.
☐ Moyenne	0.75052
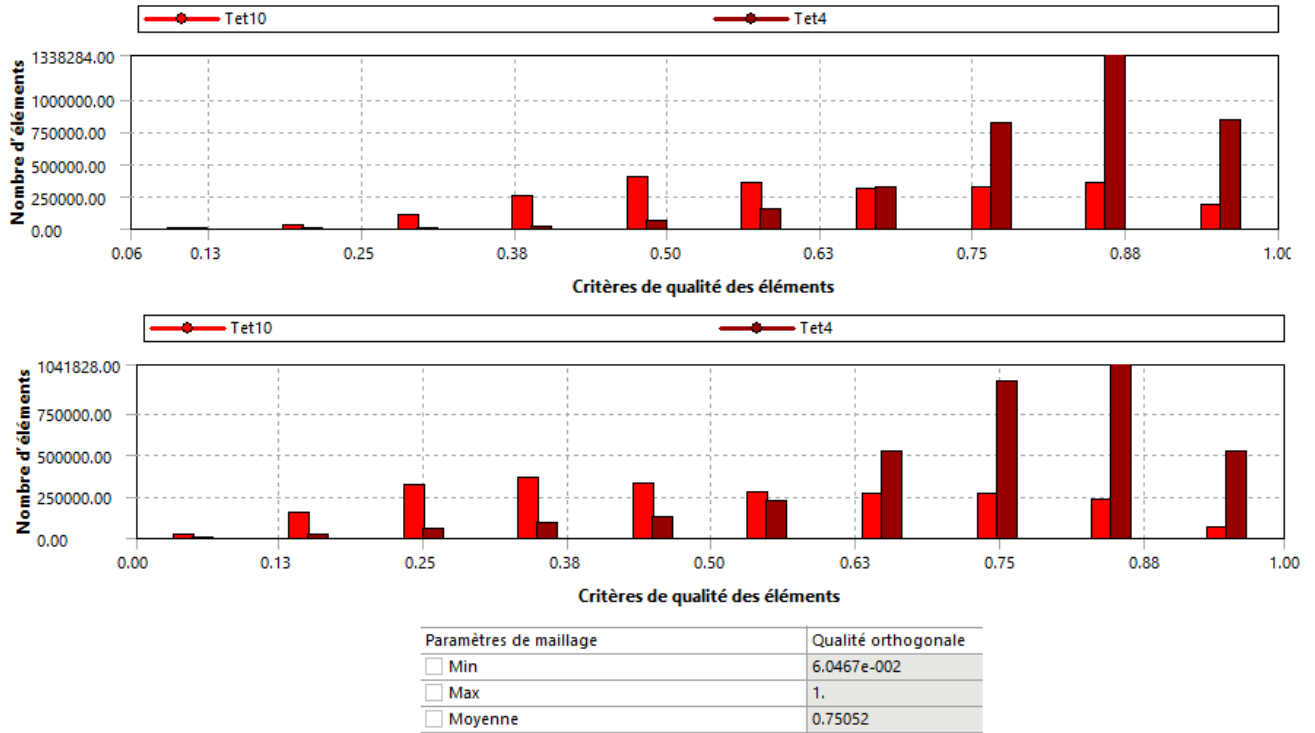
Fig 5.16: Combustor Model Meshing Quality

We can see that the meshing is on the middle spectrum of the very good quality, however this does not give the full picture to it, as the meshing was heavily based on the interior flame tume seeing that the combustion mainly occures inside of it.

5.2.2. The Turbulent Model Used in calculation

In the present simulation, k-epsilon turbulence model was used. Turbulence is represented by the realizable k-epsilon model, which provides an optimal choice and economy for internal turbulent flows.

The current study uses the realizable k–ε turbulence model. This model is in the class of two-equation models in which the solution of two separate transport equations allows the turbulent velocity and length scales to be independently determined. The realizable k–ε turbulence model is robust, economic and reasonably accurate over a wide range of turbulent flow. The realizable k–ε turbulence model solves transport equations for kinetic energy (k) and its dissipation rate (ε). It assumes that the flow is fully turbulent, and the effects of molecular viscosity are negligible. The realizable k–ε turbulence model is therefore valid for fully turbulent flows, consistent with the flow characteristics in a typical combustion chamber

5.3. Results and discussion:
5.3.1. The effect of variation of the equivalence ratio on the molar fractions of the poducts:

After calculating the mole fractions using the results of the Matlab program we get (Fig 5.17), which shows us two main parts, the major species that are CO_2, H_2O, O_2, CO and H_2. Minor species that are OH, O and H. We did not include the molar fraction of N_2 for visualisation purposes, noting that N_2 molar fraction is fluctuating between 67 and 68% which would make the minor species plots look unoticable.

We notice that the O_2 molar fraction decreases with the equivalence ratio, because with the increase of the latter the fuel quantity increases which means more consumption of O_2. When the mixture becomes rich the O_2 drops bellow 1% mole fraction which shows its total consumption

The less O_2 means a leaner combustion even with stochiometric conditions, the real combustion process relies more on the frequency of fuel/air interactions, the more the molecules hit eachother the better. Since a 100% interaction ratio is nearly impossible, the combustion will never be complete. This results in an incomplete reaction with the production of carbon monoxide and hydrogene molecules as well as the minor species.

Looking at (fig 5.18) which is taken ""Study on Direct Flame Oxide Fuel Cell Using Flat Burner and Ethylene Flame" showing the major species molar fractions for comparison purposes we note that there is a consistancy between the two with respect to molar fractions increases and decreases for different values of corse.

From the results we can notice that the H_2 mole fraction taken from the program is higher than the mole fraction from the article results. This is due to the choise of kinetic model, the main purpose of the model used as a base for the program code was to calculate and moderate the creation of soot $CH_3 - (CH_2)_m$ in the reaction products, with that the dissociation sub-reaction picked for this model result in a higher H_2 production rate which explains the results.
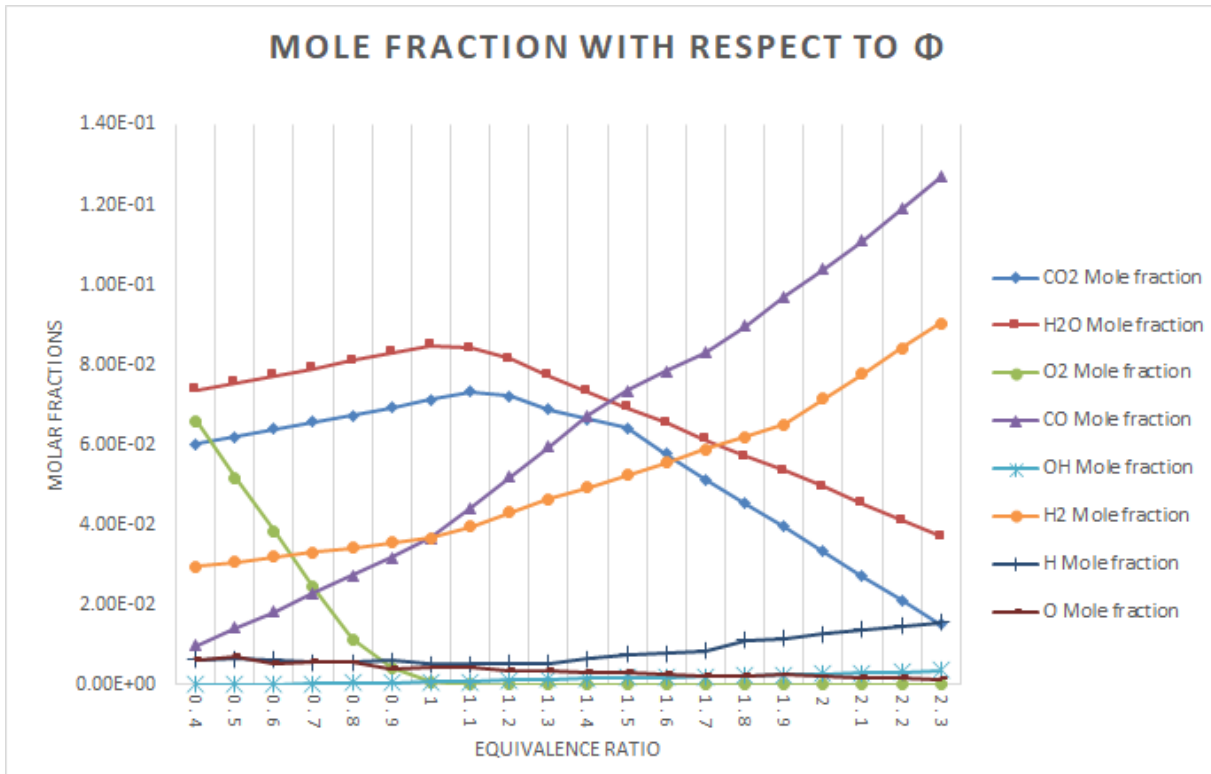
Fig 5.17: Mole fractions results of reaction products from the Newton-Raphson Program
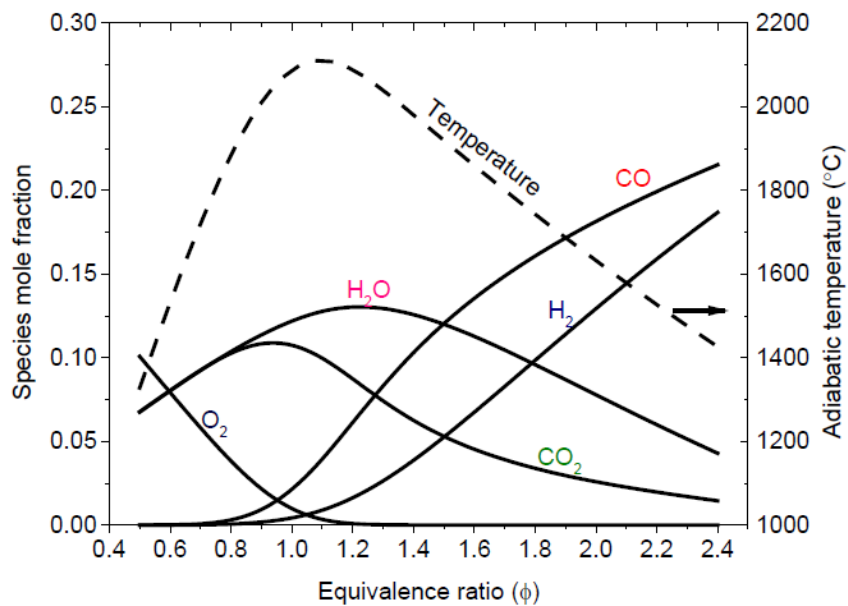
Fig 5.18: Mole fractions results from Study on Direct Flame Oxide Fuel Cell Using Flat Burner and Ethylene Flame [55]

The mass fraction contours from Ansys simulation also show the difference between the major species production and the minor species production. (Fig 5.19) (Fig 5.20) (Fig 5.21) (Fig 5.22) (Fig 5.23) (Fig 5.24) (Fig 5.25).

Major species production
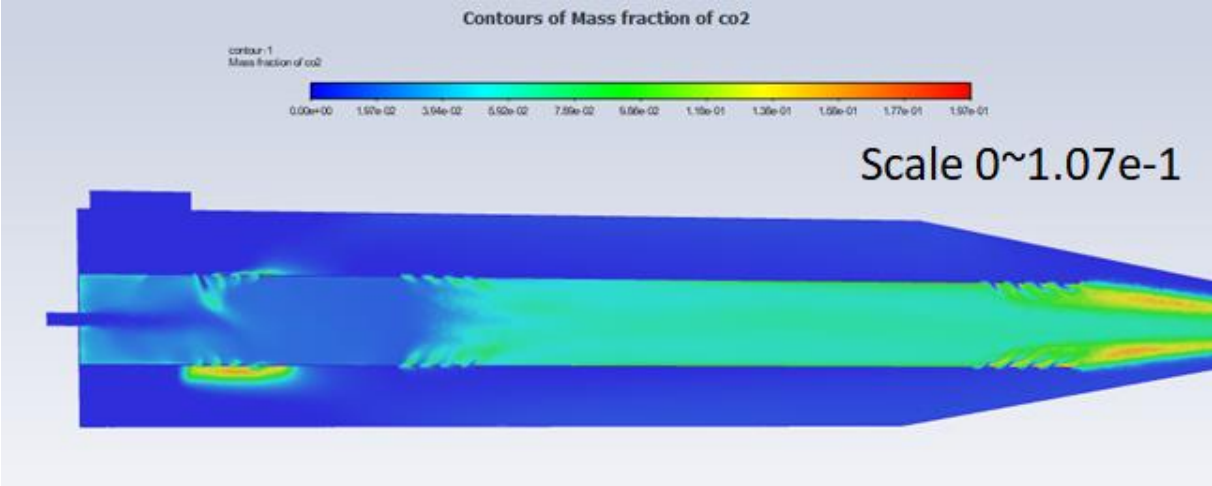
Fig 5.19: Mass fraction of CO2
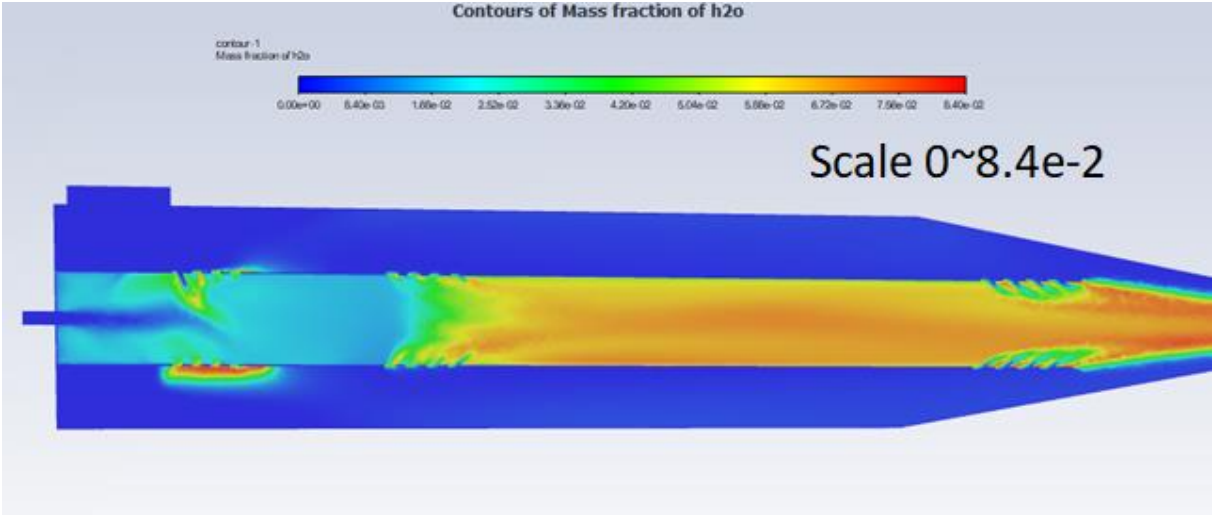
Fig 5.20: Mass Fraction of H2O
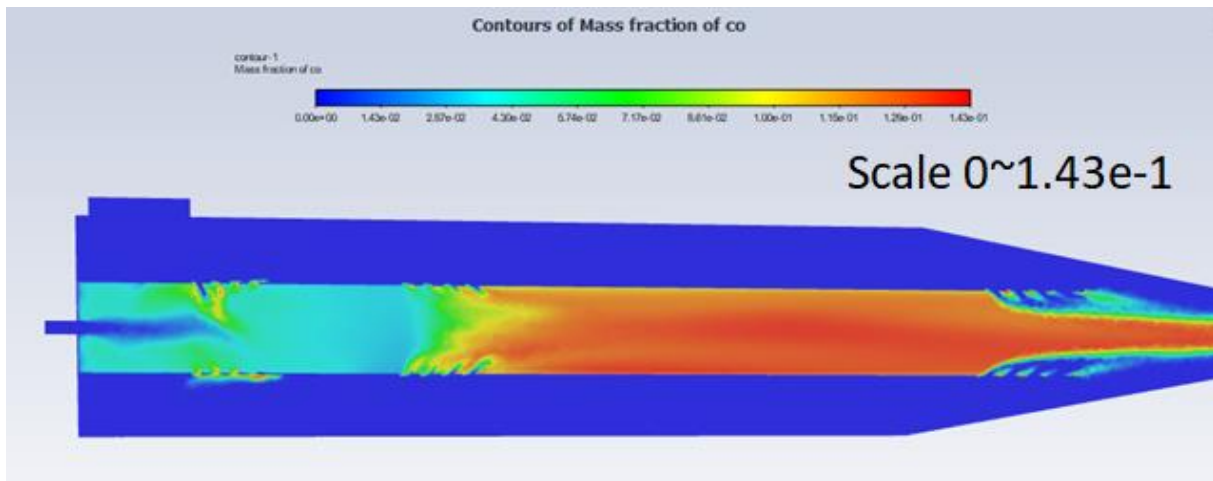
Fig 5.21: Mass Fraction of CO
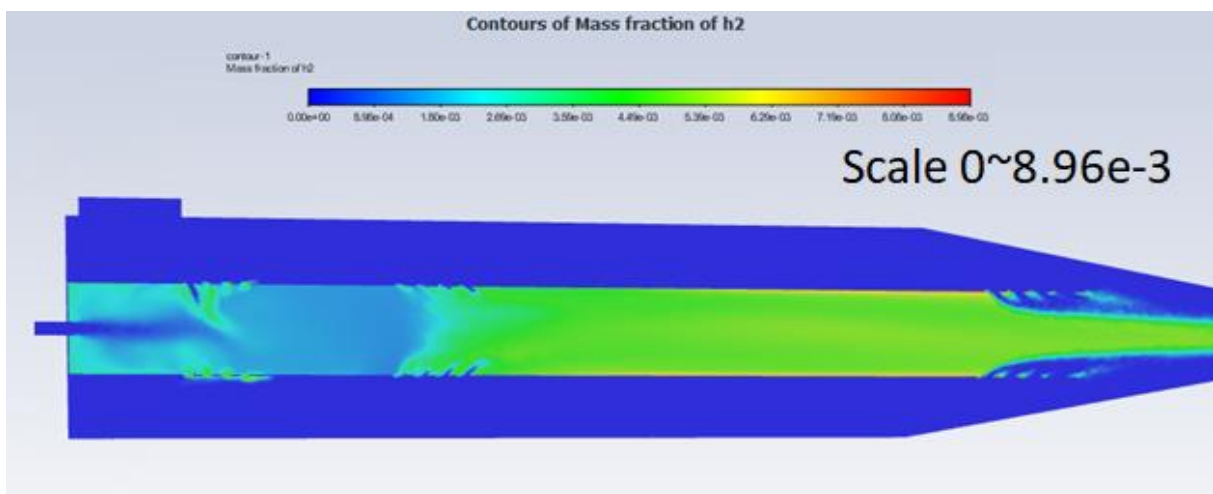
Fig 5.22: Mass Fraction of H2

Minor species production
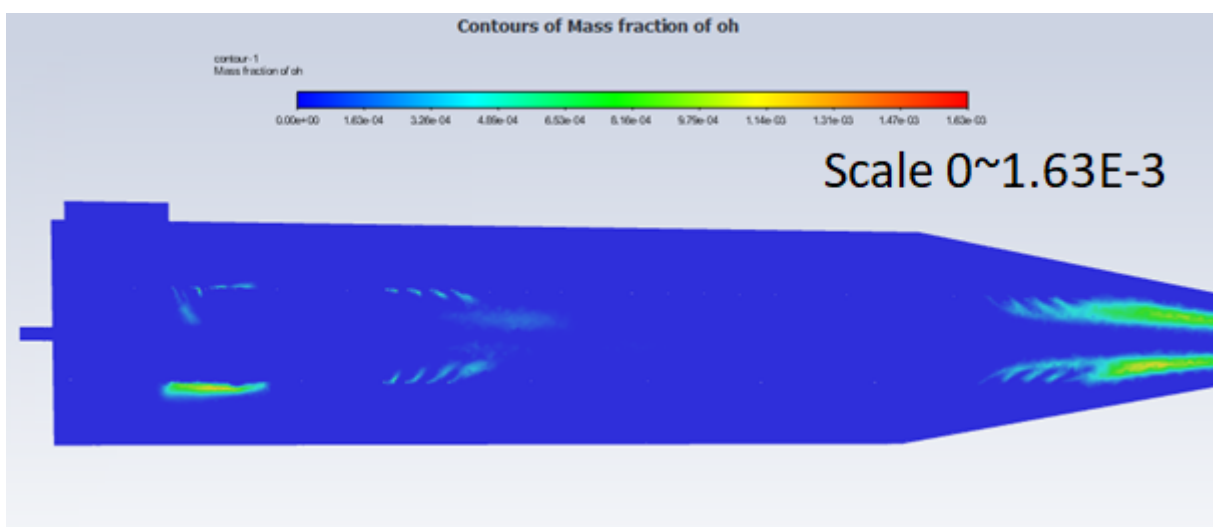
Fig 5.23: Mass Fraction of OH
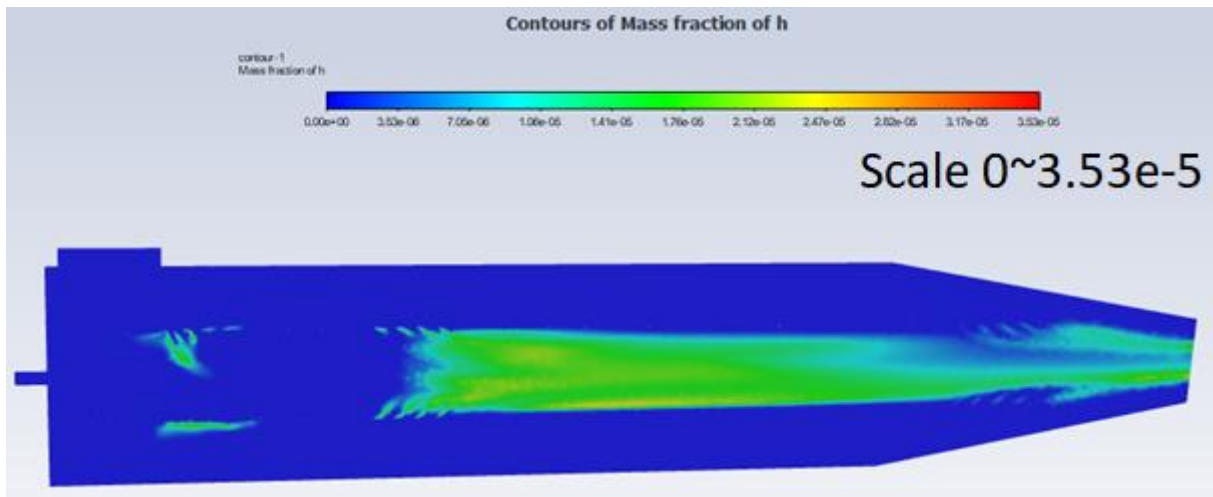
Fig 5.24: Mass Fraction Of H
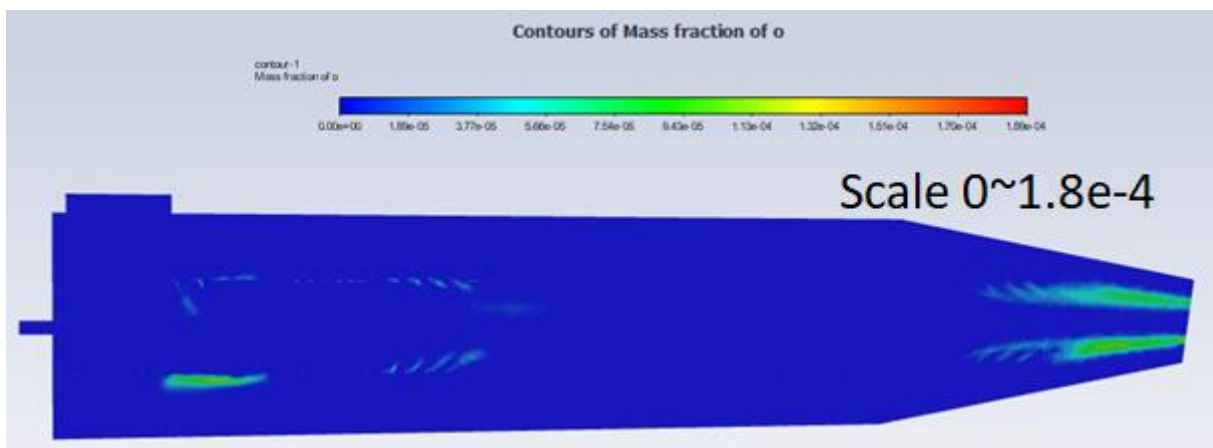
Fig 5.25: Mass Fraction Of O

As stated before; there are two main prodcuts concetration charts the first inculdes CO_2 and H_2O which are the stable for any combustion type reaction, CO which is the result of an incomplete reaction between the fuel and the air, in fact in the mechanism proposed by Singh and Jachimowski (1994), the first reaction that happen to break the initial reaction forms both CO and H_2, which leads us to our next and last major reaction product being H_2.

The minor species are H, O, and C_2H_2 which have a very small mole fractions, due to having sub-reactions that does have a very low interaction frequency.

5.3.2. The Effect of equivalence ratio and air pre-heat variation on the the final combustion temeperature

The (fig 5.26) shows that the final temperature increases with respect to the equivalence ratio change and increase toward the unit ($\phi=1$), as noticeably, air pre-heating result in an overall increase in the final temperature, that is of corse due to hotter air having more energy to spare for the molecules to use for dissociation and formation of the products.As shown in (fig 5.26) The decrease in the temperature is caused because of the formation of different species in the reaction products, those draw the activation energy required for their sub-interactions directly from the overall energy released by the reactants, and for an equivalence ratio higher than the unit ($\phi>1$) then more the increase the lower the temperature will be due to the cause previously mentioned.

We can tell that there are two main parts, one with a lean mixture (fuel relative) and another with a rich mixture, Since fuel is the deciding factor here, we can get the same temperature for different equivalence ratio values (before and after the reaction hits the maximum adiabatic temperature).
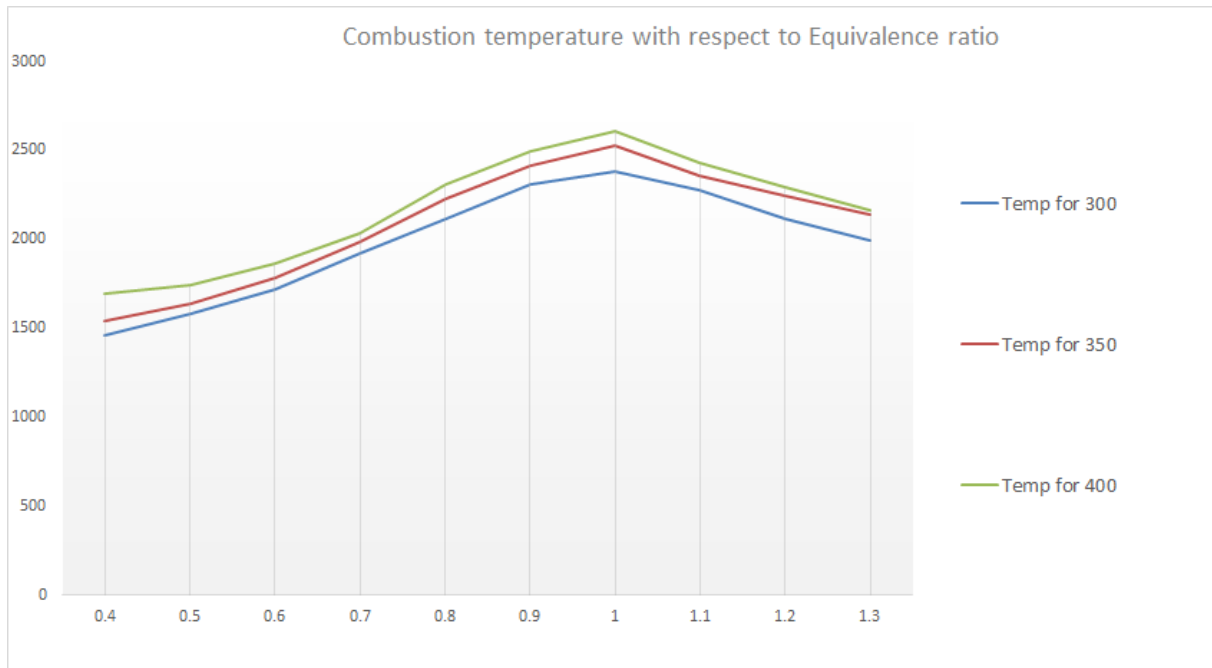
Fig 5.26: Combustion temperature variation with respect to ϕ for different Pre-Heat Temperatures

The (fig 5.27) shows the experimental values for the p9005 gas turbine temperature variation, and as predicted the temperature increases with respect to the fuel/air ratio as long as it is smaller than the stochiometric value (resulting in a smaller than unit equivalence ratio).

FUEL FLOW			AIR FLOW		OIL	PRESSURES			TEMPERATURES				
M_f	T_g	P_g	g/sec	P-RP	T_{oil}	P_3	P_4	P_2-P_3	T_1	T_2	T_3	T_4	T_5
gram/sec	°C	KPa		mm H_2O	°C	bar	bar	mm Hg	°C	°C	°C	°C	°C
2.34	18.26	154	148.72		64.40	0.69	0.15		18.99	93.98	726.07	624.76	501.95
2.12	18.47	148	134.45		65.63	0.58	0.13		18.77	83.59	713.38	622.31	505.86
1.87	19.06	150	120.53		62.89	0.48	0.10		19.17	74.45	699.71	615.97	500.73
1.69	19.56	152	107.92		60.50	0.40	0.09		19.31	67.07	700.20	618.65	501.95
1.54	19.92	154	96.51		58.64	0.33	0.08		19.25	60.94	712.16	630.13	511.23
1.43	21.09	150	83.91		56.45	0.27	0.06		19.54	55.27	747.31	656.25	529.05

T3 OVER TEMPERATURE SETTING   900°C

BELT TENSIONING RAM PRESSURE   KPa

PITOT - REVERSE PITOT CONSTANT

AIR FLOW CALIBRATION EQUATION:-

$$M_{air} = 11.51\{h\}^{0.5}$$

Fig 5.27: Temperature variation with respect to ϕ [29]

Almost Hydrocarbon fuels show a simmilar behaviour for a variation of equivalence ratio, the rise of temperature for a lean mixture, and a decay for a rich mixture as shown in the next fig (Fig 5.28).
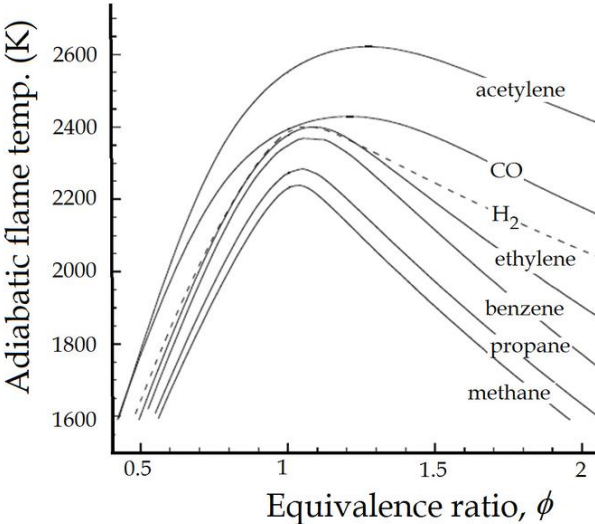
Fig 5.28: Different Fuels Adiabatic flame temperature with respect to equivalence ratio [56]

The air entering from the inlet circulate the area around the interior flame tube, the different entrences in the tube will allow fuel access to the air which will start the combustion process, this is what the total temperature contour taken from a general benchmark of the combustor (fig 5.29)
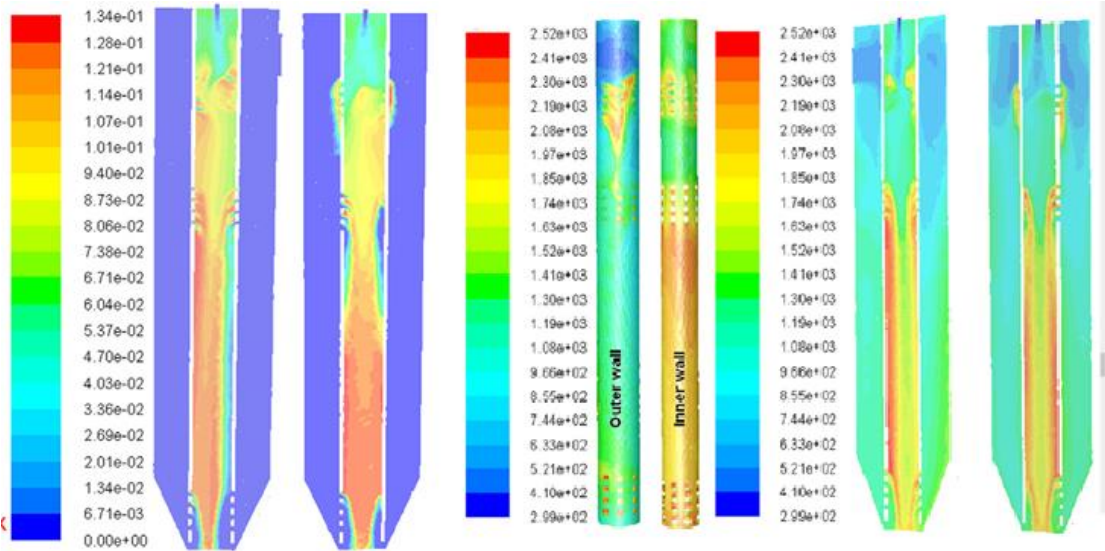
Fig 5.29: Combustor Benckmark Results [54]

The temperature rise happens in the contact zones scattered across the surface of the interio flame tube. The next 2 figures (Fig 5.30) (Fig 5.31) show the maximum temperature change with a non pre-heated air and 100K pre-heated air combustion processes. Pre-heating air will allow a higher free energy range than the non pre-heated one allowing for a higher TIT to be achieved.
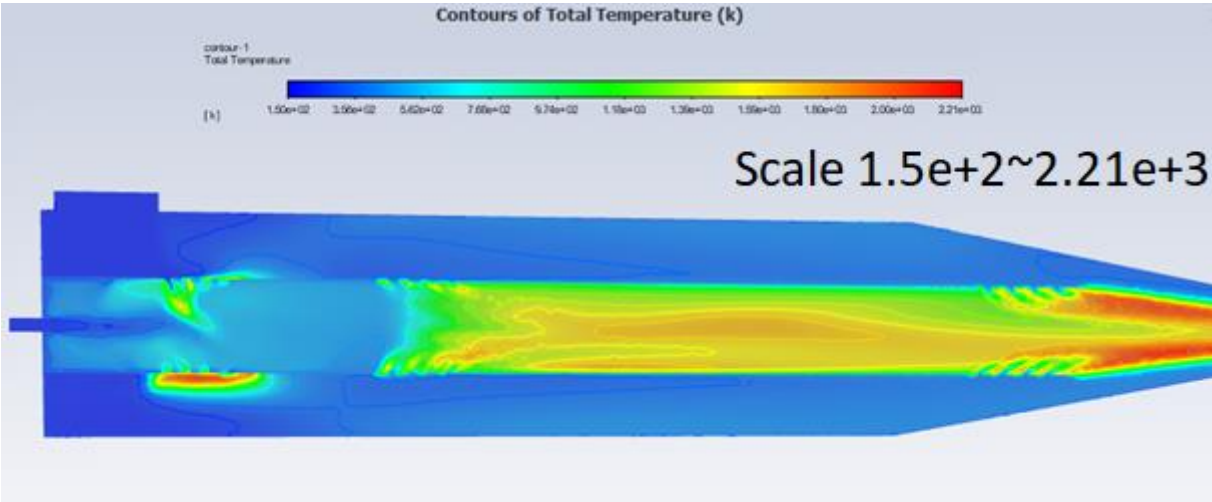
Fig 5.30: The total temperature contour for 350K air temperature
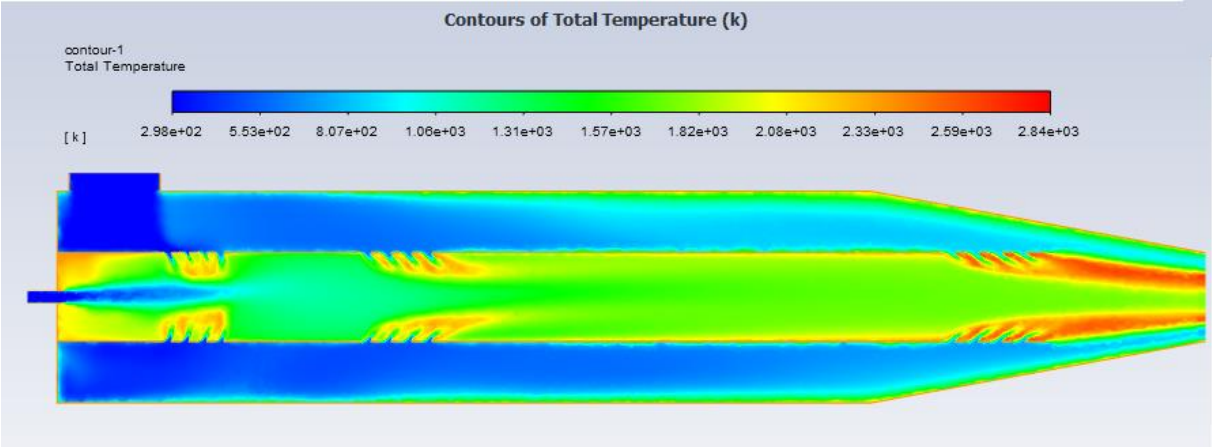
Fig 5.31: The total temperature contour for 400K air temperature

Here in the next figure (Fig 5.32) (Fig 5.33) we show a side by side comparison between different stations of iso-temperature contours showing the effect of pre-heat air on the final adiabatic temperature.
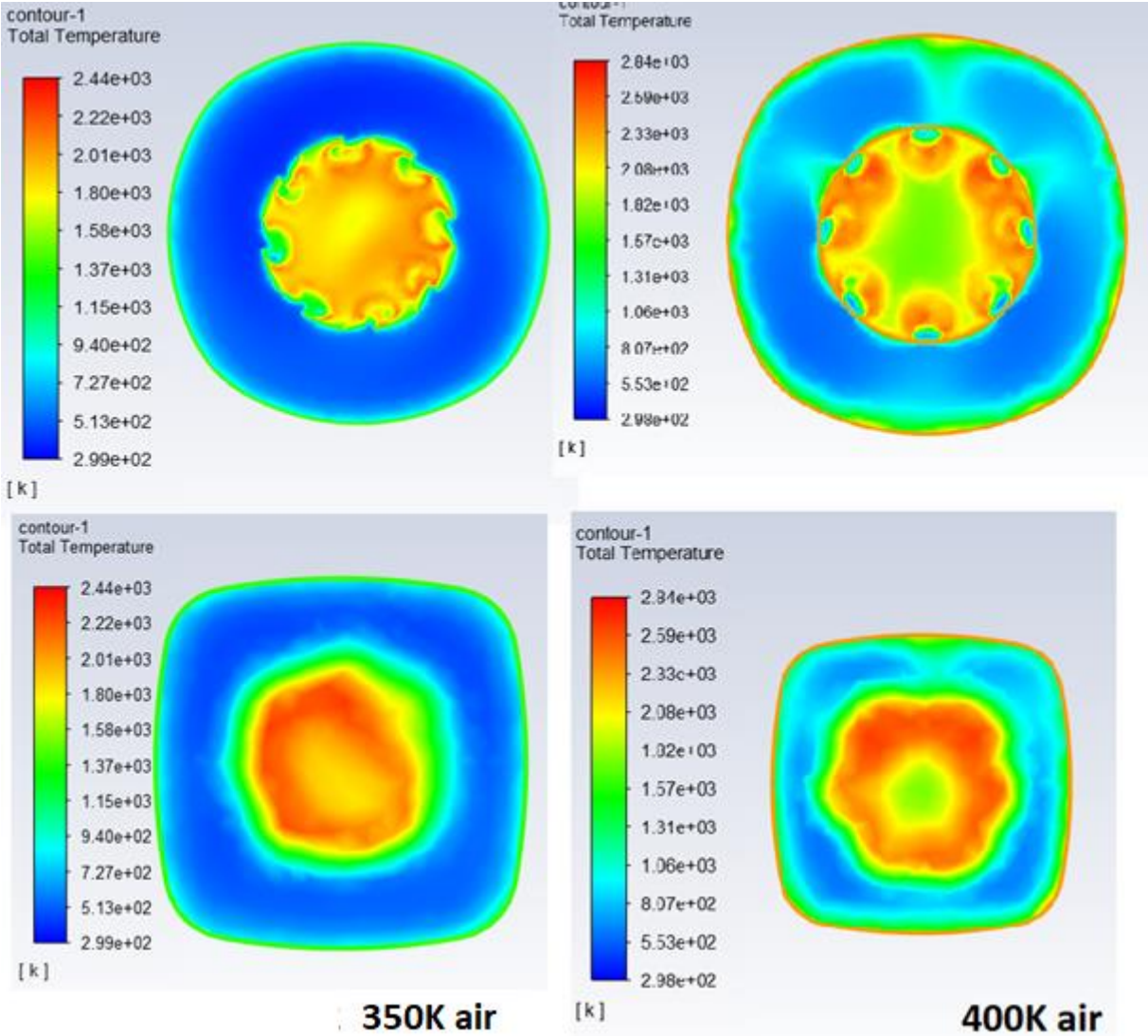
Fig 5.32: Side By Side Comparison between Iso Stations of Total Temperature For Different Air Pre-Heating Temperatures
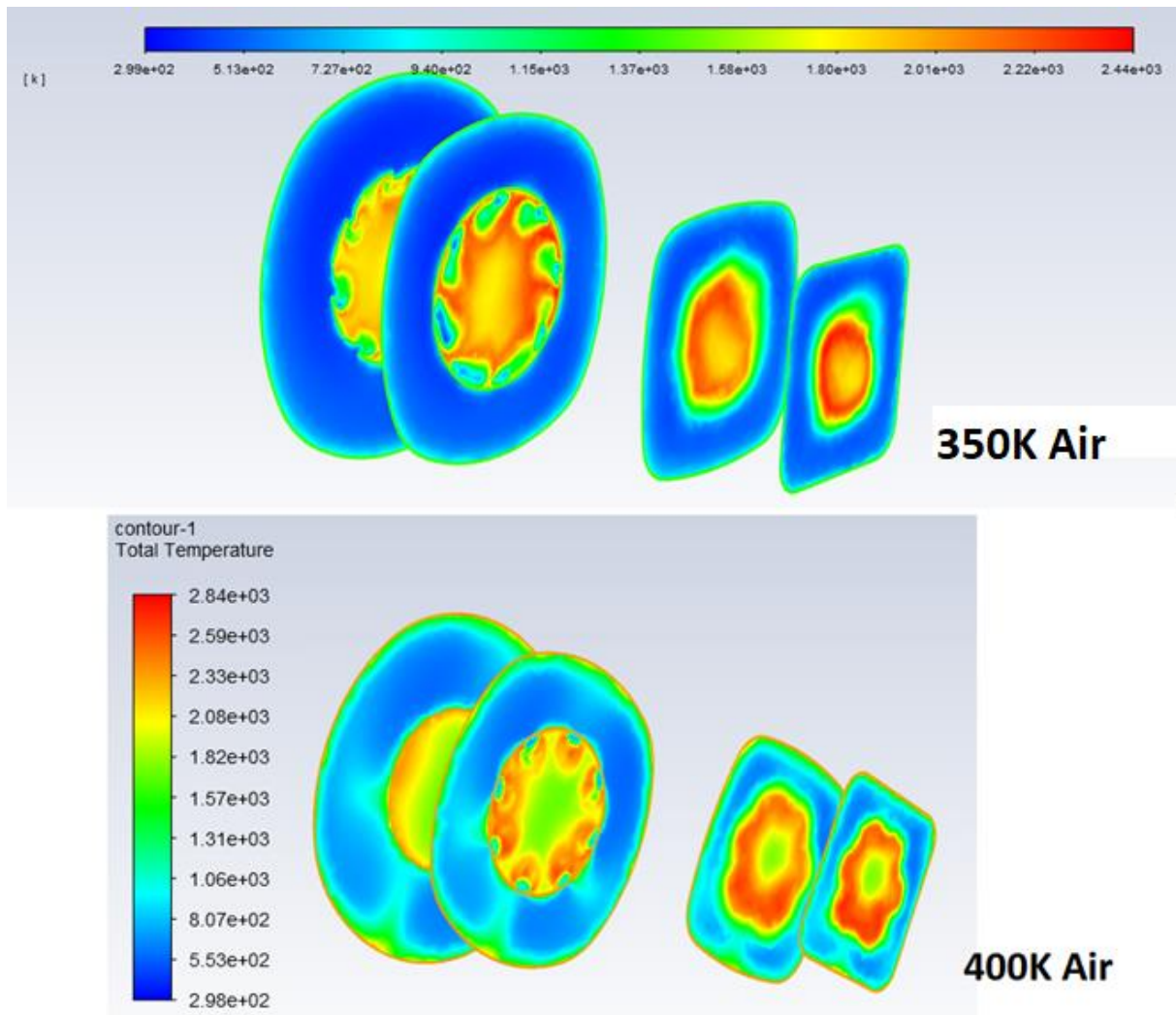
Fig 5.33: Comparison Between Overlay of Different Iso Stations of Total Temperature For Different Air Pre-heating Temperature

5.3.3. The effect of pre-heat on the production of CO

The (Fig 5.34) (Fig 5.35) (Fig 5.36) taken from the simulation of combustion in Ansys show different pre-heating air temperatures for different air pre-heating temperature, in more detail, with a higher pre-heating temperature the mass fraction of CO shows a noticeable drop.

According to the kinetic model's dissociation equations, every sub-equation that has CO as product has also a relatively higher activation energy requirement, meaning that the more CO is present in the combustion product the lower the overall adiabatic temperature will be.

As shown before the CO production is lower for a lower equivalence ratio, meaning if we want to keep its production as low as possible it is preferably better to use a lean mixture. The same result will take place if the air used in the combustion is pre-heated, the higher the preheating temperature the lower CO production will be.
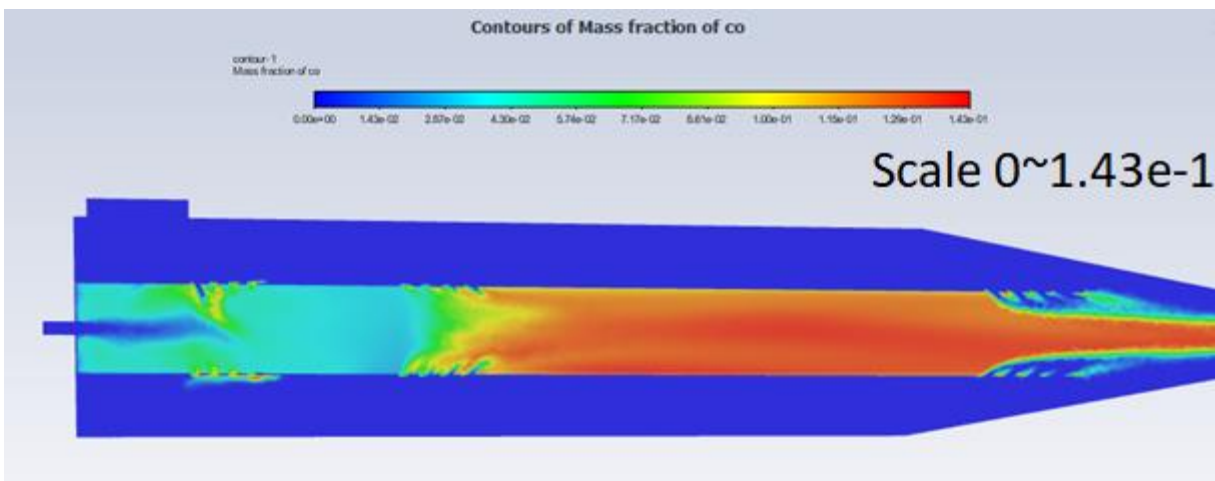
Fig 5.34: CO Mass fraction contour with 50K air preheat
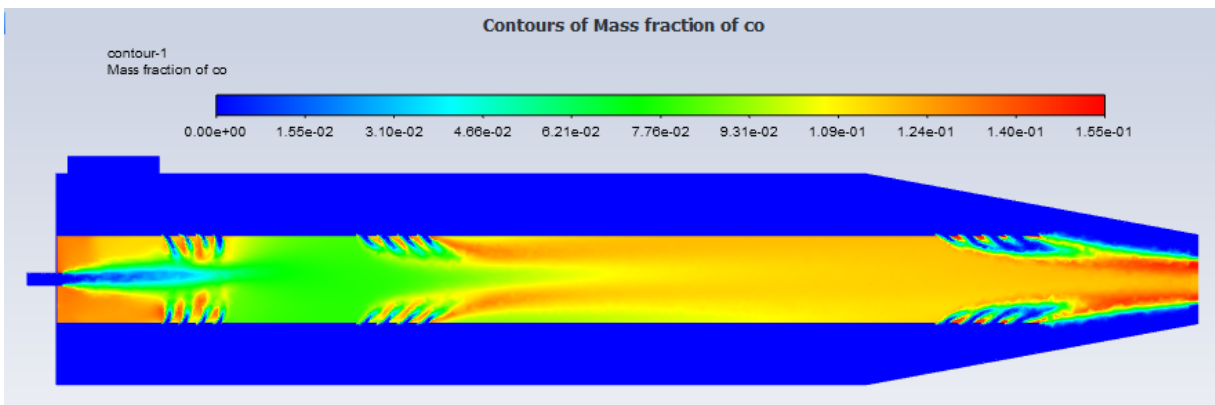
Fig 5.35: CO Mass fraction contour with 100K air preheat

In these plots, we confirm the decrease in mass fraction of carbon monoxide for different inlet pre-heating temperatures, that of corse is due to the meduim having an overall increase in total energy to use, in better terms the temperature rise means the molecules will have a higher vibration and movement, which allow for a better mixing of the air/fuel which results in better and more complete combustion process, that translate into a drop in mass fraction of CO.
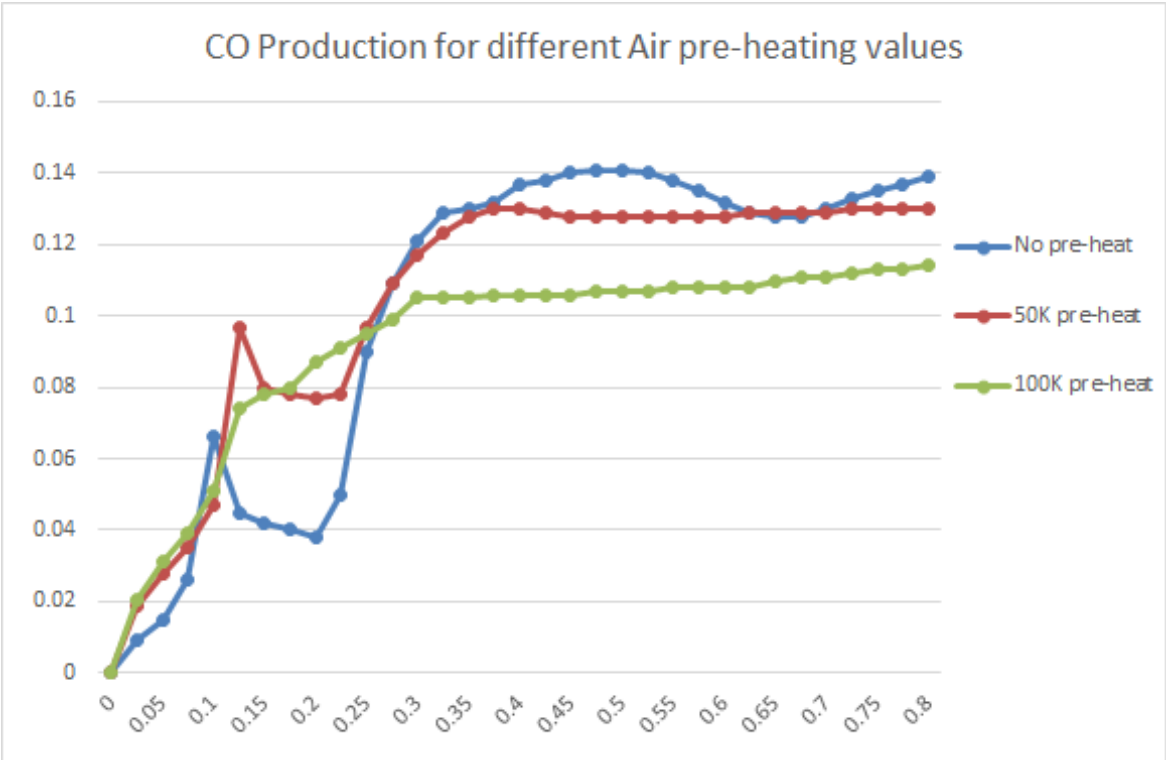
Fig 5.36: Mass fraction of CO for different pre-heat temperatures

The next simulation results taken from "The Effect of Inlet Air Preheat on CO And NO Production in the Combustion of Diesel in Canister Burner" article, the purpose was to study the Computational Fluid Dynamics (CFD) prediction on the formation of carbon monoxide and oxide of nitrogen (CO-NO) inside the canister burner with inlet air pre-heating of 100 K and 250 K by designing an appropriate air swirler to produce stable, efficient and low emission combustion with low pressure losses, the results show a drop in the CO production for the 100K and 250K inlet air pre-heating temperatures.
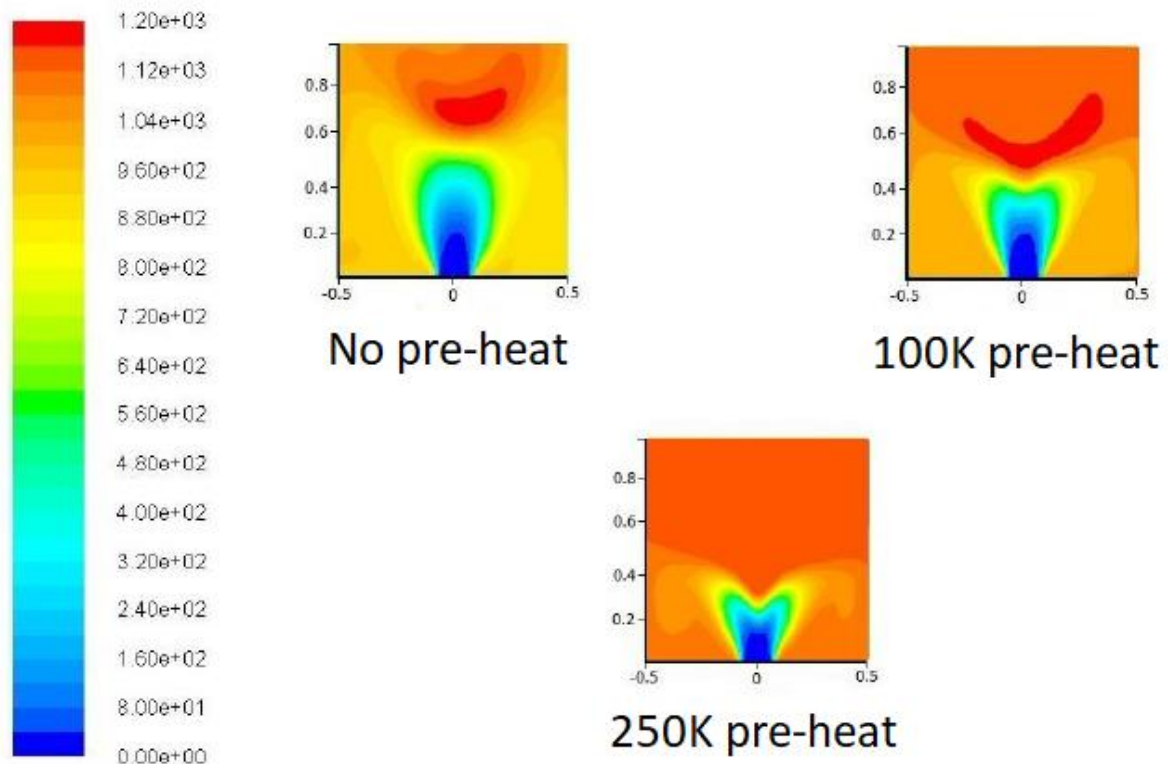
Fig 5.37: Effect of preheat on the production of carbon monoxide (Scale in PPM) [57]

The CFD simulation described in this paper shows that the combustion with inlet air pre-heat results in improved CO emission production. The CO concentration improved from 1200 ppm for combustion without inlet air pre-heat to 1000 ppm for combustion with 250 K inlet air pre-heat.

5.3.4. Pressure variation within the combustor

Since the gas turbine combustion happens at a constant pressure according to the Brayton cycle, we would be expecting a constant pressure value within the combustion zone, this is exactly what the pressure plot (Fig 5.38) taken from the Ansys simulation shows as it stays relatively constant during the whole process but drops at the exit, a sign of dynamic pressure increase as shown in (Fig 5.39) which tells us that there is an increase of flow velocity at that area due to the reaction gas expanding pre-entering the turbine inlet.
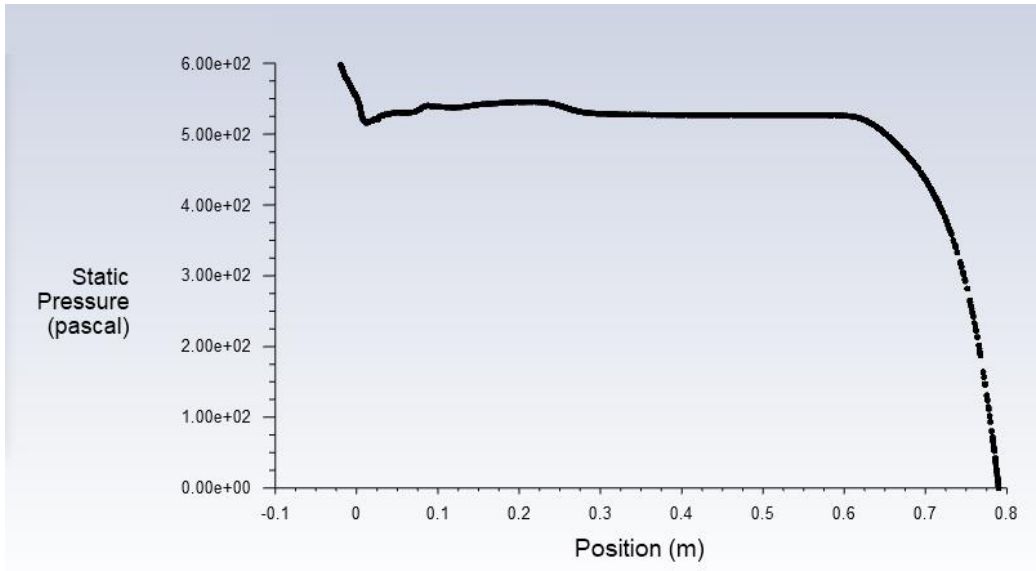
Fig 5.38: Static pressure with respect to the combustor length
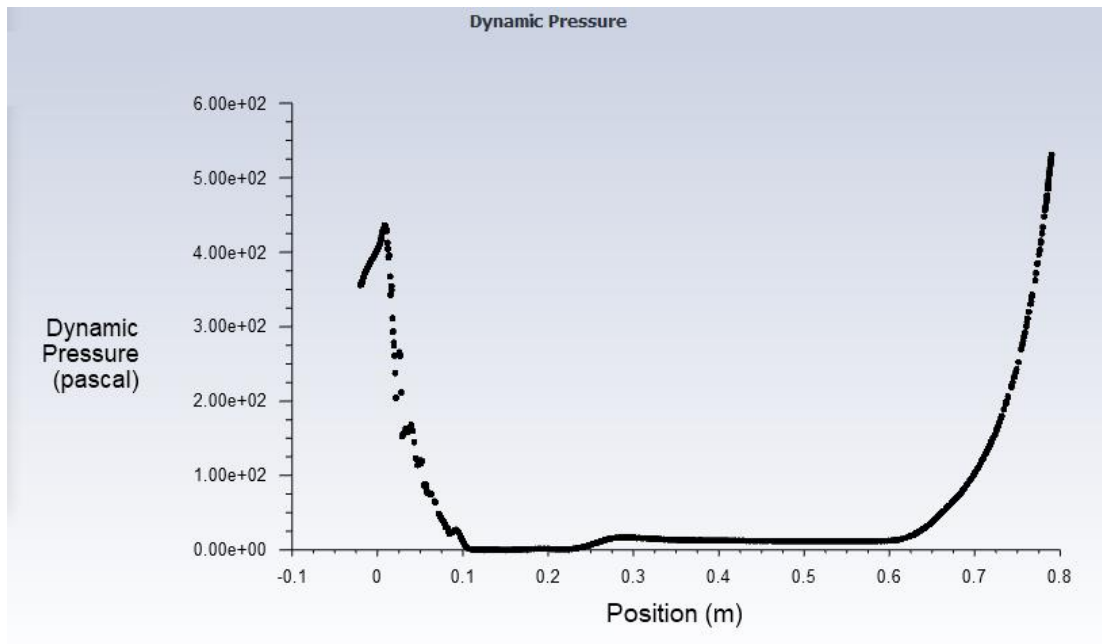
Fig 5.39: Dynamic pressure with respect to the combustor length

The next the simulation run with 400 air pre-heating temperatures along side the static pressure variation across the combustor section (Fig 5.40) (Fig 5.41). The results show a slightly different but overall stable static pressure, as the combustion occurs in an isobar medium.
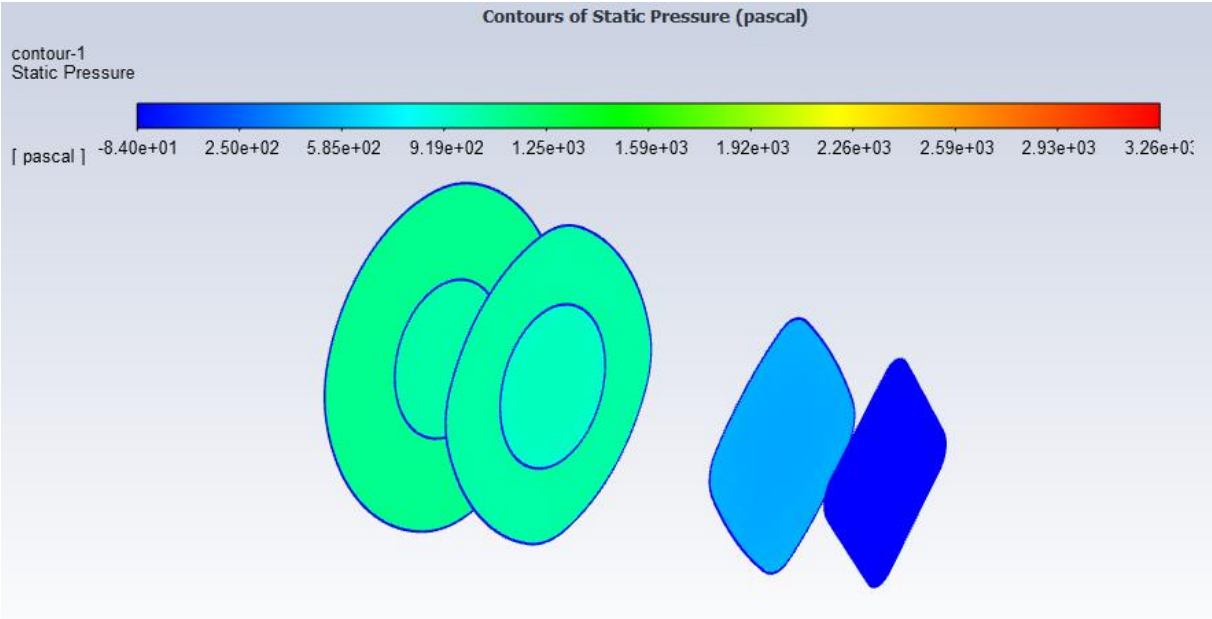
Fig 5.40: Iso-Static Pressure Contours Overlay
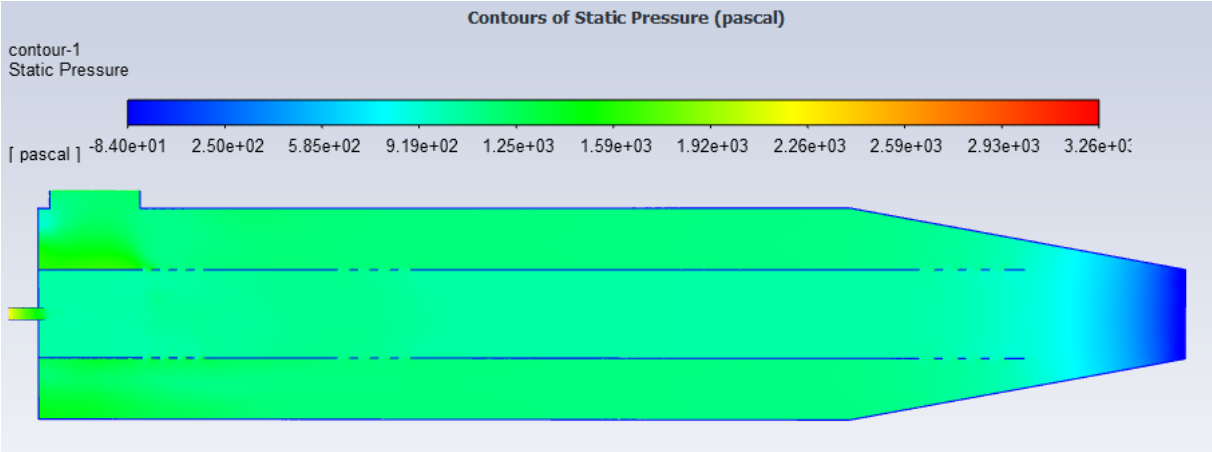
Fig 5.41: Static Pressure Contour Along The Combustor

We notice from the next figure (Fig 5.42) that the pressure has a slight effect on the adiabatic flame temperature, for a higher pressure the tempearature will rise a bit, however at a threshold of 0.8 Mpa the temperature does no longer have a significant increase, that is due to the fact that at high pressure the dissociation of stable molecules is decreased, and since there is no change in the chemical composition effected by the pressure rise it wont have an effect on the temperature.
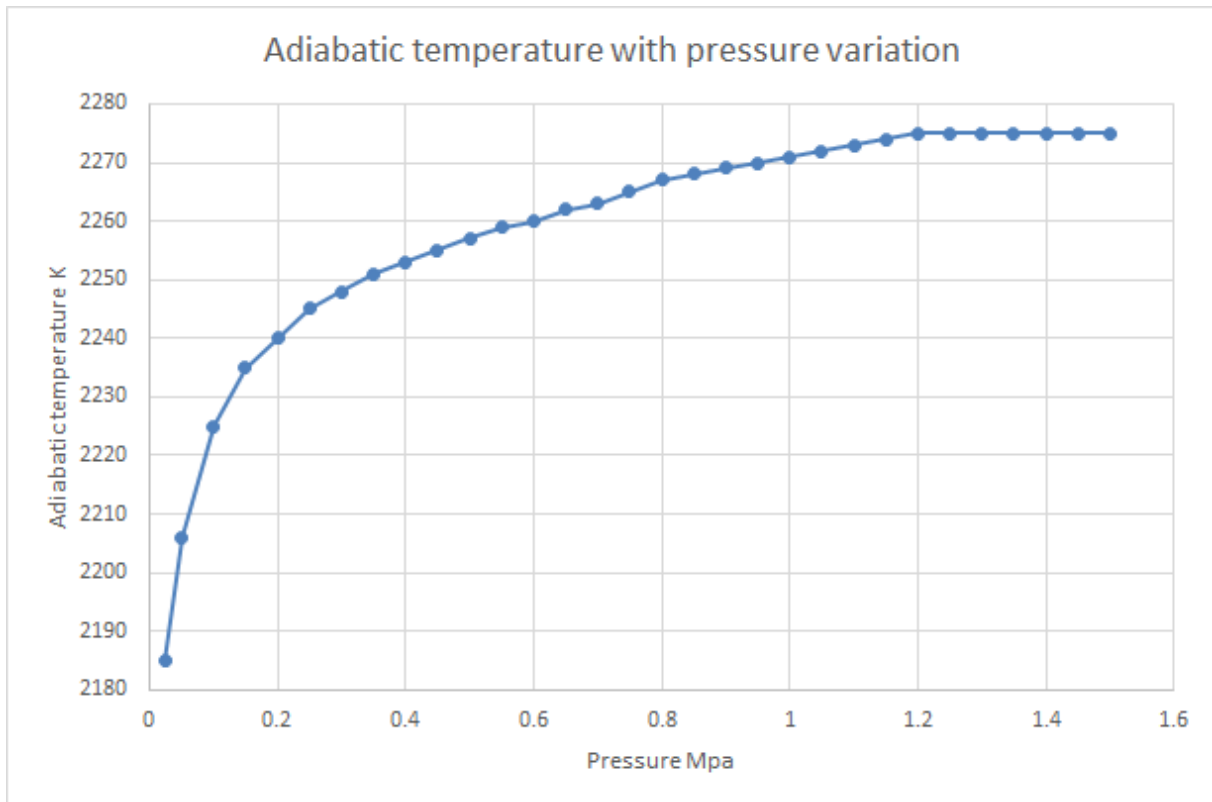
Fig 5.42: The effect of pressure rise on the adiabatic temperature [58]

5.3.5. <u>Flame velocity</u>

The (Fig 5.43) shows the velocity of the gas peaking at the exit of the flame tube, this is due to the expansion of the gas entering the convergant area of the combustor which explains the drop in static pressure. The contour of the velocity shows that it reaches a value of 80m/s for no pre-heated air 100m/s for 300k air and 120m/s for 400k air before entering the turbine. Total pressure is conserved for a drop of static pressure cause the dynamic pressure to increase, thus increasing the velocity of the flow
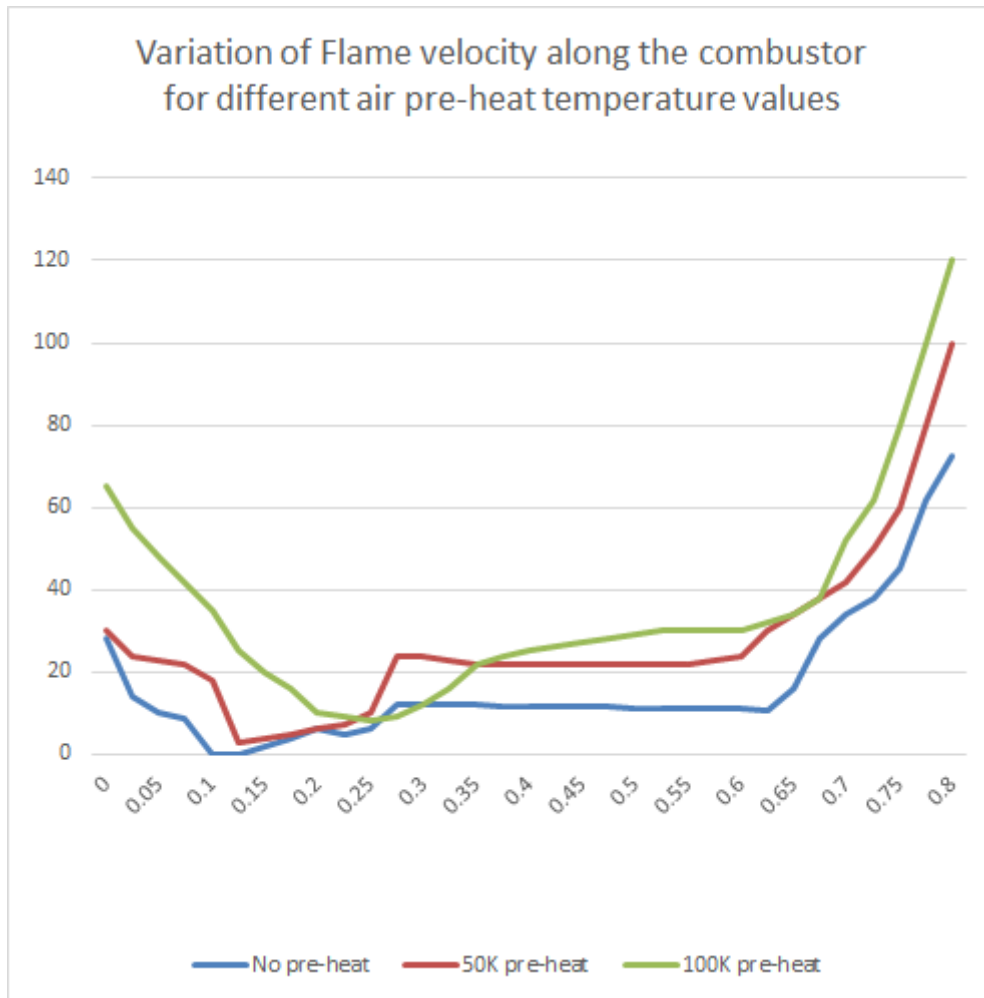
Fig 5.43: Flame Velocity Magnitude for no pre-heated air/50K pre-heated air/100K pre-heated air respectively

Here in (Fig 3.44) (Fig 5.45) we have a side by side velocity vectors in different stations in the direction toward the outlet, between a 350K pre-heated air and a 400K pre-heated air.

First station

Second station

Third Station
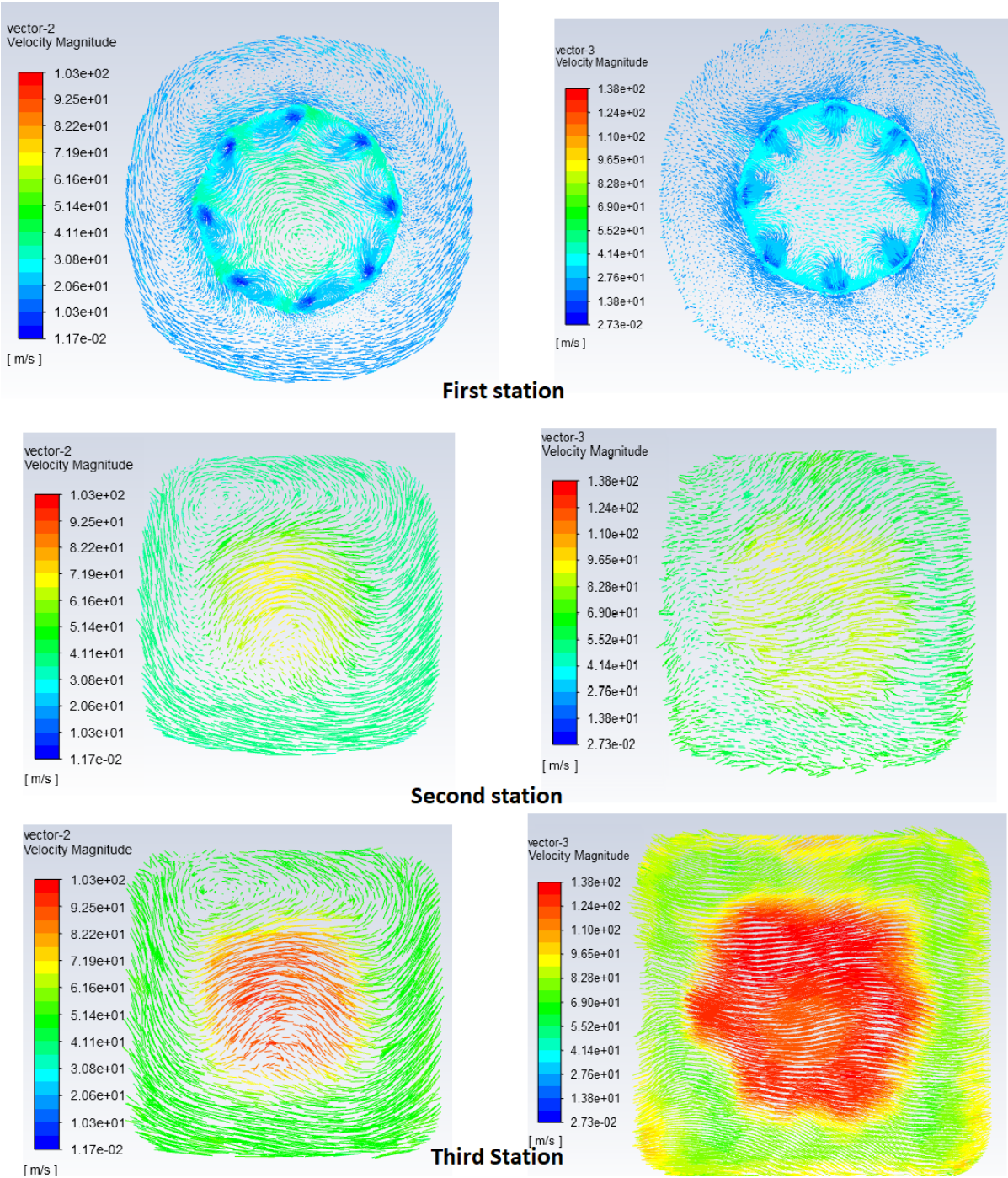
Fig 5.44: Side by side comparison of velocity vectors in different stations across the combustor section for 50K/100K pre-heated air
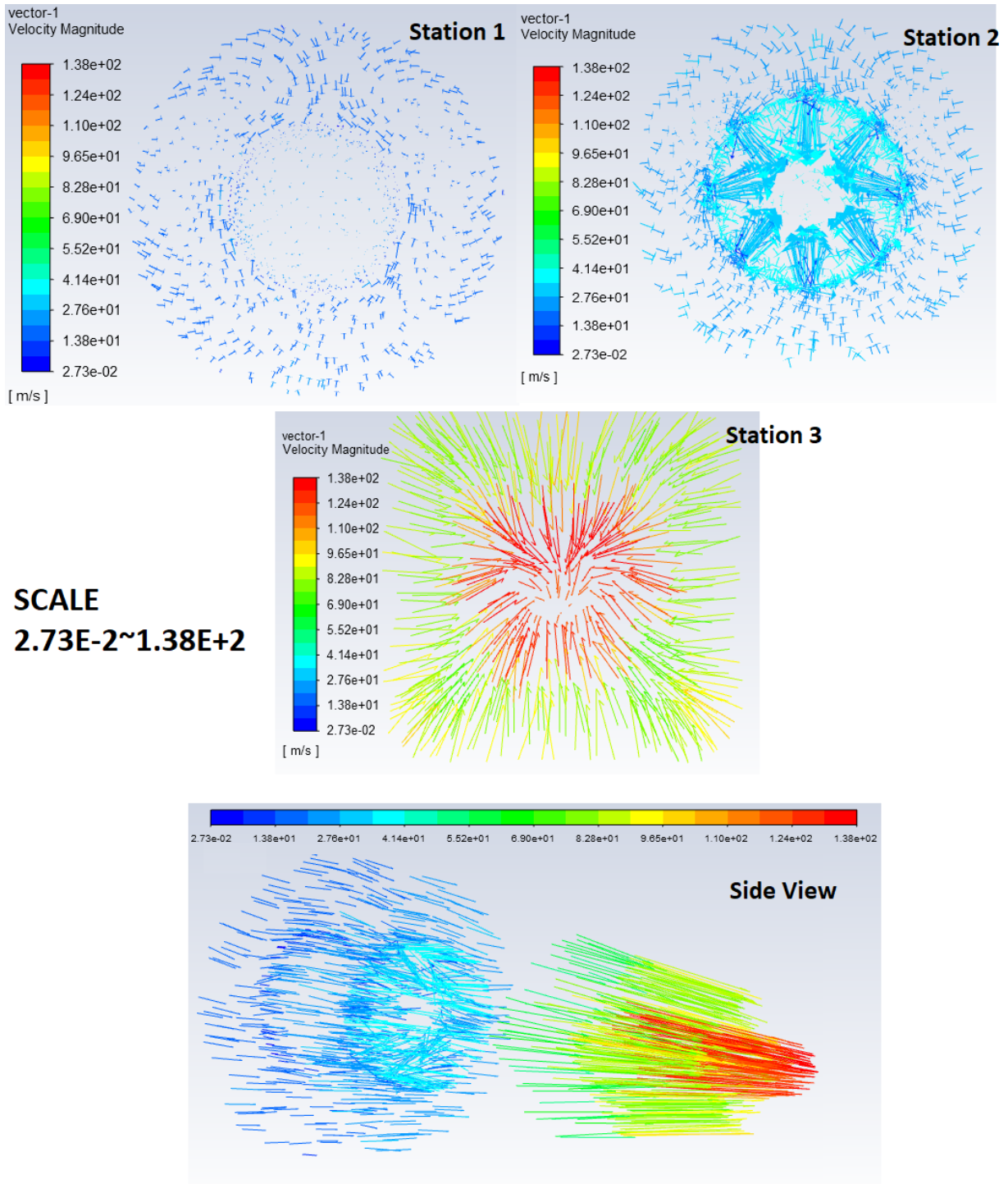
Fig 5.45: Velocity Vectors orientation with low vector density
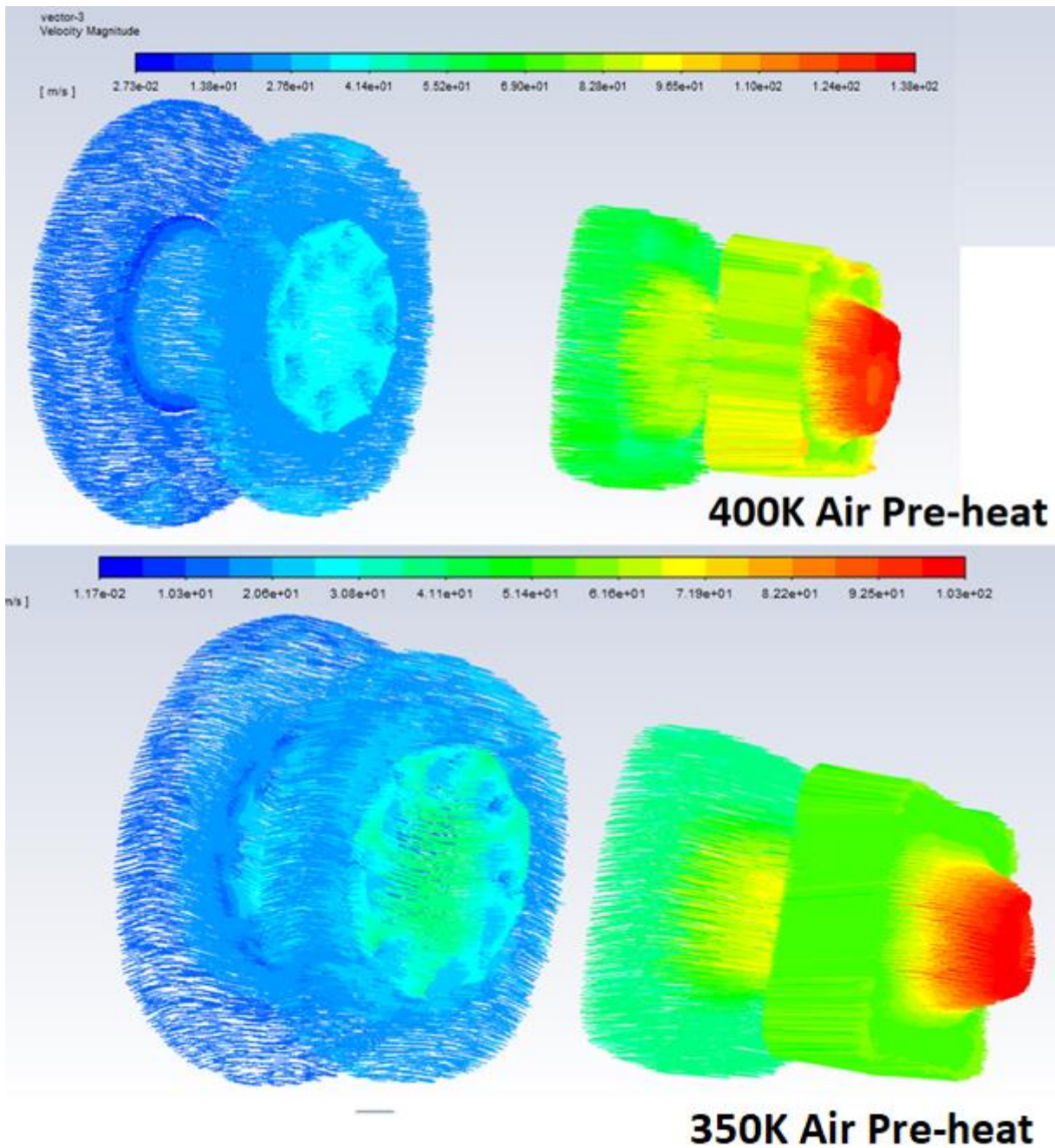
Fig 5.46: Velocity Vectors Overlay for different Air pre-heating temperatures

Heat, like sound, is a form of kinetic energy. Molecules at higher temperatures have more energy, thus they can vibrate faster. Since the molecules vibrate faster, they travel at a higher velocity throught the medium, meaning, the increasing temperature increases the speeds at which molecules move. (Fig46) (Fig47) (Fig48) (Fig49) (Fig50) (Fig51)
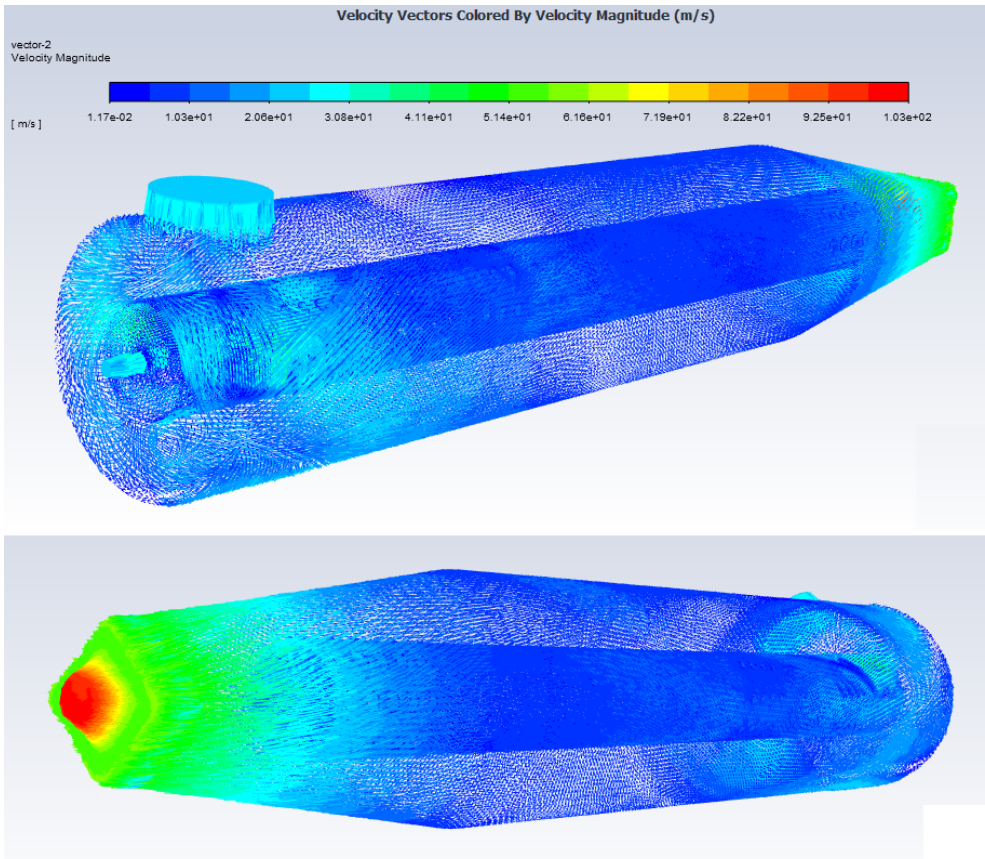
Fig 5.47: 350K air Velocity vectors 3D
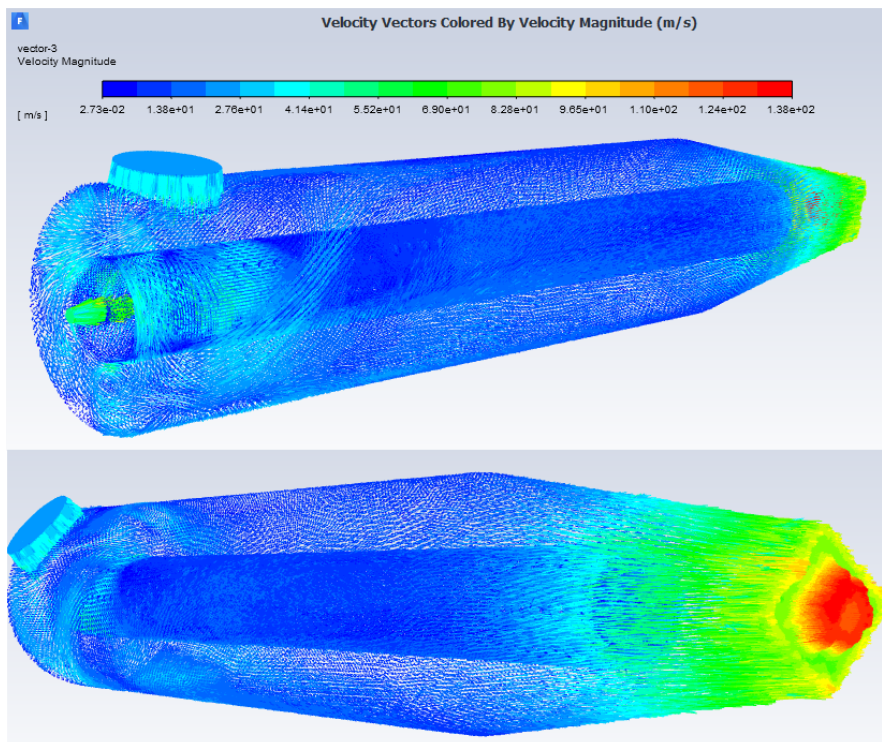
Fig 5.48: 400K air Velocity vectors 3D
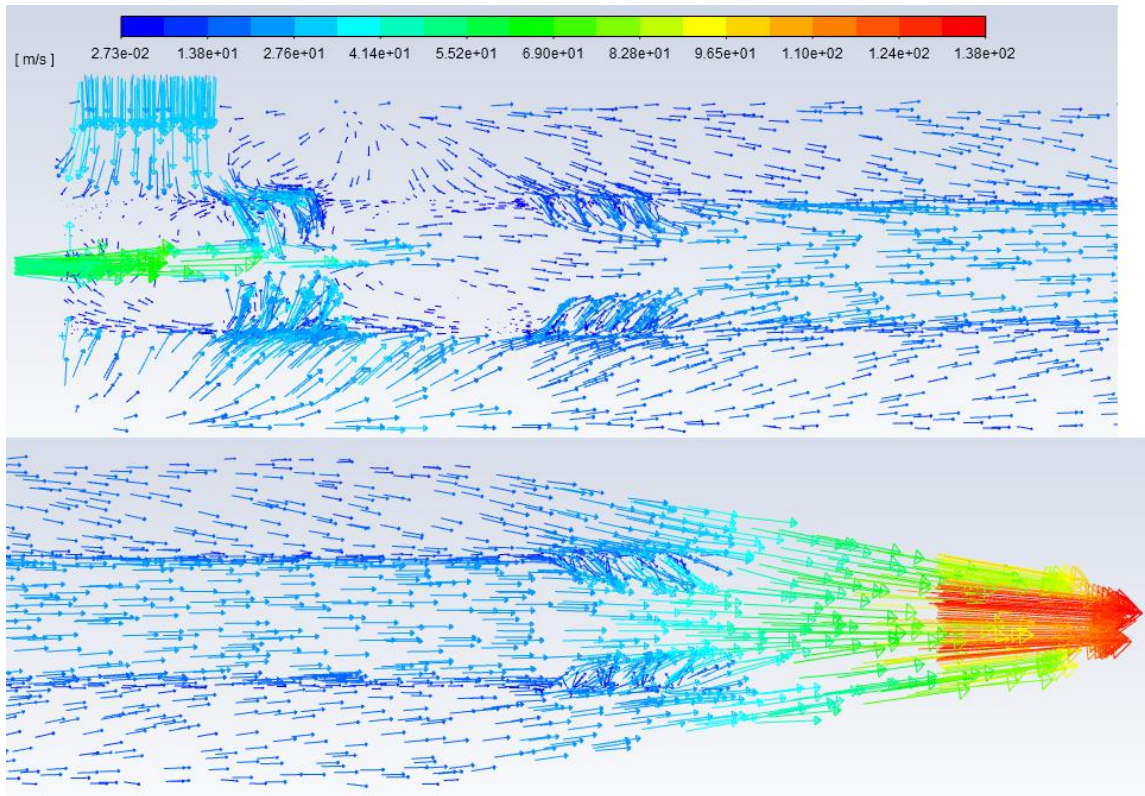
Fig 5.49: 100K pre-heat air velocity Vectors close up
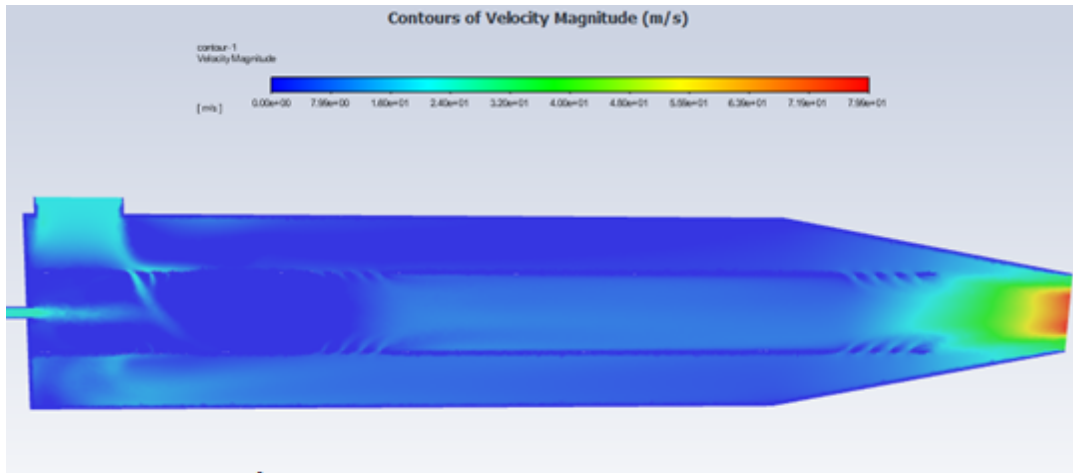
Fig 5.50: No pre-heat air velocity contour
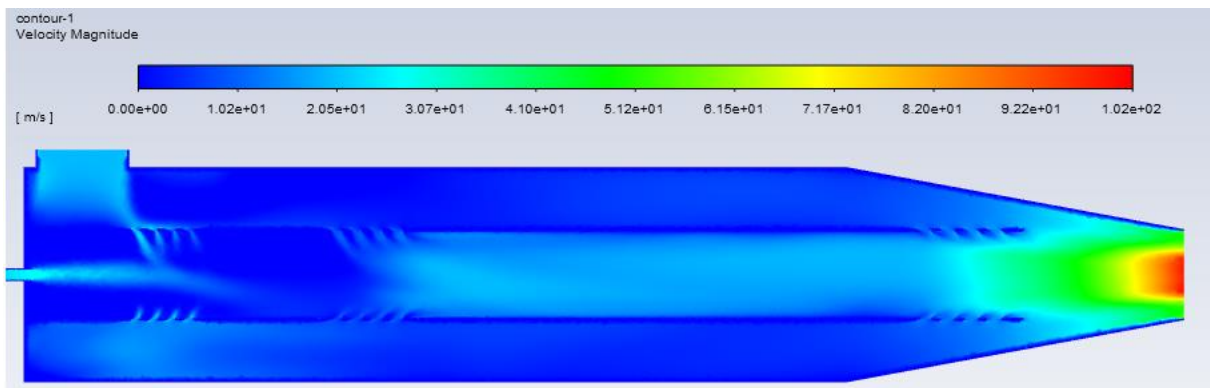
Fig 5.51: 50K pre-heat air velocity contour
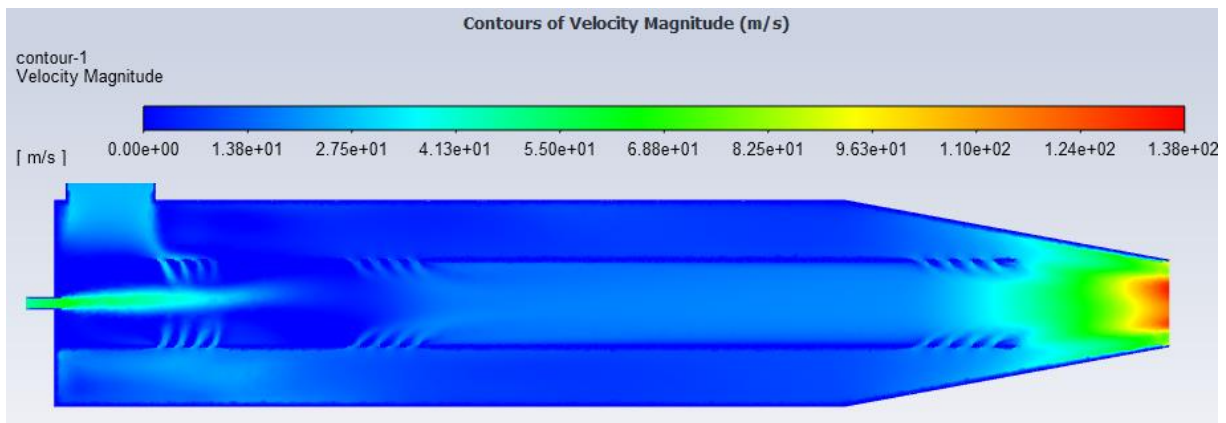
Fig 5.52: 100K pre-heat air velocity contour

Conclusion

To finalize our work the following conclusions are derived from the matlab program and CFD simulation described in this paper.

The mole fractions of the product species can be divided into two main categories, major species and minor species, depending on the equivalence ratio value. For a lean mixture the Major products are CO_2, H_2O, O_2, H_2 and CO not to mention N_2 since it did not have any dissociation reaction so it stays the same, as for a rich mixture the major products are the same but with different mole fractions, as the CO_2 and H_2O fractions start decreasing, where the CO and H_2 keep increasing, the O_2 vanishes completely due to its total consumption.

The Adiabatic temperature rises with the equivalence ratio as long as the mixture is lean, reaches a maximum at the stoichiometric value, then start decaying for a richer mixture, this can be explained by the increase in the mole fractions of the reaction product, since those reaction are endothermic, more heat is absorbed to create them which leads to an overall decrease in the final temperature. It is also noticeable that the air pre-heating causes the adiabatic temperature to rise as well, the pre-heat temperature can be translated into more energy that the combustion reaction takes advantage of by easing the production of the different species, however the pre-heating effect does not change the general shape of the temperature graph, it still rises for a lean mixture and drops significantly for a rich mixture. With that, we can conclude that for a better adiabatic temperature it is better to use a lean mixture, with an inlet air pre-heating.

The CO production is heavily effected by two parameters, the equivalence ratio, and the pre-heating temperature, for a low pollutant production, it is deduced from the previous analysis and simulations that the mixture should be lean, due to the reaction being more complete than the case of a rich mixture, this alongside an inlet air pre-heating which provides and overall increase in the reaction energy should keep the mole fractions of the pollutants as low as possible.

The combustion occurs at a somehow constant pressure, the final temperature slightly increases with the increase of the pressure, until it reaches a certain threshold of ~0.8 Mpa, after which the increase of the pressure does not have a significant effect on the adiabatic temperature, which is the result of the negligible change in the chemical composition at high pressure.

The flame velocity increases with the increase of the air pre-heating temperature, which is explained by the fact that a higher temperature means higher energy, and the more energy is given to the molecules the more they vibrate, giving them a higher velocity.

Figures

Annex A: Gordon_Mc Bride constants for calculating enthalpy

Thermodynamic data for many individual species can be conveniently stored for use with computer programs in the form of coefficients associated with equations that reproduce the data. The following dimensionless form was chosen for this report:

$$C_p^o(T)/R = a_1 T^{-2} + a_2 T^{-1} + a_3 + a_4 T$$
$$+ a_5 T^2 + a_6 T^3 + a_7 T^4 \quad (1)$$

Enthalpy was obtained by integrating $C_p^0(T)$, with respect to T:

$$H^o(T)/RT = -a_1 T^{-2} + a_2 lnT/T + a_3 + a_4 T/2$$
$$+ a_5 T^2/3 + a_6 T^3/4 + a_7 T^4/5 + b_1/T \quad (2)$$

Some species coefficients that were used in the process of making this thesis

```
C2H2,acetylene     Hf:TRC(10/93) w-3040. Gurvich,1991 pt1 p47 pt2 p39.
 2 g 1/91 C   2.00H   2.00    0.00    0.00    0.00 0   26.0372800      228200.000
    200.000   1000.0007 -2.0 -1.0  0.0  1.0  2.0  3.0  4.0  0.0        10005.839
 1.598112089D+05-2.216644118D+03 1.265707813D+01-7.979651080D-03 8.054992750D-06
-2.433307673D-09-7.529233180D-14                 3.712619060D+04-5.244338900D+01
   1000.000   6000.0007 -2.0 -1.0  0.0  1.0  2.0  3.0  4.0  0.0        10005.839
 1.713847410D+06-5.929106660D+03 1.236127943D+01 1.314186993D-04-1.362764431D-07
 2.712655786D-11-1.302066204D-15                 6.266578970D+04-5.818960590D+01


C2H4              TRC(4/88) w2600. Chao,1975. Knippers,1985.
 2 g 1/00 C   2.00H   4.00    0.00    0.00    0.00 0   28.0531600       52500.000
    200.000   1000.0007 -2.0 -1.0  0.0  1.0  2.0  3.0  4.0  0.0        10518.689
-1.163605836D+05 2.554851510D+03-1.609746428D+01 6.625779320D-02-7.885081860D-05
 5.125224820D-08-1.370340031D-11                -6.176191070D+03 1.093338343D+02
   1000.000   6000.0007 -2.0 -1.0  0.0  1.0  2.0  3.0  4.0  0.0        10518.689
 3.408763670D+06-1.374847903D+04 2.365898074D+01-2.423804419D-03 4.431395660D-07
-4.352683390D-11 1.775410633D-15                 8.820429380D+04-1.371278108D+02


CO2               Gurvich,1991 pt1 p27 pt2 p24.
 3 g 9/99 C   1.00O   2.00    0.00    0.00    0.00 0   44.0095000     -393510.000
    200.000   1000.0007 -2.0 -1.0  0.0  1.0  2.0  3.0  4.0  0.0         9365.469
 4.943650540D+04-6.264116010D+02 5.301725240D+00 2.503813816D-03-2.127308728D-07
-7.689988780D-10 2.849677801D-13                -4.528198460D+04-7.048279440D+00
   1000.000   6000.0007 -2.0 -1.0  0.0  1.0  2.0  3.0  4.0  0.0         9365.469
 1.176962419D+05-1.788791477D+03 8.291523190D+00-9.223156780D-05 4.863676880D-09
-1.891053312D-12 6.330036590D-16                -3.908350590D+04-2.652669281D+01
   6000.000  20000.0007 -2.0 -1.0  0.0  1.0  2.0  3.0  4.0  0.0         9365.469
-1.544423287D+09 1.016847056D+06-2.561405230D+02 3.369401080D-02-2.181184337D-06
 6.991420840D-11-8.842351500D-16                -8.043214510D+06 2.254177493D+03


H2O               Hf:Cox,1989. Woolley,1987. TRC(10/88) tuv25.
 2 g 8/89 H   2.00O   1.00    0.00    0.00    0.00 0   18.0152800     -241826.000
    200.000   1000.0007 -2.0 -1.0  0.0  1.0  2.0  3.0  4.0  0.0         9904.092
-3.947960830D+04 5.755731020D+02 9.317826530D-01 7.222712860D-03-7.342557370D-06
 4.955043490D-09-1.336933246D-12                -3.303974310D+04 1.724205775D+01
   1000.000   6000.0007 -2.0 -1.0  0.0  1.0  2.0  3.0  4.0  0.0         9904.092
 1.034972096D+06-2.412698562D+03 4.646110780D+00 2.291998307D-03-6.836830480D-07
 9.426468930D-11-4.822380530D-15                -1.384286509D+04-7.978148510D+00


N2                Ref-Elm. Gurvich,1978 pt1 p280 pt2 p207.
 3 tpis78 N   2.00    0.00    0.00    0.00    0.00 0   28.0134000           0.000
    200.000   1000.0007 -2.0 -1.0  0.0  1.0  2.0  3.0  4.0  0.0         8670.104
 2.210371497D+04-3.818461820D+02 6.082738360D+00-8.530914410D-03 1.384646189D-05
-9.625793620D-09 2.519705809D-12                 7.108460860D+02-1.076003744D+01
   1000.000   6000.0007 -2.0 -1.0  0.0  1.0  2.0  3.0  4.0  0.0         8670.104
 5.877124060D+05-2.239249073D+03 6.066949220D+00-6.139685500D-04 1.491806679D-07
-1.923105485D-11 1.061954386D-15                 1.283210415D+04-1.586640027D+01
   6000.000  20000.0007 -2.0 -1.0  0.0  1.0  2.0  3.0  4.0  0.0         8670.104
 8.310139160D+08-6.420733540D+05 2.020264635D+02-3.065092046D-02 2.486903333D-06
-9.705954110D-11 1.437538881D-15                 4.938707040D+06-1.672099740D+03
```

```
O                    D0(O2):Brix,1954. Moore,1976. Gordon,1999.
 3 g 5/97 O   1.00    0.00    0.00    0.00    0.00 0   15.9994000     249175.003
    200.000   1000.0007 -2.0 -1.0  0.0  1.0  2.0  3.0  4.0  0.0       6725.403
-7.953611300D+03 1.607177787D+02 1.966226438D+00 1.013670310D-03-1.110415423D-06
 6.517507500D-10-1.584779251D-13                 2.840362437D+04 8.404241820D+00
    1000.000   6000.0007 -2.0 -1.0  0.0  1.0  2.0  3.0  4.0  0.0       6725.403
 2.619020262D+05-7.298722030D+02 3.317177270D+00-4.281334360D-04 1.036104594D-07
-9.438304330D-12 2.725038297D-16                 3.392428060D+04-6.679585350D-01
    6000.000  20000.0007 -2.0 -1.0  0.0  1.0  2.0  3.0  4.0  0.0       6725.403
 1.779004264D+08-1.082328257D+05 2.810778365D+01-2.975232262D-03 1.854997534D-07
-5.796231540D-12 7.191720164D-17                 8.890942630D+05-2.181728151D+02




OH                   D0(H-OH): Ruscic,2002. Gurvich,1978 pt1 p110 pt2 p37.
 3 g 4/02 O   1.00H   1.00    0.00    0.00    0.00 0   17.0073400      37278.206
    200.000   1000.0007 -2.0 -1.0  0.0  1.0  2.0  3.0  4.0  0.0       8813.106
-1.998858990D+03 9.300136160D+01 3.050854229D+00 1.529529288D-03-3.157890998D-06
 3.315446180D-09-1.138762683D-12                 2.991214235D+03 4.674110790D+00
    1000.000   6000.0007 -2.0 -1.0  0.0  1.0  2.0  3.0  4.0  0.0       8813.106
 1.017393379D+06-2.509957276D+03 5.116547860D+00 1.305299930D-04-8.284322260D-08
 2.006475941D-11-1.556993656D-15                 2.019640206D+04-1.101282337D+01
    6000.000  20000.0007 -2.0 -1.0  0.0  1.0  2.0  3.0  4.0  0.0       8813.106
 2.847234193D+08-1.859532612D+05 5.008240900D+01-5.142374980D-03 2.875536589D-07
-8.228817960D-12 9.567229020D-17                 1.468393908D+06-4.023555580D+02




O2                   Ref-Elm. Gurvich,1989 pt1 p94 pt2 p9.
 3 tpis89 O   2.00    0.00    0.00    0.00    0.00 0   31.9988000          0.000
    200.000   1000.0007 -2.0 -1.0  0.0  1.0  2.0  3.0  4.0  0.0       8680.104
-3.425563420D+04 4.847000970D+02 1.119010961D+00 4.293889240D-03-6.836300520D-07
-2.023372700D-09 1.039040018D-12                -3.391454870D+03 1.849699470D+01
    1000.000   6000.0007 -2.0 -1.0  0.0  1.0  2.0  3.0  4.0  0.0       8680.104
-1.037939022D+06 2.344830282D+03 1.819732036D+00 1.267847582D-03-2.188067988D-07
 2.053719572D-11-8.193467050D-16                -1.689010929D+04 1.738716506D+01
    6000.000  20000.0007 -2.0 -1.0  0.0  1.0  2.0  3.0  4.0  0.0       8680.104
 4.975294300D+08-2.866106874D+05 6.690352250D+01-6.169959020D-03 3.016396027D-07
-7.421416600D-12 7.278175770D-17                 2.293554027D+06-5.530621610D+02




H2                   Ref-Elm. Gurvich,1978 pt1 p103 pt2 p31.
 3 tpis78 H   2.00    0.00    0.00    0.00    0.00 0    2.0158800          0.000
    200.000   1000.0007 -2.0 -1.0  0.0  1.0  2.0  3.0  4.0  0.0       8468.102
 4.078323210D+04-8.009186040D+02 8.214702010D+00-1.269714457D-02 1.753605076D-05
-1.202860270D-08 3.368093490D-12                 2.682484665D+03-3.043788844D+01
    1000.000   6000.0007 -2.0 -1.0  0.0  1.0  2.0  3.0  4.0  0.0       8468.102
 5.608128010D+05-8.371504740D+02 2.975364532D+00 1.252249124D-03-3.740716190D-07
 5.936625200D-11-3.606994100D-15                 5.339824410D+03-2.202774769D+00
    6000.000  20000.0007 -2.0 -1.0  0.0  1.0  2.0  3.0  4.0  0.0       8468.102
 4.966884120D+08-3.147547149D+05 7.984121880D+01-8.414789210D-03 4.753248350D-07
-1.371873492D-11 1.605461756D-16                 2.488433516D+06-6.695728110D+02

H                    D0(H2):Herzberg,1970. Moore,1972. Gordon,1999.
 3 g 6/97 H   1.00    0.00    0.00    0.00    0.00 0    1.0079400     217998.828
    200.000   1000.0007 -2.0 -1.0  0.0  1.0  2.0  3.0  4.0  0.0       6197.428
 0.000000000D+00 0.000000000D+00 2.500000000D+00 0.000000000D+00 0.000000000D+00
 0.000000000D+00 0.000000000D+00                 2.547370801D+04-4.466828530D-01
    1000.000   6000.0007 -2.0 -1.0  0.0  1.0  2.0  3.0  4.0  0.0       6197.428
 6.078774250D+01-1.819354417D-01 2.500211817D+00-1.226512864D-07 3.732876330D-11
-5.687744560D-15 3.410210197D-19                 2.547486398D+04-4.481917770D-01
    6000.000  20000.0007 -2.0 -1.0  0.0  1.0  2.0  3.0  4.0  0.0       6197.428
 2.173757694D+08-1.312035403D+05 3.399174200D+01-3.813999680D-03 2.432854837D-07
-7.694275540D-12 9.644105630D-17                 1.067638086D+06-2.742301051D+02
```

References:

[1]   Mohd Aidil Bin Ziani "The Study of Performance of Gas Turbine for Power Generation" Thesis. Faculty of Chemical and Natural Resources Engineering University Malaysia Pahang (UMP).Malaysia. 2008.

[2]   "Massachusetts Institute of Technology Gas Turbine Lab" a website.

[3]   UK patent no. 1833 "Obtaining and Applying Motive Power, & c. A Method of Rising Inflammable Air for the Purposes of Procuring Motion, and Facilitating Metallurgical Operations" a website.

[4]   Apparatus for generating mechanical power. US635919A United States a website

[5]   Gavin Mortimer "A History of the North East in 100 objects" Book. FSC. Pine street London. United Kingdom. 2013

[6]   Bakken, Lars E et al. "Centenary of the First Gas Turbine to Give Net Power Output: A Tribute to Ægidius Elling". Volume 2: Turbo Expo Book. International Gas Turbine Institute. Vienna, Austria. 2004

[7]   "MIT Gas Turbine Laboratory" a website

[8]   "Deutsches-Museum.de" a website

[9]   "Biographical Memoirs of Fellows of the Royal Society". Article. Academic journal Royal Society. United Kingdom 2005

[10]   University of Bochum. In Touch Magazine. E.magazine. American Media, Inc. Englewood Cliffs. United States 2005

[11]   Clausius, Rudolf "On the Motive Power of Heat, and on the Laws, which can be deduced from it for the Theory of Heat" An Article Poggendorff's Annalen der Physik. Dover Reprint, Original was written in 1850

[12]   Stephen R. Turns "An Introduction to Combustion Concepts and Applications" 3rd edition Book. McGraw-Hill. New York, New York, United States. 1996

[13]   Peter Atkins "The Laws of Thermodynamics_ A Very Short Introduction." Book. OXFORD. UK. 2007

[14]   Jürg Waser "Basic Chemical Thermodynamics" Imperial College press. London, United Kingdom. 1966.

[15]   "Encyclopaedia Britannica" The website

[16]   J. Wilks "The Third Law of Thermodynamics" Oxford University Press. London, United Kingdom. 1961.

[17]   Richard Feynman. "The Feynman Lectures on Physics Vol 1". Addison Wesley. Boston, Massachusetts, United State. 1970

[18] "Enthalpy and internal energy liquids, solutions and vapours" Royal Society of Chemistry The website.

[19] F Reif "Statistical Physics." McGraw-Hill. London. UK. 1949

[20] Freeman "Thermal Physics." W. H. Freeman. Macmillan Publishers. London. United Kingdom. 1969

[21] Springer Spektrum "Theoretische Physik" Springer. Berlin Germany.1988

[22] "Physical and theoretical chemistry E.textbook". Chem.libretexts.org the website

[23] "Auburn.edu-Combustion" the website

[24] L. A. Tavadyan, G. A. Martoyan "Analysis of Kinetic Models of Chemical Reaction Systems Value Approach." NOVA. Hauppauge, New York. United States. 2005

[25] IUPAC "Gold Book definition of rate law". A Website. Last revised in 2014

[26] "www.mpoweruk.com". The website

[27] Claire Soares "Gas Turbines a Handbook of Air, Land and Sea Applications." Book. Butterworth-Heinemann. Oxford, United Kingdom. 2008.

[28] Pearson "Gas Turbine Theory." Book. 7th Edition. Pearson Publishing. London, United Kingdom. 2017

[29] Cussons Technology – "Two Shaft Gas Turbine Guide". Machine Hand guide. 102, Great Clowes Street. Manchester M7 1RH. U.K 2004

[30] Taylor & Francis "Combustion Science and Technology-Global Reaction Mechanism for Ethylene Flames with Preferential Diffusion." Article. Department of Environmental Science and Process Engineering BTU Cottbus, Cottbus, Germany. 2010

[31] Autar Kaw and E. Eric Kalu "Numerical Methods with Applications Abridged." Book. 2nd Edition. University of South Florida. Florida. United States. 2009

[32] Peter Deuflhard "Newton Methods for Nonlinear Problems Affine Invariance and Adaptive Algorithms." Book. Springer. New York, New York, United States. 2004

[33] Geoffrey J McLachlan "The EM Algorithm and Extensions" Article. Wiley Interscience. Bangalore India. 1997.

[34] N S Senanayake "Applied Thermodynamics, Gas Turbine Cycles" a Website Document.

Figures References

[12] Stephen R. Turns "An Introduction to Combustion Concepts and Applications" 3rd edition Book. McGraw-Hill. New York, New York, United States. 1996

[14]   Jürg Waser "Basic Chemical Thermodynamics" Book. Imperial College press London, United Kingdom. 1966.

[27]   Claire Soares "Gas Turbines a Handbook of Air, Land and Sea Applications." Book. Butterworth-Heinemann. Oxford, United Kingdom. 2008.

[28]   Pearson "Gas Turbine Theory." Book. 7th Edition. Pearson Publishing. London, United Kingdom. 2017.

[29]   Cussons Technology – "Two Shaft Gas Turbine Guide". Machine hand guide. 102, Great Clowes Street. Manchester M7 1RH. U.K 2004

[32]   Peter Deuflhard "Newton Methods for Nonlinear Problems Affine Invariance and Adaptive Algorithms." Book. Springer. New York, New York, United States. 2004

[34]   N S Senanayake "Applied Thermodynamics, Gas Turbine Cycles" a Website Document.

[35]   M.Vikraman "EXPERIMENTAL INVESTIGATION OF ELECTRICAL-TRUST AERO ENGINE" Article. Anna University Regional Centre Thirunelveli. Tirunelveli Region, Nagercoil Road, Tirunelveli, Tamil Nadu 627007, India. 2016

[36]   "deutsches-museum.de/ausstellungen/werkstoffe energie/ kraftmaschinen/ gasturbinen/" Website

[37]   "lemondeetnous.cafe-sciences.org/2014/03/le_pouvoir_de_la_vapeur" Website

[38]   "calypteaviation.com/silniki-historia-i-budowa-cz2-silniki/" Website

[39]   "deacademic.com/dic.nsf/dewiki/2373216" Website

[40]   "www.gracesguide.co.uk/Brown_Boveri_and_Co" Website

[44]   "www.industrial-electronics.com/engineering-industrial/process-plant-mach_3.html" Website

[45]   "www.sciencedirect.com/topics/engineering/aircraft-engines" Website

[48]   "grabcad.com/tutorials/tutorial-modeling-turbine-rotor-in-solidworks" Website

[49]   "www.sciencedirect.com/topics/engineering/flow-radial-turbine" Website

[51]   2145392 "Gas Turbine Somsak Chaiyapinunt Alongkorn Pimpin" Website

[53]   "youtube.com/channel/UCcqQi9LT0ETkRoUu8eYaEkg" YouTube Channel

[54]   Ibrahim I. Enagi, K.A. Al-attab, Z.A. Zainal. "Combustion chamber design and performance for micro gasturbine application" Article. Elsevier B.V. Amsterdam, Netherlands. 2017

[55]   Moinul Hossain, Jae-ha Myung, Rong-Lan Mark "Study on Direct Flame Solid Oxide Fuel Cell Using Flat Burner and Ethylene Flame" Article. Cassidy ECS Transactions. University of Kent. Canterbury, Kent, United Kingdom. 2015

[56]   Sara Moghtadernejad, Ali Dolatabadi "A Comprehensive Review on Fluid Dynamics and Transport of Suspension/Liquid Droplets and Particles in High-Velocity Oxygen-Fuel (HVOF) Thermal Spray" Article. Coatings an online open Access Journal. 2015

[57]   Ishak M.s.a, Mohammad Nazri, Mohd Jaafar, Wan Zaidi Wan Omar "The Effect of Inlet Air Preheat on CO And NO Production in the Combustion in Canister Burner" Article in Jurnal Teknologi an international journal. Penerbit University. Teknologi Malaysia. 2014.

[58]   "www.youtube.com/channel/UC3okdrCwHBb2DamA3d6wXOw" a YouTube Channel.

[59]   "allaboutcfd-tomersblog.com/2019/02/01/know-thy-mesh-mesh-quality-part-i/" a Website